

Daptomycin: Mechanism of Action and Bacterial Resistance

by

TianHua Zhang

A thesis
presented to the University of Waterloo
in fulfillment of the
thesis requirement for the degree of
Doctor of Philosophy
in
Chemistry

Waterloo, Ontario, Canada, 2015

© TianHua Zhang 2015

Author's Declaration

I hereby declare that I am the sole author of this thesis. This is a true copy of the thesis, including any required final revisions, as accepted by my examiners.

I understand that my thesis may be made electronically available to the public.

Abstract

Daptomycin is an important lipopeptide antibiotic used for treating severe infections caused by Gram-positive bacteria, including methicillin-resistant *Staphylococcus aureus* (MRSA) and vancomycin-resistant *Enterococcus* species. Its bactericidal activity requires calcium and the presence of phosphatidylglycerol (PG) in the target membrane and correlates with membrane depolarization. Daptomycin has also been shown to form oligomers on target membranes. Based on these findings, it has been proposed that the bactericidal effect of daptomycin arises from the formation of oligomeric pores or channels. This thesis reports experiments that test and further characterize this proposed mode of action.

In the first project, reported in chapter 2, it is demonstrated that oligomer formation is necessary for the bactericidal effect. The semisynthetic lipopeptide CB-182,462, which is similar to daptomycin in terms of structure and activity, was mixed with daptomycin. Fluorescence energy transfer studies showed that this mixture indeed produces stable hybrid oligomers, but at the same time, it was found that the mixture produces a significantly less than additive antibacterial effect. The existence of functionally impaired oligomers indicates that oligomer formation is indeed important for antibacterial function. However, it also shows that oligomerization is not sufficient; once formed, the oligomers must take another step in order to acquire antibacterial activity.

The assumption that daptomycin forms channels or pores in the target membranes is based on the observation that it induces bacterial cell membrane depolarization. However, these channels or pores have not been shown in a simple membrane model system. In the second project, a liposome model was used to detect and characterize the permeability properties of the daptomycin pores. These pores are selective for cations and allow for a higher permeating rate for smaller ions. Among all the tested cations, Na^+ and K^+ have the highest permeation rate, which suggests the *in vivo* depolarization is mainly due to sodium influx.

Genetic studies have indicated that an increased content of cardiolipin in the bacterial membrane may contribute to bacterial resistance against the drug. In the third project, it was shown that daptomycin no longer forms pores, even though it could still form oligomers, when 10 or 20 molar % cardiolipin were included in otherwise susceptible liposomal membranes. The oligomers formed on cardiolipin-containing membranes had approximately half the number of subunits ($n \approx 4$) of their pore-forming counterparts, and they were confined to the outer leaflets of the membranes. These findings not only reaffirm the suggestion raised in the first project that oligomerization is not quite enough, but also lead to a more detailed model: daptomycin first forms tetramers on the outer leaflet before being translocated to the inner leaflet, then two tetramers on the opposite leaflets align to create an octameric pore. Cardiolipin may mediate resistance to daptomycin by preventing its membrane translocation and subsequent permeabilization.

Acknowledgements

First and foremost, I would like to express my deepest appreciation to my supervisor Dr. Michael Palmer, a humble scholar, true gentleman, and inspiring mentor. I am deeply grateful for the opportunity of working in his research group. Without his knowledgeable guidance and persistent support, this dissertation would have not been possible. His encouragement and sense of humor have made the whole experience an absolute delight.

I would also like to thank my advisory committee members, Drs. Jean Duhamel, Qing-Bin Lu, and Richard Manderville; and my external committee member, Dr. Stanley Dunn for their valuable suggestions and comments.

I would also like to extend my sincere appreciation to Drs. Jared Silvermann, Scott Taylor, and Evan Mintzer for their fruitful collaborative support and discussions.

I am also very grateful for all the help from these wonderful friends and colleagues: Dr. Jawad Muraih, Eric Brefo-Mensah, Dr. Lisa Pokrajac, Mohamed Salah, Ben MacCormick, Robert Taylor, Bradley Scott, Celine Desert, and Stephanie Uwumarenogie. In particular, I am thankful to Dr. Jawad Muraih for his generous help throughout the whole research project.

To all my friends from chemistry department, especially all the biochemists from the 2nd floor of ESC, thank you for all the encouragement, help, and the great times, which will always be remembered. And to all the administrative staff members, thank you for all your help throughout the years.

Dedication

To my family

Contents

Author's Declaration	ii
Abstract	ii
Acknowledgements	iv
Dedication	v
List of Figures	x
List of Tables	xii
List of Abbreviations	xiii
1 Introduction	1
1.1 The arms race against bacteria	2
1.1.1 The antibiotic era: Golden age and crisis	3
1.2 Action modes of antibacterial agents	5
1.2.1 Inhibition of murein synthesis	5
1.2.2 Inhibition of mycolic acid synthesis	9
1.2.3 Inhibition of ribosomal protein synthesis	9
1.2.4 Inhibition of DNA and RNA synthesis	13
1.2.5 Inhibition of folate metabolism	14
1.2.6 Disruption of bacterial cell membranes	17
1.3 Bacterial resistance to antibiotics	17
1.3.1 Target modification	18
1.3.2 Target overexpression	21

1.3.3	Drug inactivation	23
1.3.4	Efflux and reduction of uptake	25
1.3.5	Origin and spread of resistance	28
1.3.6	Antibacterial combination therapy	34
1.4	Daptomycin	35
1.4.1	Preclinical development	37
1.4.2	Clinical trials and applications	43
1.4.3	Mode of action	44
1.4.4	Resistance to daptomycin	48
1.5	Research Objectives	51
2	The role of oligomer formation in the antibacterial activity of daptomycin	53
2.1	Introduction	53
2.2	Materials and Methods	55
2.2.1	Synthesis and purification of NBD-CB-182,462 and of perylene-dap- tomycin	55
2.2.2	Preparation of PC/PG large unilamellar vesicles (LUV)	56
2.2.3	Isothermal titration calorimetry (ITC)	56
2.2.4	Steady-state fluorescence measurements on PC/PG liposomes and on bacterial cells	57
2.2.5	Antibacterial activity of daptomycin and CB-182,462	58
2.3	Results	58
2.3.1	Oligomerization of CB-182,462 on liposome membranes	58
2.3.2	Formation of daptomycin/CB-182,462 hybrid oligomers on liposomes .	60
2.3.3	Formation of hybrid oligomers on bacterial cells	61
2.3.4	Antibacterial activity of daptomycin/CB-182,462 mixtures	64
2.4	Discussion	64

3	Daptomycin forms cation- and size-selective pores in model membranes	68
3.1	Introduction	68
3.2	Materials and Methods	69
3.2.1	Preparation of indicator-loaded large unilamellar vesicles	69
3.2.2	Fluorescence measurements	70
3.2.3	Spectrophotometric measurements	71
3.2.4	Assessment of flow rate of different cations through daptomycin pores .	72
3.3	Results	72
3.3.1	Effect of daptomycin on cation permeability	72
3.3.2	Effect of daptomycin on the permeability for anions	76
3.3.3	Effect of daptomycin on the permeability for neutral solutes	77
3.3.4	Estimation of the rate of ion flow across daptomycin pores	78
3.4	Discussion	80
4	Cardiolipin Prevents Membrane Translocation and Permeabilization by Daptomycin	83
4.1	Introduction	83
4.2	Materials and Methods	85
4.2.1	Preparation of liposomes (LUV) for fluorescence experiments	85
4.2.2	Preparation of liposomes (LUV) for ITC experiments	85
4.2.3	Measurement of membrane permeabilization with pyranine-loaded liposomes	85
4.2.4	Measurements of perylene excimer fluorescence	86
4.2.5	Isothermal calorimetry	86
4.2.6	Langmuir monolayers	86
4.2.7	Determination of daptomycin oligomer subunit stoichiometry by FRET	87
4.2.8	Dithionite quenching of NBD fluorescence	87
4.3	Results	88

4.3.1	Cardiolipin Inhibits Membrane Permeabilization by Daptomycin	88
4.3.2	Binding and oligomerization of daptomycin on membranes containing cardiolipin	88
4.3.3	Interaction of daptomycin with membranes containing CL by surface pressure and isothermal calorimetry (ITC)	92
4.3.4	Cardiolipin inhibits membrane translocation of daptomycin	94
4.4	Discussion	96
5	Summary and future work	101
5.1	Summary	101
5.2	Future work	104
5.2.1	Solid-state NMR for daptomycin pore structure	104
5.2.2	Mechanism of resistance caused by lysyl-PG	104
5.2.3	Interaction between daptomycin and the bacterial cell wall	105
5.2.4	Quantitative analysis of membrane binding and oligomerization	105
5.2.5	Potentials with synthetic daptomycin analogues	106
	Bibliography	108

List of Figures

1.1	Timeline of antibacterial development	4
1.2	Inhibition of murein biosynthesis by antibiotics	6
1.3	Structures of fosfomicin and of its related metabolites	7
1.4	Structures of cycloserine and of its related metabolites	8
1.5	Inhibition of bacterial ribosomal protein biosynthesis	10
1.6	Structure and action mode of puromycin	12
1.7	Inhibition of DNA and RNA biosynthesis	13
1.8	Inhibition of folate metabolism	15
1.9	Inhibitors of bacterial folate metabolism.	16
1.10	Action mechanisms of serine β -lactamases and of clavulanic acid.	24
1.11	Schematic representation of efflux pumps that confer bacterial drug resistance . . .	26
1.12	Schematic representation of gene transfer by bacterial conjugation	30
1.13	Schematic representation of transposons	31
1.14	Schematic representation of Tn3 replicative transposition.	32
1.15	Schematic representation of an integron	33
1.16	Structures of daptomycin and amphomycin	36
1.17	Biosynthesis of daptomycin by the Dpt non-ribosomal machinery.	39
1.18	Combinatorial biosynthesis of daptomycin analogues.	41
1.19	Proposed action mode of daptomycin.	47
1.20	Structures of PG, CL, and lysyl-PG.	51
2.1	Structures of daptomycin and of CB-182,462 and of their labeled derivatives	54

2.2	Formation of CB-182,462 oligomers on PC/PG liposomes	59
2.3	Formation of hybrid oligomers of native CB-182,462 and daptomycin on liposomes.	60
2.4	Interaction of homogeneous and hybrid oligomers with DOPC/DOPG membranes.	62
2.5	Formation of hybrid CB-182,462 oligomers on <i>Bacillus subtilis</i> cell membranes	63
2.6	Mutual inhibition of bactericidal action between daptomycin and CB-182,462	65
2.7	Hypothetical model for daptomycin action	66
3.1	Binding of daptomycin to PC/PG membranes at pH 6 and pH 8	71
3.2	Schematic of the pyranine-based liposome permeabilization assay	73
3.3	Permeabilization experiments with pyranine-loaded liposomes	74
3.4	Permeabilization of pyranine-loaded liposomes by gramicidin.	75
3.5	Schematic of the structure of daptomycin	76
3.6	Absence of liposome permeabilization toward chloride and cysteine	77
3.7	Conversion of observed pyranine fluorescence changes to cation flow rates	79
4.1	Structure of daptomycin	84
4.2	Permeabilization by daptomycin of liposomes composed of PC, PG, and CL	88
4.3	Fluorescence of perylene-daptomycin on liposomes	89
4.4	Estimation of subunit stoichiometry of daptomycin oligomer	91
4.5	Surface pressure change of lipid monolayers in response to daptomycin	92
4.6	ITC experiments on daptomycin binding to model membranes	93
4.7	Hypothetical action model of daptomycin.	94
4.8	NBD fluorescence quenching using dithionite	95
5.1	Structure of a synthetic daptomycin dimer	105
5.2	Structures of daptomycin and analogues.	107

List of Tables

1.1	Mechanisms of bacterial resistance to antibiotics.	19
3.1	Buffers and indicators used to detect membrane permeabilization toward different solutes.	70

List of Abbreviations

AMA	aspergillomarasmine A
A-site	aminoacyl-site (ribosome)
CCCP	carbonyl cyanide m-chlorophenyl hydrazine
CDA	calcium-dependent antibiotic
CL	cardiolipin
D-Ala	D-alanine
DHF	dihydrofolate
DHFR	dihydrofolate reductase
DHPS	dihydropteroate synthase
DMPC	1,2-dimyristoyl-sn-glycero-3-phosphocholine
DMPG	1,2-dimyristoyl-sn-glycero-3-phospho-rac-(1'-glycerol)
DNA	deoxyribonucleic acid
dTMP	deoxythymidine 6-monophosphate
DTNB	5,5'-dithiobis-(2-nitrobenzoic acid)
<i>E. coli</i>	<i>Escherichia coli</i>
EF-G	elongation factor G
GlcNAc	N-acetylglucosamine
HEPES	4-(2-hydroxyethyl)-1-piperazineethanesulfonic acid
Hexamethonium	N,N,N,N',N',N'-hexamethylhexane-1,6-diaminium
IR	inverted repeat

IS	insertion sequence
ITC	isothermal titration calorimetry
LPS	lipopolysaccharide
LUV	large unilamellar vesicles
MBL	metallo- β -lactamase
MES	2-(N-morpholino)ethanesulfonic acid
MLS	macrolides, lincosamides, and streptogramins
MOA	mechanism of action
mRNA	messenger RNA
MRSA	methicillin-resistant <i>Staphylococcus aureus</i>
MurA	UDP-GlcNAc enolpyruvate transferase
MurNAc	N-acetyl-muramic acid
MurY	phospho-MurNAc-pentapeptide translocase
NAD	nicotinamide adenine dinucleotide
NBD	nitrobenzoxadiazole
NRPS	non-ribosomal peptide synthetase
PABA	<i>p</i> -aminobenzoic acid
<i>P. aeruginosa</i>	<i>Pseudomonas aeruginosa</i>
PBP	penicillin-binding protein
P-site	peptidyl-site (ribosome)
PC	phosphatidylcholine
PEP	phosphoenolpyruvate
PG	phosphatidylglycerol

Pyranine	8-hydroxypyrene-1,3,6-trisulfonic acid
RNA	ribonucleic acid
THF	tetrahydrofolate
RND	resistance-nodulation-cell division
SAM	S-adenosylmethionine
<i>S. aureus</i>	<i>Staphylococcus aureus</i>
<i>S. roseosporus</i>	<i>Streptomyces roseosporus</i>
TOCL	tetraoleyl-cardiolipin
Tricine	N-(Tris(hydroxymethyl)methyl)glycine
rRNA	ribosomal RNA
tRNA	transfer RNA
UDP	uridine diphosphate
VRE	vancomycin-resistant <i>Enterococcus</i>

Chapter 1

Introduction

While microbes have been in existence for much longer than humanity, microbes were unknown to us until the 1670s, when Dutch scientist Antonie van Leeuwenhoek first observed live microorganisms in water using his home-built microscope. His remarkable work can be considered the beginning of microbiology. About two centuries later, the breakthrough studies by Louis Pasteur and Robert Koch led to the establishment of microbiology as an exact science, and they also let us realize that, whether we like them or not, microbes play a role in many aspects of our own lives.

Pasteur first showed that yeast can bring about food fermentation, one of the many things we like about microbes today. Besides the production of good cheese and wine, microbes also play a crucial role in maintaining our ecosystem. They also benefit us in many modern applications such as drug development, waste remediation, and energy generation. On the other hand, we have every reason to dislike or be afraid of them. Pasteur discovered that bacteria could cause food spoilage. Soon after, Robert Koch showed that anthrax is caused by *Bacillus anthracis*, thus providing the first evidence bacteria can cause disease in man. Infections caused

by pathogenic microbes have claimed, and continue to claim, more human lives than any other cause of death. A great number of these pathogens are from the kingdom of bacteria.

The discoveries by Pasteur, Koch, and others enabled us to combat bacterial infections through hygiene, vaccines, and antibiotic chemotherapy. While antibiotics have been used to great success for several decades, their utility is diminishing, as bacterial resistance continues to emerge and spread. Renewed research into the discovery, characterization, and optimization of antibiotics is therefore imperative.

This chapter will first present a brief up-to-date review of major antibacterial agents. We will consider both how they attack bacteria, and how the bacteria fight back against them. Daptomycin, a lipopeptide antibiotic that is the main topic of this thesis, will be introduced in Section 1.4. The subsequent chapters will present my experimental work on the action mode of this antibiotic.

1.1 THE ARMS RACE AGAINST BACTERIA

Although written records and archaeological discoveries indicate that we have a very long history of using antibacterial medicine, all early applications were empirical and met with limited success.^{15,39,43,150} The extent of bacterial infection was never under control, and we can call this period the pre-antibacterial era.

It was not until around 1900 that Paul Ehrlich introduced the concept of a “magic bullet”, meaning a compound that could selectively target a pathogenic microbe but not its host. Following this concept, Ehrlich and colleagues started the first large-scale drug screening, which eventually led to the discovery of the anti-syphilis drug Salvarsan (arsphenamine) in 1909. Using the same approach, Prontosil (sulfamidochrysoidine), the first sulfonamide drug, was developed and used clinically to treat a wide range of bacteria beginning in the 1930s. In the meantime, a serendipitous incident happened in Fleming’s lab in 1928, which led to the discovery of penicillin and its clinical use beginning in the early 1940s.^{7,69,160} With the introduction of these three drugs, the antibiotic era had begun.

In the following years, a variety of successful antibacterial drugs were obtained from different sources. Some of them are chemically synthesized, just as Salvarsan and Prontosil had been. The rest of them are antibiotics that are either naturally produced by microorganisms, such as penicillin by the fungus *Penicillium notatum*, or are the semisynthetic derivatives of such natural compounds. With these drugs in hand, humans seemed to get the upper hand in the war against bacteria. But instead of surrendering, the bacteria came up with biochemical mechanisms of resistance to these drugs. Therefore, newer and more powerful antibacterial drugs are constantly required, which means that we have entered a perpetual arms race against bacteria.

1.1.1 The antibiotic era: Golden age and crisis

After realizing the tremendous healing power of antibacterial chemotherapy, vast resources were put into the search for more and better antibacterial drugs. The efforts paid off, as a great number of new drug classes were soon discovered. In retrospect, most of the antibiotic classes we know today were discovered in the two decades following the clinical introduction of penicillin, and this period is also considered as the “Golden age” of antibiotics. Silver¹⁸² has summarized them all in a discovery timeline (Figure 1.1).

After the “Golden age”, antibiotic discovery entered a protracted period of drought, during which only a few new drug classes were discovered. Silver has termed this period the “Discovery void”. Several factors contributed to this dearth of discoveries:

1. Most of the antibacterials are natural products that were discovered through empirical screening. After a while, the low-hanging fruit had been harvested, and screening costs increased.
2. Modification of existing drugs promises more immediate results and financial returns, while requiring less resources, and therefore came to be preferred over new discovery.
3. Big pharmaceutical companies abandoned the development of antibacterials, focusing their resources instead on potentially more profitable therapeutic areas.¹⁸²

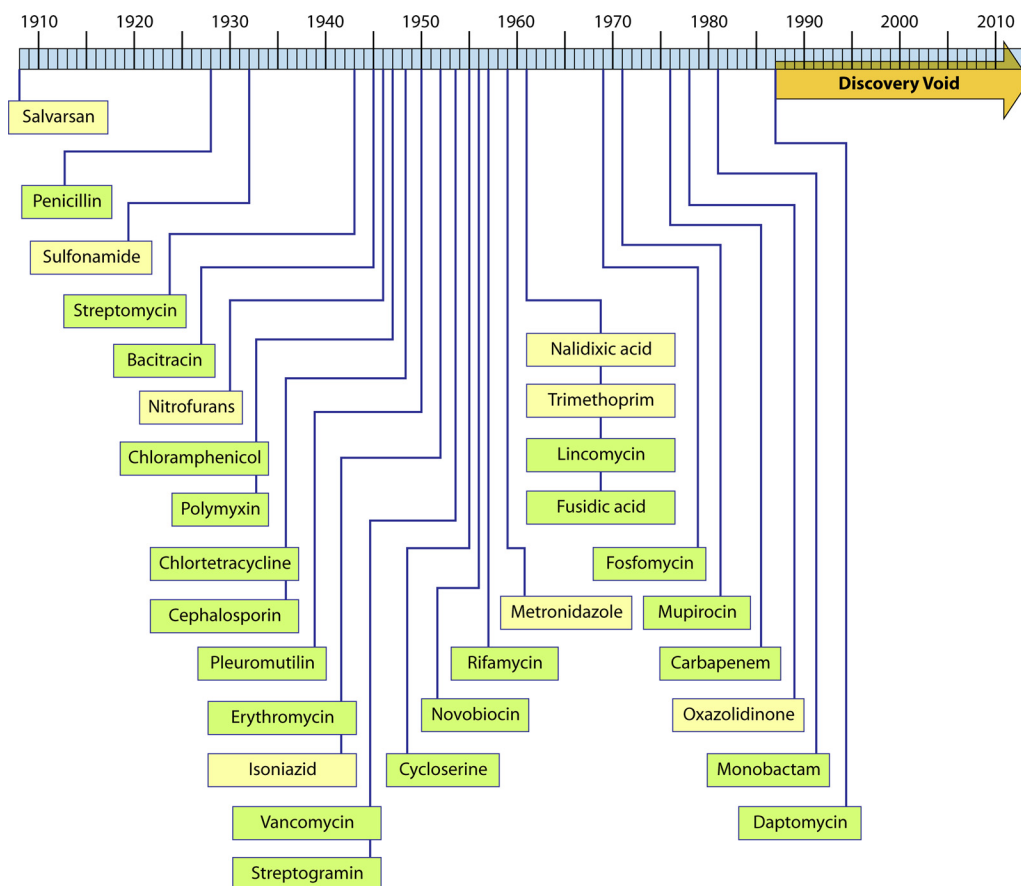


Figure 1.1 The development in antibacterial agents. The dates shown are of their initial discoveries. Each agent represents a new drug class.¹⁸²

For several decades, this decrease in development activity remained under the radar and did not cause much concern. However, the situation has since deteriorated. Antibacterials are mass-produced and widely distributed for use not only health care, but also in other fields, mainly in animal husbandry. Under the enormous selection pressure exerted by ubiquitous antibiotics, bacteria started developing different means to adapt and survive. It soon became very clear that the question was not if bacteria would become resistant to a new drug, but only how long it will take them to do it. Due to the severity and prevalence of antibacterial resistance, many infections that until recently could be considered manageable have again become potentially life-threatening. Therefore, we are now facing a renewed crisis of bacterial infections.³³

1.2 ACTION MODES OF ANTIBACTERIAL AGENTS

To overcome this crisis, it is obvious that we have to keep upgrading our antibacterial arsenal. And hence it is worthwhile to learn lessons from our existing drugs. In this section, I will use the targets as the focal points to explain the mechanisms of action (MOA) of different drug classes mentioned in Silver's timeline (Figure 1.1).

A safe antibacterial agent needs to have very selective toxicity towards bacteria but not its host organism, which means it needs to act upon a target that is specific for the bacteria. Many drugs that meet this criterion find their targets in the synthesis the bacterial cell wall or in the biosynthesis of DNA, RNA, and protein.

1.2.1 Inhibition of murein synthesis

The cell wall of bacteria is an essential structure for their viability and is also the first obstacle that any antibacterial drug has to deal with before exerting its activity. In contrast to mammalian cells, all bacteria other than mycoplasmas have a murein (peptidoglycan) layer on top of their cytoplasmic membrane. Many antibacterial drugs take advantage of this difference by inhibiting the biosynthesis of murein at various steps (Figure 1.2). This is a length pathway with multiple enzyme-catalyzed reactions, as follows:

Synthesis of N-acetylmuramic acid from N-acetylglucosamine. The basic building block N-acetylglucosamine (GlcNAc) is converted to N-acetyl-muramic acid (MurNAc) by the enzyme UDP-GlcNAc enolpyruvate transferase (MurA), which transfers enolpyruvate from phosphoenolpyruvate (PEP) to GlcNAc. Fosfomycin is structurally similar to both glycerophosphate and PEP (Figure 1.3). Due to the former similarity, fosfomycin is picked up and transported across the membrane by the glycerophosphate transporter. Inside the cell, fosfomycin behaves as an antimetabolite of PEP. It attaches covalently to the active site of enzyme MurA, causing its inactivation.^{26,97,160}

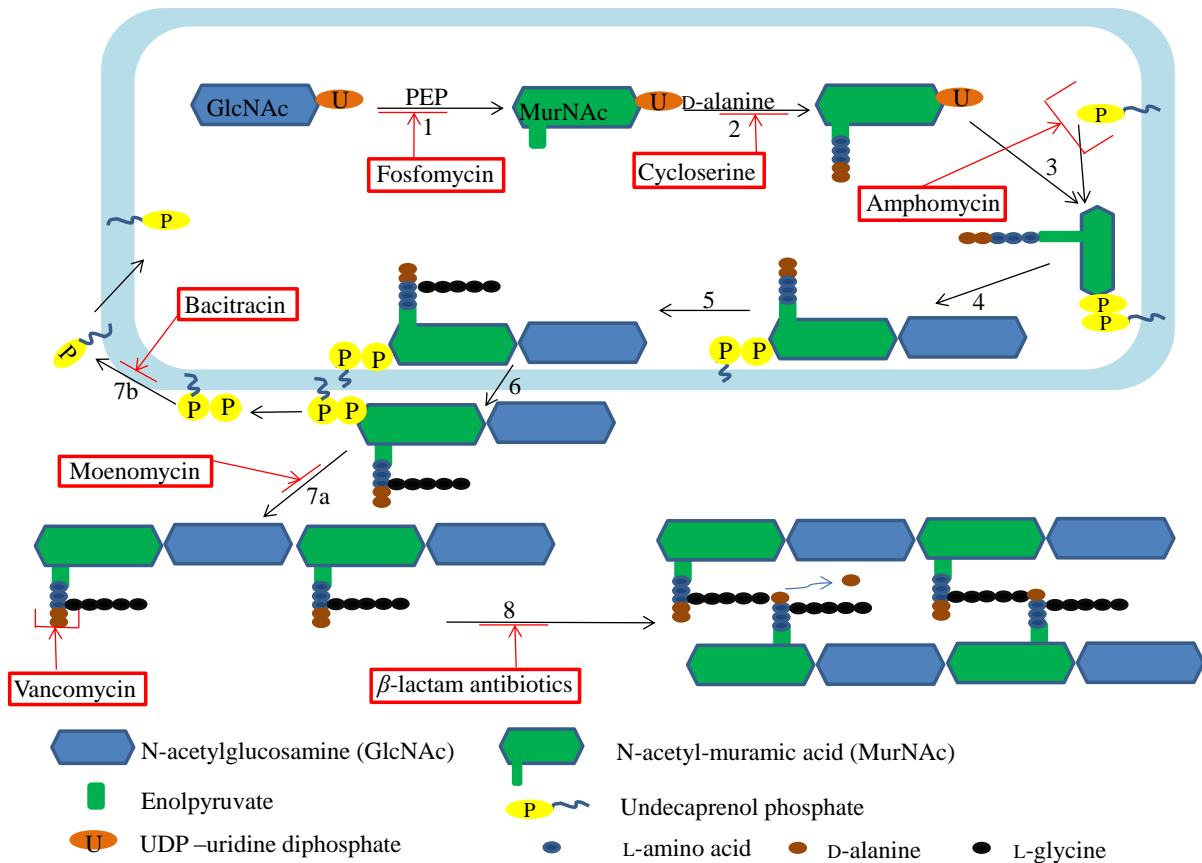


Figure 1.2 Murein biosynthesis is inhibited at various steps by antibacterial agents. The intracellular synthesis of lipid II is carried out in steps 1–5. GlcNAc is first converted to MurNAc by the enzyme MurA using the substrate phosphoenolpyruvate (PEP). This is followed by the stepwise addition of a pentapeptide that includes two D-alanine (D-Ala) residues. Fosfomycin and cycloserine are antimetabolites to PEP and D-Ala, respectively, and inhibit these first two steps. In step 3, MurNAc is further activated and transferred to an undecaprenol phosphate lipid carrier by MraY. Amphomycin inhibits this step by binding and sequestering the carrier lipid. In step 4, GlcNAc is added to the carrier-bound MurNAc, whose peptide moiety is further extended in step 5 with pentaglycine to form lipid II. In step 6, lipid II is flipped to the outer leaflet of the cytoplasmic membrane, where the polymerization begins. The glycopeptide moiety is transferred from lipid II to a nascent peptidoglycan strand by transglycosylase in step 7a, which can be inhibited by moenomycin. Meanwhile, the undecaprenol bisphosphate carrier is converted back to the monophosphate and returns to the cytosol for the next cycle. Bacitracin inhibits the regeneration of undecaprenol phosphate and thereby affects step 3 in the next cycle. In the final step, adjacent peptidoglycan strands are cross-linked via their side peptide chains by transpeptidase. This step can be inhibited by vancomycin and by β -lactam antibiotics.

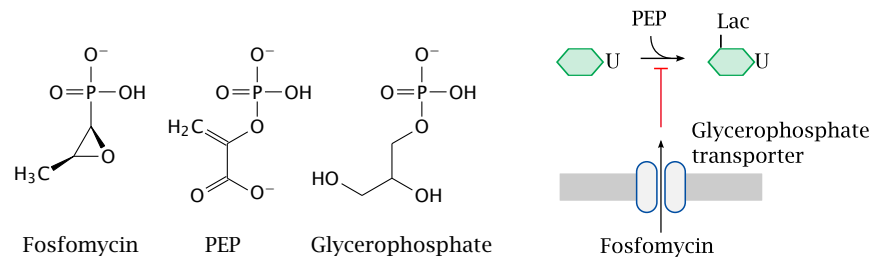


Figure 1.3 Structures of fosfomicin and of its related metabolites. The antibacterial activity of fosfomicin is due to its structural similarity with the metabolites PEP and glycerophosphate. Prior to reaching its cytoplasmic enzyme target MurA, fosfomicin is first transported across the cytoplasmic membrane by the glycerophosphate transporter. Inside the cell, fosfomicin deactivates MurA by attaching to its active site.¹⁶⁰

Attachment of a pentapeptide to MurNac. A pentapeptide that contains two D-alanine residues at its free end is added to MurNac. This pentapeptide is crucial for the cross-linking of adjacent murein strands in the final step 8 of murein synthesis. The D-alanine that is part of this peptide is supplied by alanine racemase and ligated by D-alanine ligase. Cycloserine is an antimetabolite of D-alanine that can effectively inhibit both enzymes (Figure 1.4).^{66, 154, 160, 212}

Attachment of peptidyl-MurNac to undecaprenol phosphate. The new building block is transferred to undecaprenol phosphate, a carrier lipid, by phospho-MurNac-pentapeptide translocase (MraY). This step is inhibited by the lipopeptide antibiotic amphomycin. Unlike the previous two drugs, which interact directly with enzyme molecules, amphomycin binds to the lipid carrier substrate. It is worth noting that, while amphomycin is structurally quite similar to daptomycin (see Figure 1.16), the two antibiotics have very different action modes.^{35, 169, 200}

Completion of the lipid II precursor. The activated building block is extended with another GlcNac moiety, which is followed by the addition of a pentapeptide containing only glycine residues. This glycine pentapeptide is attached to a lysine, which is the third amino acid residue on the pentapeptide previously attached in step 2. This step completes the synthesis of lipid II.

Transport of lipid II to the outer membrane leaflet. The cytoplasmic lipid II is flipped across the membrane for the final stage of murein assembly. The exact mechanism involved in translo-

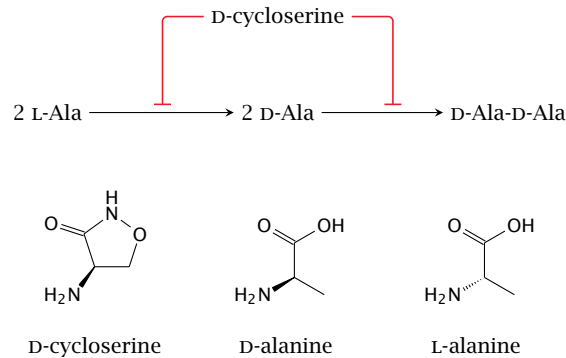


Figure 1.4 Structures of cycloserine and of its related metabolites. Cycloserine is an antimetabolite of D-alanine. It inhibits both alanine racemase and D-alanine ligase.¹⁶⁰

cation of lipid II across membrane has been studied by many researchers, yet it still remains controversial. Protein transporters FtsW and MurJ are the two potential candidates that have been investigated in great detail and debated between two research groups.^{139,178,223}

Transfer of the precursor to a nascent murein strand. The glycopeptide moiety of lipid II is transferred to a nascent murein strand by transglycosylase; this leaves behind the carrier lipid as a diphosphate. Moenomycin, a glycolipid antibiotic, is the only known antibiotic to inhibit this step; it binds and inactivates the enzyme.^{156,224}

The undecaprenol diphosphate carrier released by the transglycosylase reaction is converted back to undecaprenol phosphate by a pyrophosphatase; it is then flipped back across the membrane to join step 3 of the subsequent cycle. Undecaprenol pyrophosphatase is inhibited by bacitracin, which sequesters the carrier lipid in the outer membrane leaflet. This indirectly inhibits step 3.^{191–193}

Covalent cross-linking of murein strands. Adjacent murein strands are cross-linked to form the final murein mesh structure. The cross-linking reaction takes place between the terminal residue of the pentaglycine of one strand and the subterminal D-alanine residue of another; the terminal D-alanine residue is released in the process. This enzymatic reaction can be inhibited by vancomycin, which binds to the D-Ala-D-Ala peptide substrate denies it access to the active site of the transpeptidase. It is also inhibited by β -lactam antibiotics, which include

the penicillins, cephalosporins, carbapenems, and monobactams. These antibiotics have structural similarity with the D-Ala-D-Ala peptide moiety. Moreover, the β -lactam ring is “spring-loaded” and is ready to react covalently with the transpeptidase, which can inhibit the enzyme function completely.^{160,205,213}

1.2.2 Inhibition of mycolic acid synthesis

Isoniazid (isonicotinic acid hydrazide) is one drug specifically used for tuberculosis treatment. It targets cell wall synthesis as well. However, instead of attacking any of the steps involved in murein synthesis, it targets the synthesis of mycolic acids. Mycolic acids are fatty acids with very long chains that are precursors for constructing the unique cell wall of mycobacteria, a class of pathogenic bacteria that includes the causative agent of tuberculosis. Isoniazid is a prodrug; it is first activated by the mycobacterial catalase-peroxidase KatG to form an isonicotinic acid radical. The radical then forms an adduct with NAD^+ that inhibits the enzyme InhA, which in turn is directly involved in mycolic acid synthesis.^{160,204}

1.2.3 Inhibition of ribosomal protein synthesis

Protein synthesis is another major target exploited by many classes of antibacterial agents (Figure 1.5). The ribosomes of bacteria and of eukaryotes differ significantly in size and structure. The bacterial ribosome has a sedimentation velocity of 70S; it consists of a large (50S) subunit and a small (30S) subunit. In contrast, the eukaryotic ribosome has 80S with subunits of 60S and 40S, respectively. Some antibiotics, for example puromycin, inhibit both the eukaryotic and the prokaryotic ribosome; however, many others selectively inhibit the bacterial ribosome and are therefore useful in antibacterial chemotherapy.

Most drugs that target the ribosome bind to the 23S ribosomal RNA (rRNA) molecule, which is part of the large 50S subunit and contains the peptidyl transferase active site.¹⁷³ These drugs include chloramphenicol, pleuromutilin, erythromycin, lincomycin, and streptogramin.

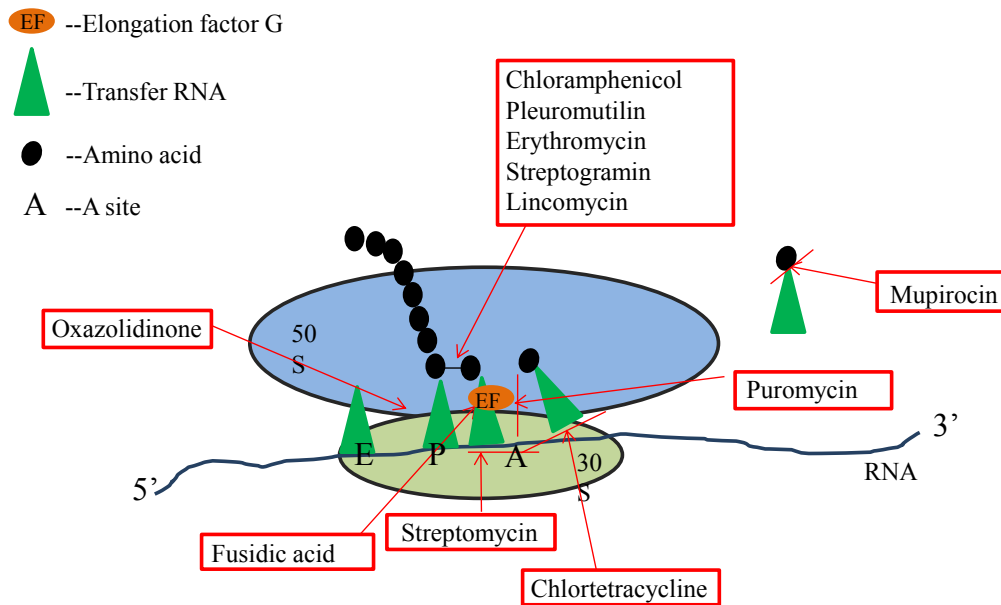


Figure 1.5 Inhibition of bacterial ribosomal protein biosynthesis. Most of the antibiotics that bind to the 50S subunit interfere with the extension of the peptide. An exception are the oxazolidinone antibiotics, which inhibit the initiation of translation. The antibiotics chlortetracycline and streptomycin bind to the 30S subunit and interact with A-site; they interfere with the binding and the proofreading of the tRNA, respectively. Fusidic acid binds to elongation factor G (EF-G) and stops translocation of peptidyl-tRNA from the aminoacyl-site (A-site) to the peptidyl-site (P-site). Puromycin acts as a false aminoacyl-tRNA, which terminates the peptide extension. Mupirocin inhibits the synthesis of isoleucyl-tRNA.

Peptidyl transferase is responsible for elongating the nascent peptide with an incoming amino acid by catalyzing the formation of a peptide bond.

Erythromycin, lincomycin, and streptogramin belong to the drug classes of macrolides, lincosamides, and streptogramins, respectively. While these three drug classes have very different chemical structures, they are nevertheless often grouped together as the MLS antibiotics because of their very similar binding sites and action mechanisms. This similarity also accounts for their notorious cross-resistance (Section 1.3.1). The binding of these drugs to the peptidyl transferase active site interferes with the binding of incoming aminoacyl-tRNA to the A-site of the ribosome, which subsequently inhibits the formation of a new peptide bond and forces the premature release of peptidyl-tRNA.^{121, 138, 168, 202}

Oxazolidinones are another class of drugs that bind to 23S rRNA on the 50S subunit and even compete for the binding site with chloramphenicol and lincomycin.^{115,219} They also inhibit peptide synthesis, but this effect is mechanistically distinct from the other 50S-bound inhibitors. Unlike the others, which act on a growing peptide, oxazolidinones prevent the translation right from the start by inhibiting the formation of the ternary initiation complex between N-formylmethionyl-tRNA, the ribosome, and mRNA.^{162,181,198}

Despite the great similarity of activity shared among all of these 23S rRNA targeting drugs, structural and resistance studies have shown that there were still some subtle differences in their exact mechanisms of action.²¹⁶

There are fewer drug classes that bind to the 30S subunit, but there is a great diversity in their mechanisms of action. Example of such drugs include streptomycin, chlortetracycline, and fusidic acid. Streptomycin, an aminoglycoside, interacts with the aminoacyl-site or A-site, where tRNA binding to the ribosome and pairing with mRNA take place. The A-site serves as the proofreader for mRNA translation; it ensures that only the correct tRNA-mRNA pairs will form. The interaction between streptomycin and the A-site causes structural changes to the latter, which still allow it to bind tRNA but interfere with its ability to recognize and reject incorrect pairs. This translational miscoding leads to the synthesis of faulty protein molecules, which in turn causes cell damage.^{119,160}

Chlortetracycline interacts with the A-site as well; it blocks the binding of aminoacyl-tRNA directly and stops the mRNA from being translated.⁷¹ Fusidic acid interferes with protein synthesis by binding to and inhibiting the function of peptide elongation factor G (EF-G), which promotes the translocation of tRNA from the A-site to the peptidyl or P-site.^{2,28,102}

Mupirocin inhibits protein synthesis but does not bind to either the 50S or the 30S subunits. It inhibits protein synthesis by limiting the supply of one specific aminoacyl-tRNA, namely, isoleucyl-tRNA, to the ribosome. It binds to the active site of isoleucyl-tRNA synthetase as an analogue of isoleucyladenylate, which stops the production of isoleucyl-RNA.^{40,86,187,208,220}

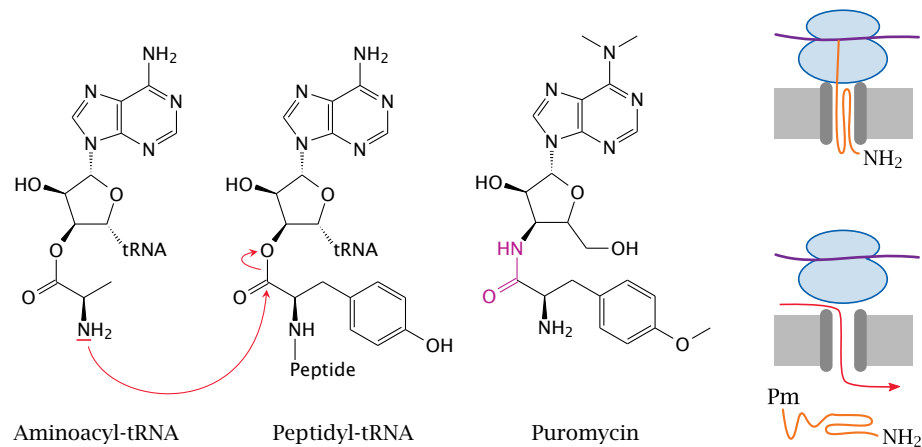


Figure 1.6 Structure and mechanism of action of puromycin. Puromycin (Pm) is structurally similar to the aminoacyl moiety of aminoacyl-tRNA and is attached to the c-terminal of a growing peptide. The presence of an amide bond (purple) instead of an ester bond terminates the synthesis of the peptide and causes its premature release. With ribosomes engaged in the synthesis of membrane proteins, the premature release of the peptide will leave the translocon pore stuck in an open state, which will make the membrane leaky to small solutes.¹⁶⁰

Puromycin is an analogue of the aminoacyl moiety in aminoacyl-tRNA, which is mistakenly picked up by the ribosome and added to the C-terminal of a growing peptide (Figure 1.6). Instead of an ester bond that would yield to nucleophilic attack by the next incoming amino acid, puromycin has an amide bond, which cannot participate in the subsequent elongation reaction and leads to the termination of peptide synthesis.^{11, 149, 222} In addition to the direct harm caused by the incomplete peptide synthesis, the premature release of the peptide from ribosome can also lead to a secondary damage on membranes. When the protein undergoing synthesis is an integral membrane or secretory protein, the ribosome will be attached to a translocon pore that spans the cytoplasmic membrane (or in eukaryotes, the ER membrane). The nascent proteins are guided to their destinations by these pores. Once the peptide is prematurely released, the translocon pore is left open and becomes a pathways for small solutes to permeate across the membrane freely.^{185, 186}

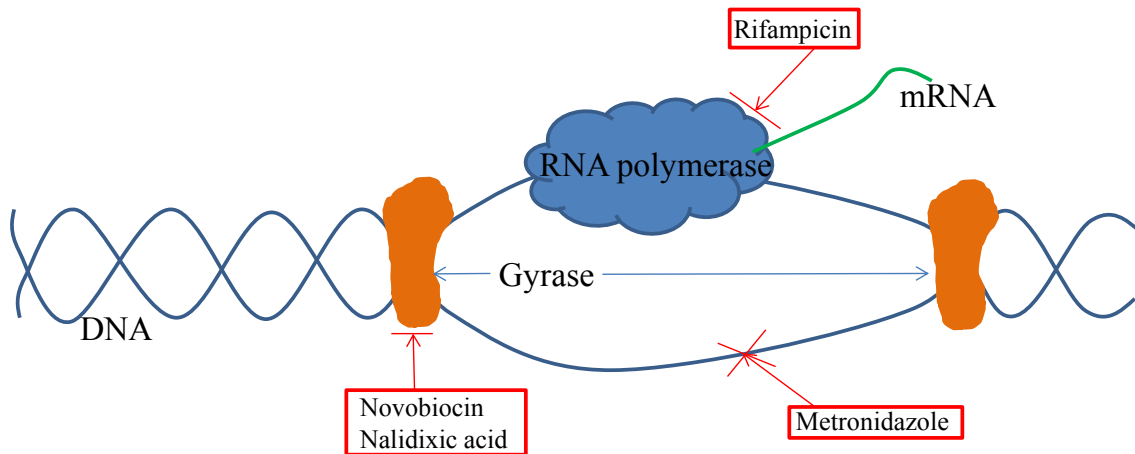


Figure 1.7 Inhibition of bacterial DNA and RNA biosynthesis. Rifampicin (rifamycin class), novobiocin (aminocoumarin class) and nalidixic acid (quinolone class) exert their activity by deactivating enzymes. Metronidazole can break DNA strands directly.

1.2.4 Inhibition of DNA and RNA synthesis

Another group of drugs find their targets upstream of ribosomal protein synthesis, that is, in DNA and RNA synthesis. They can either interrupt DNA and RNA replication or directly damage DNA (Figure 1.7). Some representative drugs are rifampicin (rifamycin class), novobiocin (aminocoumarin class), nalidixic acid (quinolone class), and metronidazole (nitroimidazole class).

Bacterial DNA-dependent RNA polymerase comprises multiple subunits. Rifampicin binds to the active site of the β -subunit, which catalyzes the polymerization. The binding strongly inhibits DNA transcription and particularly the initiation stage.^{30,70,188,214} The eukaryotic enzymes are much less sensitive to inhibition by rifampicin.⁸¹ Novobiocin and nalidixic acid both exert their antibacterial activity by inhibiting the function of bacterial DNA gyrase, a type II topoisomerase (also see Section 1.3.1). Though neither novobiocin nor nalidixic acid are clinically important these days, some of the newer generation drugs from their classes are widely used, such as ciprofloxacin (a gyrase inhibitor from the quinolone class).

The unique and essential functions of enzyme topoisomerases make them excellent drug

targets. The length of a cell's DNA is much longer than that of the cell contains it. In order to be accommodated inside the cell, these DNA strands are coiled and supercoiled to adopt a much more compact form. This process requires topoisomerase. On the other hand, DNA strands need to be relaxed and disentangled before replication or transcription, which again requires topoisomerase.^{42, 180, 196, 197} Gyrase (type II topoisomerase) can cut both strands of one DNA double helix and then re-ligate them after passing an intact double helix across the gap. This relaxation of DNA coils grants access to DNA-associated enzymes.

Metronidazole acts selectively against anaerobic bacteria. After entering the cells, it is reduced by the low-redox-potential enzyme pyruvate:ferredoxin oxidoreductase and ferredoxin to a highly reactive nitro intermediate form. This unstable intermediate may attack and break DNA strands.¹¹⁶ In addition to infections with anaerobic bacteria, nitroimidazoles are also useful in treating infections caused by anaerobic eukaryotic pathogens, such as *Trichomonas vaginalis*.^{58, 160}

1.2.5 Inhibition of folate metabolism

The metabolism of folate plays an crucial role in many biochemical pathways (Figure 1.8). It provides single carbon units for the biosynthesis of thymine (dTMP), purine bases, and the amino acid methionine, which serve as basic building blocks in the synthesis of DNA, RNA, and proteins. Methionine is also an important intermediate in the S-adenosylmethionine (SAM) cycle that brings about a number of methylation reactions. The two well-known antibiotics that inhibit folate metabolism are sulfonamides and trimethoprim.

In all of these folate-dependent pathways, tetrahydrofolate (THF) is the pivotal compound. THF is reduced from dihydrofolate (DHF) by dihydrofolate reductase (DHFR). The synthetic drug trimethoprim works as a DHFR inhibitor due to its structural resemblance of DHF (Figure 1.9). Even though DHFR is required in both bacteria and human folate metabolism, the structural differences between the human and bacterial enzymes make trimethoprim selectively toxic towards bacteria.

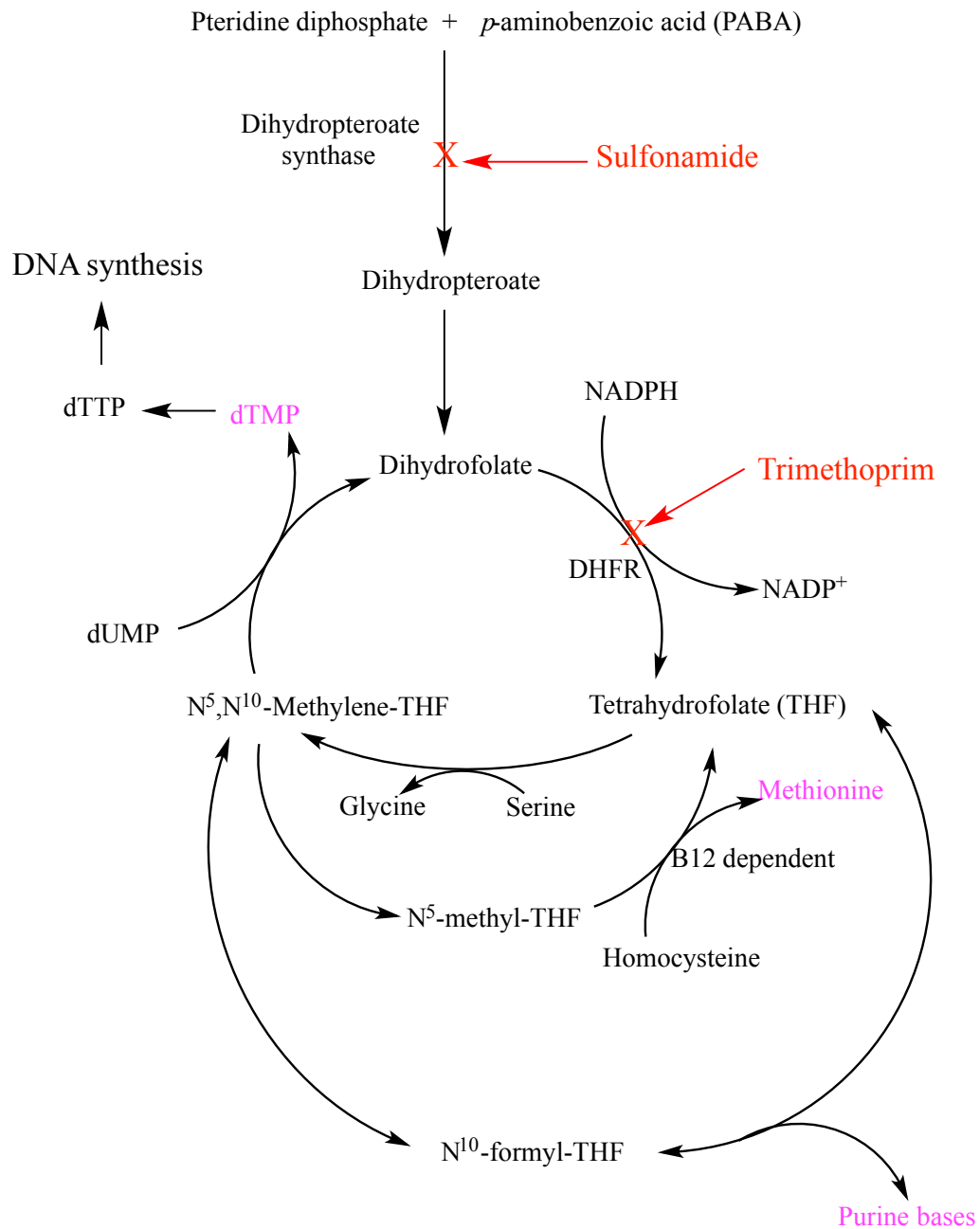


Figure 1.8 Inhibition of bacterial folate metabolism. The participation of folate is crucial in multiple biochemical pathways; some major compounds provided by these pathways are highlighted in pink. The production of THF is in the center of these pathways, and hence is the target for antibiotics. Sulfonamide and trimethoprim inhibit activities of dihydropteroylserine synthase and dihydrofolate reductase (DHFR) respectively.

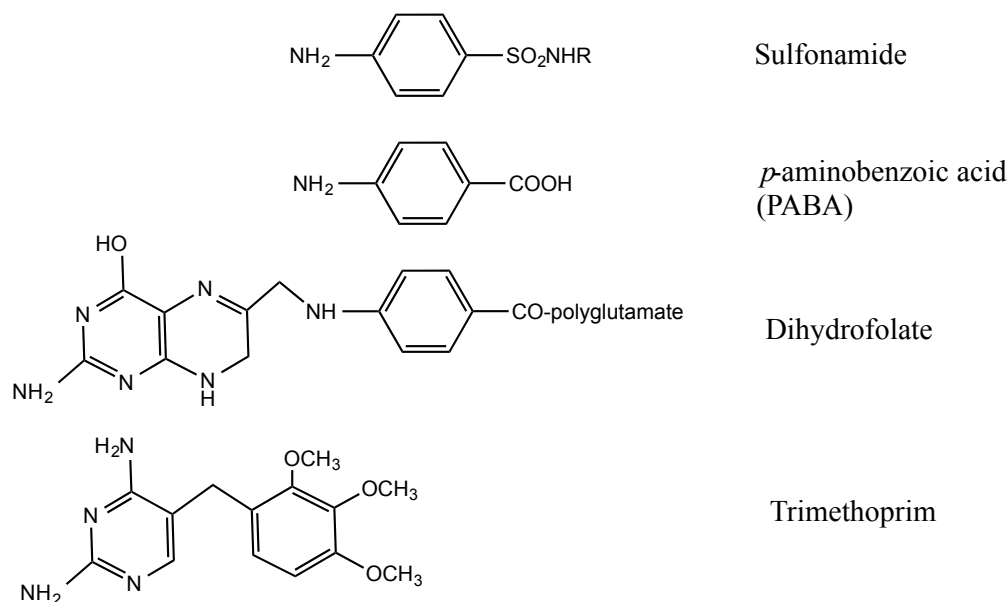


Figure 1.9 Structures of compounds that interfere bacterial folate metabolism. Sulfonamides and trimethoprim share structural similarities with PABA and with DHF, respectively, and act as their antimetabolites.

To obtain DHF, bacteria and humans utilize two completely different routes. Humans get folic acid directly from a variety of dietary sources and then convert it to DHF via a NADPH-dependent reduction reaction (also catalyzed by DHFR). On the other hand, bacteria have to synthesize DHF themselves. Firstly, dihydropteroate is produced by incorporating the precursor *p*-aminobenzoic acid (PABA) into a pteridine diphosphate, followed by the release of a diphosphate group; this reaction is catalyzed by the enzyme dihydropteroate synthase. Subsequently, the dihydropteroate is further modified to produce DHF (Figure 1.8). Sulfonamides and PABA have very similar structures and compete for enzyme substrate binding sites. This competition can effectively inhibit the synthesis of folate and any subsequent reactions.

Sulfonamides and trimethoprim inhibit the same pathway in successive steps. Their antibacterial effects are synergistic, and they are thus often used in combination. However, the prevalent resistance and the concern of allergic reactions to them have greatly limited the usage of sulfonamides.

1.2.6 Disruption of bacterial cell membranes

There are also some antibacterial agents that are not necessarily involved in enzyme function or metabolic pathways but can kill bacteria by disrupting their cell membranes. However, most of them are not selective towards bacterial cells and hence are too toxic for clinical application. So far, two such drugs have been clinically approved, namely, polymyxin and daptomycin.

Polymyxin is a positively charged cyclic lipopeptide antibiotic with a short acyl side chain. It binds to the outer membrane of Gram-negative bacteria, and more particularly to lipid A, the hydrophobic anchor of lipopolysaccharide (LPS). Adjacent LPS molecules form a network through hydrophobic forces and bridging cations (Ca^{++}). This organized network is crucial to maintain the cell wall's integrity. The binding of polymyxin interrupts the hydrophobic interaction and also displaces Ca^{++} , which leads the destabilization and disruption of the outer membrane.^{65,160,165,172} The mechanism of action for daptomycin is explained in Section 1.4.3.

Valinomycin acts on cell membranes as a potassium ionophore. It has a cyclic peptide structure which wraps tightly around a potassium ion and exposes a hydrophobic exterior. This complex can easily diffuse through membranes and dissipate the potassium concentration gradient, and thus cause the disruption of cell's membrane potential. Valinomycin is not selective for bacteria but also acts on mammalian cells. It thus is too toxic for medical use; however, its high specificity for potassium ions makes it very useful for research in biochemistry and cell biology, including some of the experiments described in the following chapters.

1.3 BACTERIAL RESISTANCE TO ANTIBIOTICS

The existence of bacterial resistance has been a concern since the beginning of the antibiotic era. Mass production and a wide range of application of antibacterials in the past 70 years has created a very strong selection pressure for bacteria and promoted the emergence and spreading of resistance.

To combat bacterial resistance, new drug classes were developed to attack different bacterial targets. As mentioned above, a variety of targets have been exploited. Notwithstanding the diversity of the antibacterials' action mechanisms and targets, the resistance mechanisms employed by bacteria toward them can be broadly divided into three categories: (1) modification of drug targets, (2) enzymatic drug inactivation, and (3) enhanced efflux and/or reduced uptake of drugs. Most drugs encounter more than one resistance mechanism in different bacterial species or strains. Even individual bacterial strains may employ multiple mechanisms of resistance toward a specific single drug. A summary of the resistance mechanisms is given in Table 1.1.

1.3.1 Target modification

Target modification is the most common way to confer resistance to bacteria, and almost all antibiotics encounter this problem. Many drug classes that were previously mentioned directly target and inhibit enzymes that have essential functions in the life of the bacterial cell. To counter this inhibition, the targeted enzymes may acquire mutations that abolish or reduce the affinity for the inhibitory drug, sometimes even at a cost to their own fitness.¹⁰⁹ One of many examples is rifampicin resistance. Rifampicin, which is an important drug in the treatment of tuberculosis, targets β -subunit of bacterial RNA polymerase that is encoded by *rpoB*. Resistance-conferring mutations in *rpoB* may take the shape of point mutations, deletions, and insertions.^{74,123} Collectively, they occur with unusually high frequency, which may lead to rapid selection of resistant strains under therapy. Rifampicin should therefore never be used for monotherapy but in combination with one or more other antibiotics (see Section 1.3.6).

Mutations that render a target enzyme resistant to its cognate antibiotic can in principle arise spontaneously in any bacterial strain. Alternatively, a bacterium can also acquire resistance through the wholesale adoption of a foreign gene that encodes a homologous enzyme which is naturally resistant to the drug. This is the case with methicillin-resistant *Staphylococcus aureus* (MRSA), which have acquired a transpeptidase enzyme from other staphylococcal species.

Table 1.1 Mechanisms of bacterial resistance to antibiotics.

Antibiotic (Class)	Target	Resistance mechanism
Inhibitors of murein synthesis		
Fosfomicin (epoxide)	Enzyme MurA	Destruction by ring-opening epoxidases; mutational inactivation of the glycerophosphate transporter
Cycloserine	Alanine racemase and D-alanine ligase	Mutations in target enzymes
Moenomycin	Transglycosylase	Not fully understood
Bacitracin	Undecaprenol pyrophosphate (UPP)	overexpression of competing UPP phosphatase
Vancomycin (glycopeptide)	D-Ala-D-Ala on lipid II pentapeptide	Replacement of D-Ala-D-Ala with D-Ala-D-Lac
Penicillins, cephalosporins, carbapenems, monobactams	β -lactam antibiotics target transpeptidases that cross-link peptidoglycan chains in the bacterial cell wall	Most commonly through deactivation by β -lactamase; MRSA express enzyme with low antibiotic binding affinity; mutation of porins
Inhibitor of mycolic acid synthesis		
Isoniazid	Activated by KatG; adduct inhibits InhA	Expression of impaired KatG; mutations on InhA
Inhibitors of ribosomal protein synthesis		
Fusidic acid (steroid)	Peptide elongation factor G (EF-G)	Mutations in EF-G
Streptomycin (aminoglycoside)	Ribosomal A-site (protein S12, 16S rRNA)	Mutations on S12 and 16S RNA; modification by aminoglycoside acetyltransferases, phosphotransferases, and nucleotidyltransferases; efflux
Chlortetracycline (tetracycline)	16S rRNA	Efflux; expression of tetracycline binding proteins; oxidation by TetX
Puromycin	Antimetabolite of aminoacyl-tRNA	Modified by puromycin acetyltransferase
Mupirocin	Isoleucyl-tRNA synthetase	Expression of resistant enzyme

Antibiotic (Class)	Target	Resistance Mechanism
Oxazolidinones	23S rRNA	Mutations of 23S rRNA
Chloramphenicol	23S rRNA	Modified by chloramphenicol acetyltransferases; mutation of porins
Pleuromutilin	23S rRNA	Mutation of 23S rRNA
Erythromycin (macrolide)	23S rRNA	Methylation and mutation of 23S rRNA; modification by by macrolide esterases or phosphotransferases; efflux
Lincomycin (lincosamide)	23S rRNA	Methylation and mutation of 23S rRNA; lincosamide nucleotidyltransferases
Streptogramin	23S rRNA	Methylation and mutation of 23S rRNA; streptogramin acetyltransferases
Inhibitors of DNA and RNA synthesis		
Novobiocin (aminocoumarin)	DNA gyrase	Mutation of DNA gyrase; efflux
Nalidixic Acid (quinolone)	DNA gyrase	Efflux; mutation of porins; mutation of DNA gyrase
Rifampicin	RNA polymerase	Mutation of RNA polymerase; ADP-ribosylation of drug; efflux
Metronidazole (Nitroimidazole)	DNA strands	Reduced drug activation; efflux
Inhibitors of folate metabolism		
Sulfonamide	Dihydropteroate synthase (DHPS)	Mutation of DHPS
Trimethoprim	Dihydrofolate reductase (DHFR)	Mutation or overexpression of DHFR; certain pathogens don't have DHFR and use alternative cofactors for carbon transfer
Cell membrane disruption		
Polymyxin B	Lipid A core of lipopolysaccharide (LPS)	Modifications on LPS
Daptomycin (lipopeptide)	Phosphatidylglycerol in cytoplasmic membrane	Changes in membrane lipid composition

Target modification applies not only to protein enzymes but also to ribosomes, and more specifically to the ribosomal RNA. As mentioned above in Section 1.2.3, the MLS group antibiotics share a common binding region on the 23S rRNA of the 50S subunit. Resistance to these antibiotics can arise through the methylation or dimethylation of a specific adenine residue, equivalent to *E. coli* coordinate 2058 (A-2058), which causes a structural change to the 23S RNA that denies drug binding. This methylation is catalyzed by adenine-specific N-methyltransferases which are encoded by the *erm* (erythromycin ribosome methylation) class of genes. The *erm* genes are found in a wide range of bacterial species, including the antibiotic-producing *Streptomyces* species and many pathogens. Due to the similarity between their binding sites, cross-resistance among MLS group drugs is fairly common.^{112, 167, 215}

1.3.2 Target overexpression

In addition to modifying targets, some bacterial strains gain resistance to antibiotics by overexpressing the corresponding drug targets. In a favorable scenario of treating bacterial infections, the activity of the target is effectively inhibited to a level at which the bacteria can no longer survive. Even though the molar concentration of an antibiotic is normally far higher than that of its target, the antibiotic will only inhibit its target to a certain extent but not completely. Assuming a reversible interaction, the residual active fraction of the target will remain constant as long as the antibiotic concentration does, too. Therefore, when target expression increases, the absolute amount of uninhibited target will increase proportionally. Once the amount of uninhibited target reaches a sufficient level of activity, the bacterial strain will have achieved resistance to the drug.

The overexpression of target would appear to be a straightforward way for bacteria to develop resistance; however, this does not hold true for all drugs. An instructive example of divergent effects of target overexpression is provided by the comparison of sulfonamides and trimethoprim. As discussed in Section 1.2.5, both are inhibitors of folate metabolism, with dihydropteroate synthase (DHPS) and DHFR as the respective targets (Figure 1.8). Both drugs

are challenged by widespread resistance. With trimethoprim, target overexpression works as expected, and it is indeed one of the major resistance mechanisms encountered in resistant strains. In contrast, resistance to sulfonamides due to overexpression of DHPS has not been observed in any resistant isolates, and when induced experimentally in laboratory strains, no change in susceptibility towards sulfonamide occurs.¹⁵⁷ Nevertheless, a much earlier study showed that resistance is conferred by an increase of PABA, the regular substrate of DHPS, as would be expected with competitive inhibition.¹¹¹

The apparent contradiction in these findings can be resolved by considering the subtleties of the action mechanism of sulfonamides.¹⁵⁷ Sulfonamides compete against PABA for binding to DHPS, but they do not inhibit the catalytic activity of DHPS. Instead, they become substrates themselves and undergo coupling with pteridine diphosphate, and the depletion of this precursor is responsible for the inhibition of folate metabolism by sulfonamides. The overexpression of DHPS will not change the proportion of correct and aberrant product formed, and thus will not affect the level of bacterial susceptibility.

Another interesting example is DNA gyrase, the target for the two antibiotics coumermycin A1 and ciprofloxacin, which belong to the aminocoumarin and the quinolone class, respectively (Figure 1.7). When susceptible *E. coli* strains were modified to overexpress DNA gyrase, they became resistant to coumermycin A1 but more susceptible to ciprofloxacin. These opposite effects are due to the two drugs' different mechanisms of action. Coumermycin A1 competes against ATP for binding, which inhibits DNA gyrase; this inhibition can be compensated by overexpression. On the other hand, ciprofloxacin inhibits gyrase only partially; it still permits the DNA cleavage by gyrase but prevents DNA re-ligation. The drug-bound gyrase will therefore induce an accumulation of DNA double-strand breaks. Therefore, ciprofloxacin changes the enzyme's activity from useful to toxic, and overexpression of gyrase would only make the host bacteria more susceptible to the drug.

These findings show that the effect on drug susceptibility conferred by target overexpression is dictated by the specific mechanism involved in the drug-target interaction. If the drug

strictly inhibits the target activity, overexpression of the target will result in drug resistance; in contrast, if the drug alters the target's activity, overexpression may not induce resistance, and may even enhance the drug's toxicity. In some cases, target overexpression may exert a heavy fitness cost to the bacterium. An example are the penicillin-binding proteins (PBPs) 1A, 1B, and 2. The overexpression of these proteins can significantly reduce the growth rates of their host *E. coli* strain,¹⁵⁷ and in case of PBP2 can even result in cell lysis.¹¹⁴

1.3.3 Drug inactivation

Instead of taking a passive approach to adapt, bacteria may also develop resistance by directly modifying and thereby inactivating drug molecules. The most common types of modifications are hydrolysis and group transfer, which are carried out by a variety of enzymes.²¹⁸

Many antibiotics have ester and amide bonds that are essential to their activity. But these bonds are also very susceptible to hydrolysis. The widespread resistance to β -lactam antibiotics due to β -lactamases is the best known and most important example. There are two major types of β -lactamases, namely, the serine enzymes and the metallo-enzymes. Inhibitors that can be used to protect the antibiotics are only available for the former, not the latter (Figure 1.10).

As briefly mentioned earlier, the β -lactam antibiotics exert their activity by forming stable covalent derivatives with the target enzyme transpeptidase, which opens the β -lactam ring and inactivates both the antibiotic and its target enzyme completely. Ring opening and formation of a covalent bond between drug and enzyme are mediated by a serine residue in the active site (Figure 1.10, middle). Serine β -lactamases can open the β -lactam ring and form a covalent bond in the same way via a catalytic serine residue (Figure 1.10, left), which inactivates the drug. The covalent intermediate is then readily hydrolyzed, which releases and reactivates the β -lactamase molecule.

Clavulanic acid by itself is a very weak β -lactam antibiotic; however, its unique interaction with serine β -lactamase makes it clinically useful (Figure 1.10, right). This interaction involves

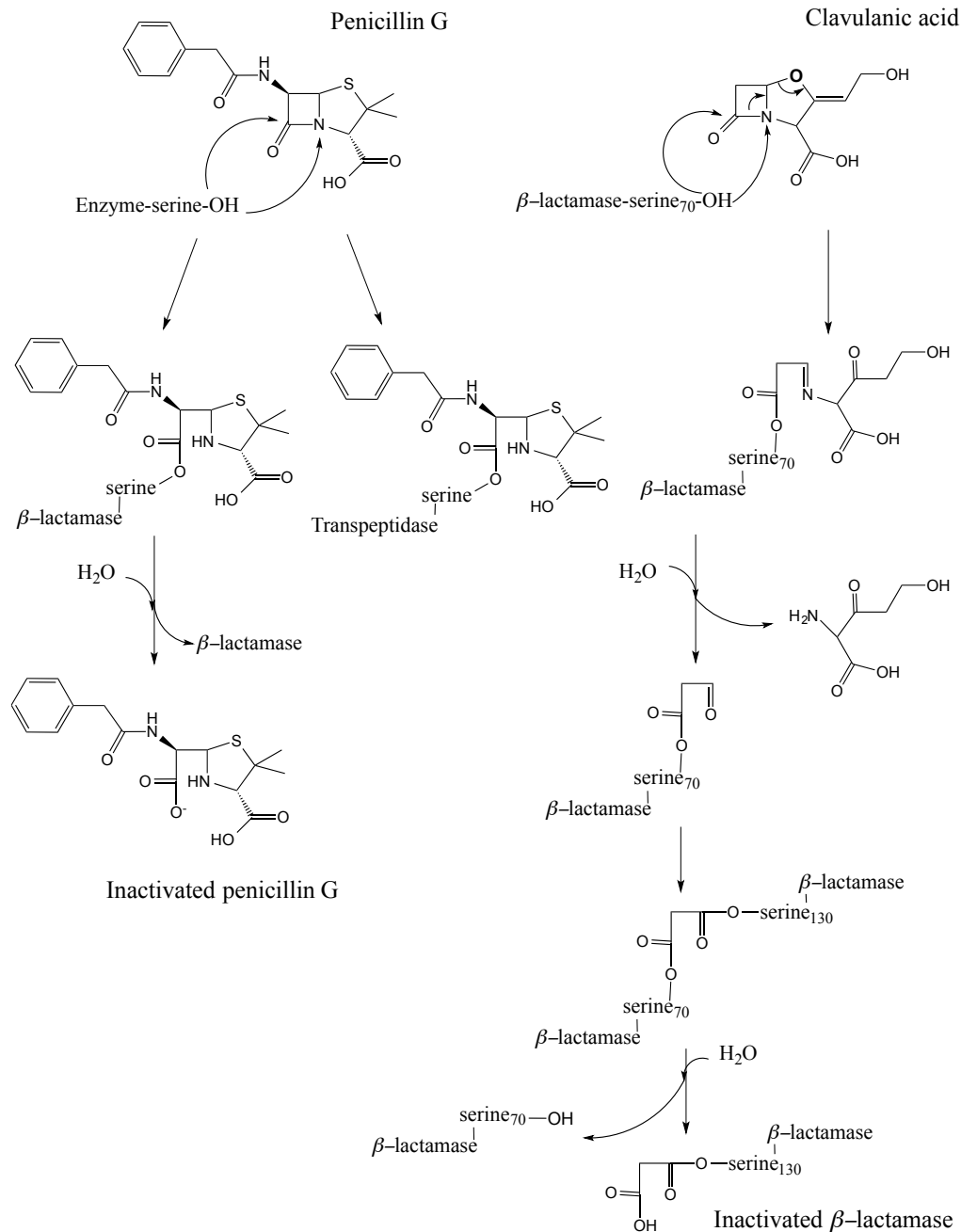


Figure 1.10 Action mechanisms of serine β -lactamases and of clavulanic acid. In the absence of β -lactamase, the catalytic serine residue of transpeptidase attacks the β -lactam ring of penicillin to form a stable and inactive derivative (middle). The same reaction is also carried out by β -lactamase (left); however, this enzyme releases itself through hydrolysis, which yields an inactivated penicillin. Clavulanic acid (right) can react with β -lactamase as well, but it engages two serine residues in the active site. The bond formed via the second serine residue is stable and hence inactivates the enzyme.

two serine residues in the active site. The covalent bond formed with the first serine residue is still easily hydrolyzed, but before this happens, the reactive intermediate forms a stable bond with the second serine residue, which leaves it attached to the β -lactamase molecule even after the first bond is cleaved. This unique feature makes clavulanic acid an effective serine β -lactamase inhibitor. Hence, it is successfully used in combination with β -lactam antibiotics like amoxicillin to overcome resistance.¹⁶⁰

The hydrolysis catalyzed by a metallo- β -lactamase (MBL) is achieved by activation of water via a Zn^{++} active center, which does not involve a serine residue and makes it immune to inhibitors like clavulanic acid. There has not been much success in finding inhibitor for MBLs until very recent. In the study done by Wright and colleges,¹⁰⁰ it was shown that a fungal natural product, aspergillomarasmine A (AMA), can function as a rapid and potent inhibitor to certain clinically important MBLs, such as NDM-1 and VIM-2. When AMA was used in combination with meropenem, a carbapenem antibiotic, the activity of meropenem was efficiently restored against bacteria strains possessing either NDM or VIM-type alleles.

Most of the enzymes that inactivate antibacterials are group transferases. These enzymes covalently link drugs with groups such as acyl, phosphoryl, thiol, and glycosyl moieties. The addition of functional group will cause structural changes and impair target binding. Example group transferases are chloramphenicol acetyltransferases and aminoglycoside kinases.

The activity of prodrugs like metronidazole and isoniazid, which were mentioned earlier, relies on activation by bacterial enzymes. Resistance may occur when bacterial strains down-regulate the expression of those enzymes, so that most of the drug molecules remain in their inactive prodrug forms.^{56,204,209,225}

1.3.4 Efflux and reduction of uptake

Another strategy for bacteria to lower the intracellular drug concentration is by reducing uptake and/or inducing efflux of drugs.¹⁰⁴ To get across a Gram-negative bacterial cell, a drug molecule needs to traverse the outer membrane, either by diffusion across the lipid bilayer or

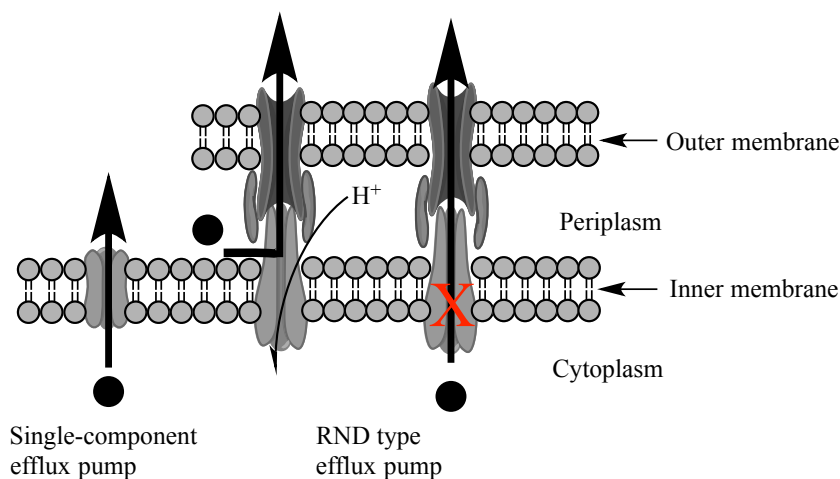


Figure 1.11 Schematic representation of efflux pumps that confer bacteria drug resistance. Single-component pumps span only one membrane, across which the target molecules are transported from the bacterial cytoplasm to the outside for Gram-positive bacteria, or to the periplasmic space for Gram-negative ones. RND type pumps span both membranes (inner and outer) and the periplasmic space. They capture the target molecules from the periplasmic space (not the cytoplasm) and extrude them to the outside.

through porin channels. The outer leaflet of the outer membrane is composed of lipopolysaccharide (LPS), which is impermeable to many compounds. Therefore, many drugs, such as β -lactams, chloramphenicol, and fluoroquinolones, have to go through porin channels. Certain bacteria have gained resistance by reducing porin expression or altering the size and selectivity of porin.^{34,47,80,206}

For the drugs that have successfully crossed the cell wall, bacteria may use efflux pumps to send them back out again. In susceptible bacterial strains, there is either no or very weak drug efflux. To develop resistance, bacteria start to enhance the efflux by overexpressing efflux pumps or acquiring more efficient pumps through gene transfer. Some of these pumps are simple single-component transporters, while others are multi-component systems, such as the resistance-nodulation-cell division (RND) transporters found in Gram-negative bacteria (Figure 1.11). Some of these transporters have low substrate selectivity, which enable them to efflux multiple distinct types of drugs and make their host bacteria multidrug-resistant. This

multidrug resistance mechanism is not only a great challenge to the current antibacterials, but also a burden for future drug development.^{104,160}

The single-component pumps span a single cell membrane. Gram-positive bacterial cells have a relatively simple envelope structure, with only a cytoplasmic membrane; therefore, single-component efflux transporters are sufficient to pump the target molecules back to the outside in this case. In contrast, Gram-negative bacterial cells have an inner and an outer membrane. Even though they also have simple single-component pumps, by which resistance to certain drugs is conferred, the most prominent ones are the multi-component RND transporters.

These tripartite RND transporters cross both the inner and the outer membrane and can efflux a wide range of antibiotics (Figure 1.11). So, are they just like the single-component pumps but with longer wingspans that can pick up the targets from the cytoplasm and send them right across two membranes to the outside? Not really, as a number of studies have shown that they have a much more intriguing and intricate mechanism, and they are capable of promoting a very strong drug resistance.

In a study done by Lomovskaya and colleagues,¹¹³ several combinations of efflux pumps (with overlapping drug specificity) were expressed in the same bacteria strains, and then the magnitude of resistance conferred by them was evaluated. Two different patterns of resistance enhancement were observed. When two pumps of the same type were combined, either single-component or RND, the resulting degree of resistance was additive. In contrast, when the combination consisted of one single-component and one RND pump, a multiplicative enhancement of drug resistance was conferred.

The authors explained the observations by a model based on the concentration gradients generated by efflux pumps. When two types of pumps were involved, two concentration gradients (crossing both inner and outer membrane) would be created, whereas the single type pumps could only create one of the gradients. However, they did not address the location where the drug molecules would be captured by the RND pumps.

In a later theoretical study by Palmer,¹⁵⁹ it was shown that, in order to achieve the observed multiplicative enhancement of drug resistance, RND pumps must be capable of capturing the drug molecules from the periplasmic space. Many functional^{62, 122, 203} and structural^{57, 118, 146} studies also supported this model.

The best-studied RND pumps are AcrAB-TolC from *E. coli*, and MexAB-OprM from *Pseudomonas aeruginosa*. These RND pumps comprise an inner membrane spanning pump (AcrB, MexB), an outer membrane pore (TolC, OprM), and a periplasmic protein (ArcA, MexA) that aligns and surrounds the first two. Some very thorough studies done on AcrAB-TolC have revealed a very detailed working mechanism of this type of pump.^{145, 175} AcrB exists as a trimer and extracts drug molecules from the periplasmic space only. The trimer-drug complex, driven by the proton-motive force across the inner membrane, rotates around the axis that goes through the center of the TolC pore. During the rotation, the three subunits are cycling through three different conformations, which correspond to three functional steps. The first step grants the substrate access to the binding pocket from the periplasm. The second step expands the binding pocket to accommodate the substrate. In the final step, the entry pathway is closed off, and the substrate is extruded through the TolC pore to the outside.

1.3.5 Origin and spread of resistance

Some of the resistant strains are the result of spontaneous mutations. Due to the large population and short reproductive cycles of bacteria, mutations that will enable a given strain to endure higher levels of some specific antibiotic tend to arise frequently, and such mutants are observed readily in the presence of the drug. Using serial passage with stepwise increases of the drug concentration, highly resistant strains can often be readily selected in vitro.

While this mechanism is straightforward and indeed accounts for the development of resistance toward single antibiotics under therapy, the limitations of its explanatory power were noticed early on. In the 1950s, streptomycin, tetracycline, and chloramphenicol were introduced and widely used as alternatives for sulfonamides in the treatment of *Shigella* dysentery.

While resistance was observed initially only to individual agents, several years later clinical isolates were obtained that had acquired resistance to all four drugs simultaneously, often including ones that had not been used on the patient in question.¹⁸⁹

It was conceptually very difficult to explain the observation by mutation and selection. Mutations that mediate resistance to a single drug arise with a frequency of about 10^{-7} to 10^{-10} per bacterium and generation; therefore, the probability of achieving resistance to four distinct antibiotics simultaneously is exceedingly low. It was then also observed that the multidrug resistance trait could readily be transferred between bacterial cells. The phenomenon of transferable resistance gave rise to extensive studies and fascinating discoveries, many of which have greatly advanced the development of molecular biology.

As we know today, a large number of bacteria acquire their resistance from others through horizontal gene transfer. This transfer can bridge species barriers and involve both pathogenic and non-pathogenic strains. In many cases, the resistance genes being transferred can be traced back either to the antibiotic producing organisms, which need them to avoid committing suicide while producing antibiotics, or to non-producing strains, which rely on them to survive in the vicinity of the former. Most antibiotics are produced by soil microorganisms. The most abundant class of soil bacteria are actinomycetes; therefore, it is not a surprise that many actinomycetes are naturally resistant to multiple antibiotics.⁴⁵

The horizontal propagation of antibiotic resistance genes is mediated by three key genetic vehicles: conjugative plasmids, transposons, and integrons.¹⁵⁵

Plasmids are extra-chromosomal, independently replicating, double-stranded circular DNA molecules. They are the major vehicle for the exchange of genetic material between bacterial cells. A particularly efficient form of plasmid transfer is known as conjugation (Figure 1.12). The plasmids involved in this process are conjugative plasmids, similar to the prototypical F-plasmid ("F" stands for fertility). The F-plasmid enables its host cell (donor cell) to produce pili and initiate conjugation. During the conjugation, one strand of the F-plasmid is released and transferred to recipient cell. Inside the latter, the complementary strand is synthesized,

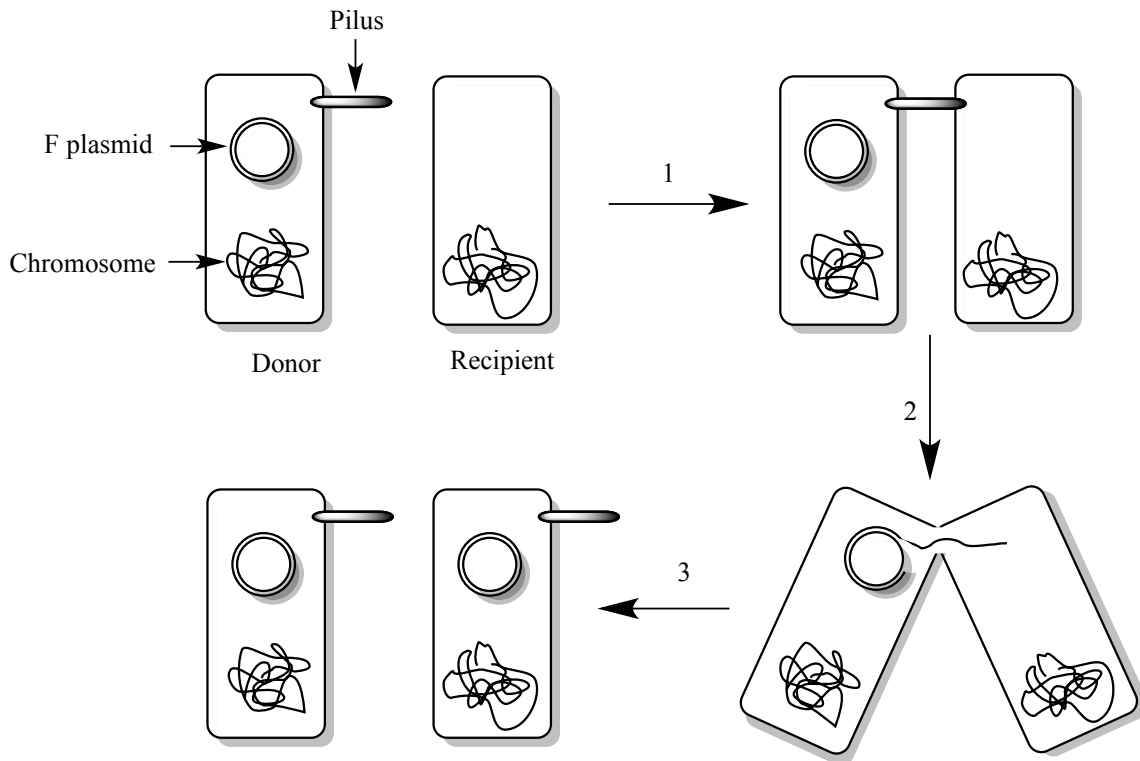


Figure 1.12 Schematic representation of gene transfer by bacterial conjugation. The donor cell contains an F-plasmid, which can initiate conjugation by expressing a pilus. The donor pilus reaches to the recipient cell and creates a bridge between both cells (1). The pilus then retracts and brings the two cells into close contact to form a channel, through which one strand of the F-plasmid is transferred to the recipient cell (2). Finally, the single-stranded plasmids in both donor and recipient cells are replicated to form complete double-stranded plasmids, and the conjugation completes (3).

which provides the recipient cell with an identical copy of the double-stranded F-plasmid. If antibiotic resistance genes are carried by these conjugative plasmids, which are then referred to as R-plasmids or R-factors, these resistance traits can be easily spread among bacterial species.

Transposons are also mobile DNA molecules. They differ from plasmids by being smaller, linear, and incapable of traveling between cells just by themselves. However, transposons are very active travelers within the cell; they can jump from plasmid to plasmid, from plasmid to chromosome, and from chromosome to plasmid. Therefore, in order to cross the cell membrane barriers, transposons need to jump aboard conjugative plasmids.

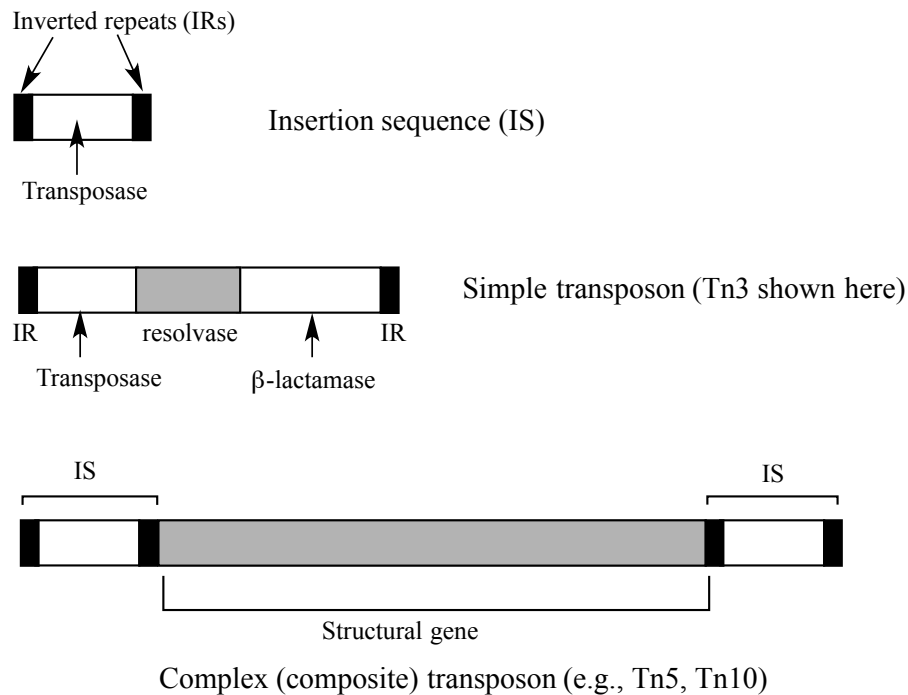


Figure 1.13 Schematic representation of transposons. Insertion sequence (IS) is the basic transposable element (top). A resistance gene can be incorporated into either a simple transposon (middle) or a complex transposon (bottom).

The basic transposable elements found on transposons are also referred to as insertion sequences (ISs). Each insertion sequence has a transposase gene plus a pair of inverted repeats (IRs) flanking it (Figure 1.13). When extra structural genes (such as antibiotic resistance genes) are associated with the ISs and become movable, the whole construct is called a transposon, which is denoted by “Tn” and a number.

In a direct transposition, or so-called “cut and paste” transposition, the transposase recognizes the terminal IR sequences and cuts at each end to excise the whole transposon from the donor DNA. The transposase also introduces a staggered cut into the recipient DNA, into which the cut-out transposon is then inserted.

In a simple transposon, only one IS element is involved. Using Tn3 as an example here (Figure 1.13, middle), the extra genes (coding for resolvase and β -lactamase) and transposase gene are located between one pair of IRs.^{76,83} Different from direct transposition, Tn3 uses

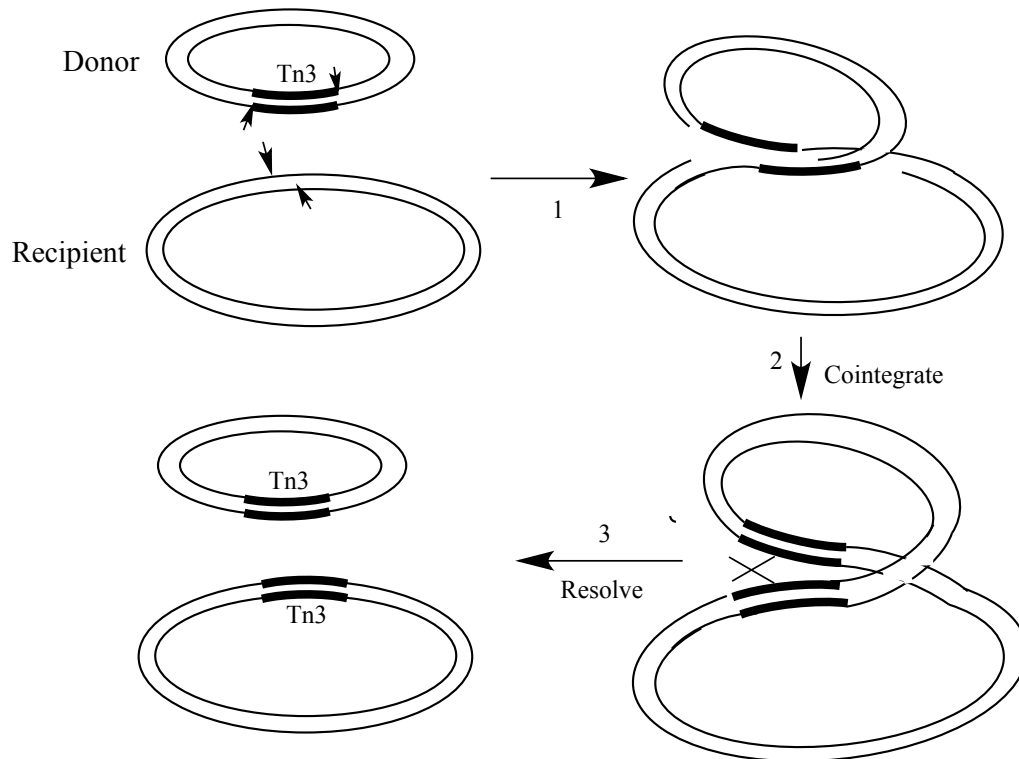


Figure 1.14 Schematic representation of Tn3 replicative transposition. Both the donor and the recipient DNA are first nicked by transposase. The donor and recipient DNA molecules are then linked covalently at their openings (1). The ensuing single-stranded gaps are filled by replication, which produces a DNA molecule with two copies of the transposon, also called a cointegrate(2). The cointegrate is resolved by resolvase through site-specific recombination between the two transposon copies, which restores the original donor DNA and also creates a transposon-carrying recipient DNA (3). The cutting sites are indicated by arrows.

a replicative transposition mechanism, which includes a replication of the transposon, so that a copy of it is left at its original site. In the model proposed by Shapiro (Figure 1.14),¹⁷⁹ the transposase first cuts the donor DNA to expose the 3'-OH groups at the ends of transposon Tn3 and also makes a staggered cut in the recipient DNA. Then the donor and recipient DNA molecules become covalently linked, with the gaps being filled by DNA replication. The result is a DNA molecule that has two copies of the transposon, which is called a cointegrate. The transposon-encoded resolvase finally resolves the cointegrate through site-specific recombination within the transposon, which release the donor DNA in its original form and the recipient

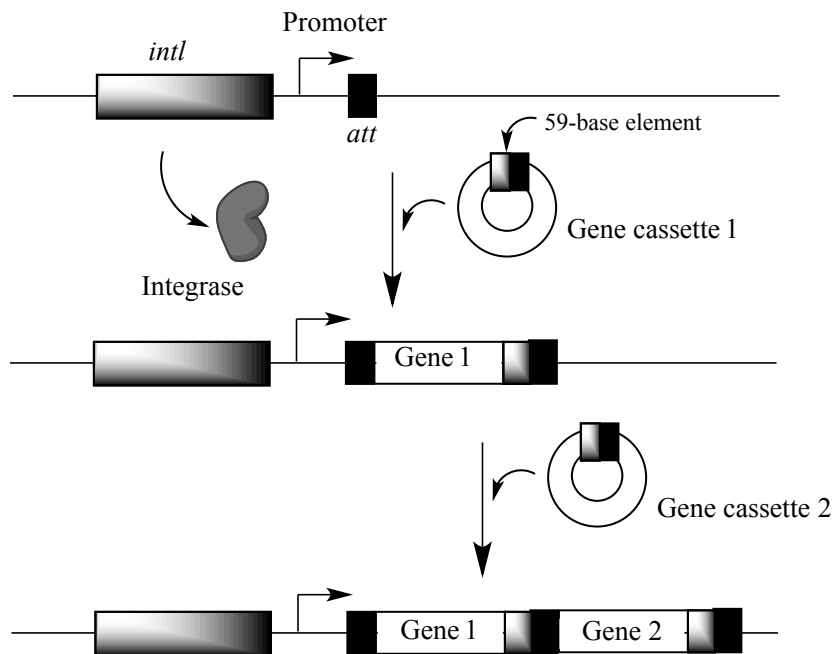


Figure 1.15 Schematic representation of an integron. Integrons consist of an attachment site (*att*), a gene (*intl*) encoding the integrase, and a promoter that drives the expression of incorporated genes. The incorporated genes are obtained from gene cassettes. The site-specific recombination events rely on the recognition of 59-base elements.¹⁵⁵

DNA with a new copy of the transposon.

In a complex (composite) transposon, the structural genes are flanked by two copies of an IS (Figure 1.13 bottom). Examples are transposons Tn5 and Tn10,¹⁵⁵ which contain genes that confer resistance to streptomycin and to tetracycline, respectively.

Integrons are gene expression platforms that incorporate promoter-less genes and convert them into functional genes. An integron consists of three elements (Figure 1.15): (1) an attachment site where the acquired sequence is integrated; (2) a gene encoding integrase, a site-specific recombinase; and (3) a promoter that drives the expression of the incorporated sequences. Integrons incorporate genes from gene cassettes, which are small circular DNA molecules that often carry antibiotic resistance genes. These gene cassettes also contain a recombination site known as a 59-base element even though it might not be exactly 59 bases long. The integrase can recognize different 59-base elements, allowing the incorporation of

multiple resistance genes within a single integron.

In contrast to plasmids and transposons, integrons are not mobile all by themselves. In order to unleash their potential in spreading resistance, integrons need to be incorporated into either a plasmid or a transposon first, and in most cases, integrons are found within transposons. An example of multi-drug resistance spreading via integrons is the *Shigella* dysentery case mentioned at the beginning of this section (1.3.5).^{127, 155}

1.3.6 Antibacterial combination therapy

Combinations of two or more antibiotics are widely used in the treatment of bacterial infections. In some cases, this approach is used because of practical limitations. For example, in severely ill patients, it is necessary to begin treatment immediately, before the pathogen can be identified and its drug susceptibility profile can be determined. At this initial stage, antibiotics will have to be selected empirically in order to cover an appropriately broad spectrum of pathogens and resistance patterns. This situation is typical of complicated infections such as sepsis and meningitis.^{24, 161}

In many cases, combination therapy is still preferred after the complete information on the pathogen is available. Carefully selected combinations can produce synergistic effects, which means that the antibacterial activity is greater than the sum of the effects of the individual agents. Such synergistic action may result in greater or more rapid therapeutic success. Examples include the treatment of *Staphylococcus aureus* and *Enterococcus* infections with aminoglycosides and β -lactams (vancomycin). Combination therapy may also overcome resistance to some important antibiotics from resistance; see for example the combination of penicillin and clavulanic acid mentioned earlier (Section 1.3.3).

Another reason for combination therapy is the serious resistance issue. The most well-known example is the treatment for tuberculosis. Tuberculosis is caused by *Mycobacterium tuberculosis*, which has very unique cell wall structure and growth properties.⁷⁵ These features allow the bacteria to survive under therapy for several months, and the treatment accordingly

takes a long time. If monotherapy was used, the risk of mutations that induce resistance would be unacceptably high. A more recent study also found that within a clonal population of mycobacteria, the cells showed unusually asymmetric division and growth, which generated many distinct sub-populations of cells. These physiologically distinct cells also showed different susceptibility profiles to the important drugs.⁴ Combination therapy with three or four drugs greatly reduces the risk of emergent resistance. The standard combination used today includes the four drugs rifampicin, isoniazid, pyrazinamide, and ethambutol.

1.4 DAPTOMYCIN

Daptomycin (Cubicin[®]), the subject of this thesis, is the first lipopeptide antibiotic approved for clinical use. Since its approval in 2003, daptomycin has become one of the most effective and widely used antibiotics for treating serious infections caused by Gram-positive bacteria, including methicillin-resistant *Staphylococcus aureus* (MRSA) and vancomycin-resistant *Enterococcus* (VRE) strains.^{9,32,199}

Daptomycin is produced by *Streptomyces roseosporus*, a soil actinomycete first isolated by researchers from Eli Lilly and Company in the early 1980s.^{49,60,61} Under normal conditions, daptomycin is produced along with other structurally similar lipopeptides that all share an identical core cyclic peptide structure but bear different lipid tails. Collectively, they are called the A21978C lipopeptides.¹⁴

The A21978C core cyclic peptide comprises 13 amino acids (Figure 1.16), including a number of non-proteinogenic and D-amino acids, namely, ornithine, kynurenine, 3-methylglutamic acid, D-alanine, D-serine, and D-asparagine. The amino acid residues Asp-7 and Asp-9 were shown to be essential for antibacterial activity.⁷⁷ Ten of the amino acids cyclize to form a ring closed by an ester bond between the side chain hydroxyl group of Thr-4 and the C-terminal kynurenine (Kyn-13). The fatty acyl tail is attached to the N-terminal Trp-1 on the exocyclic peptide, which comprises the residual three amino acids. Unlike the structurally related antibi-

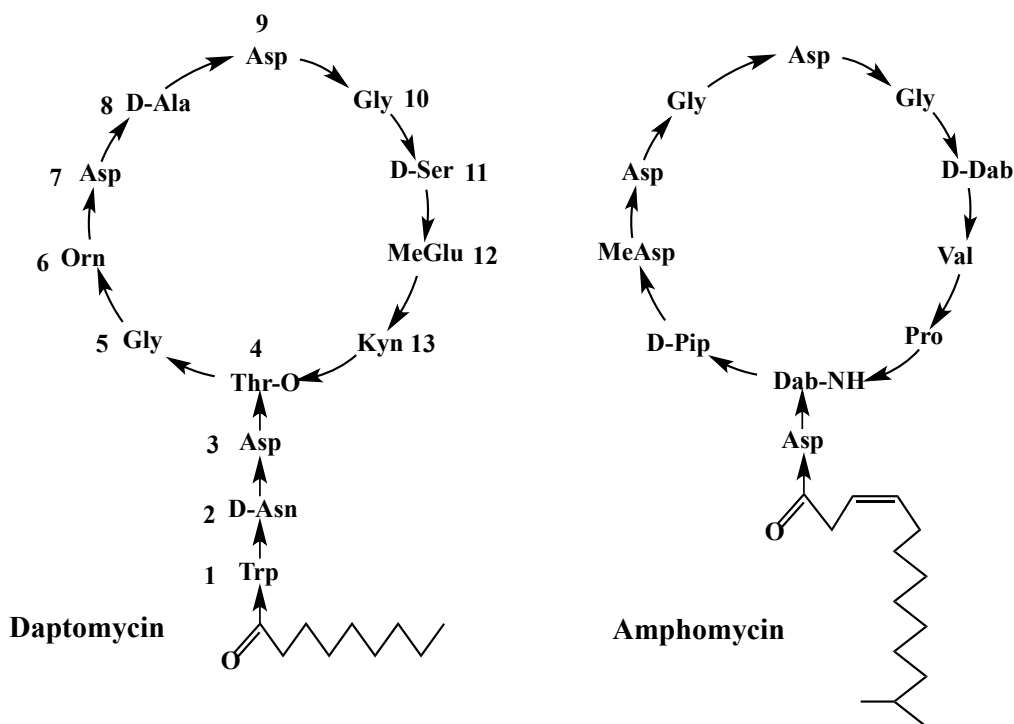


Figure 1.16 Structures of daptomycin and amphomycin. Non-standard amino acids are ornithine (Orn), kynurenine (Kyn), 3-methylglutamic acid (MeGlu), pipecolic acid (Pip), diaminobutyric acid (Dab), and β -methylaspartic acid (MeAsp).

otic amphomycin, the peptide ring is closed by an ester bond instead of an amide bond; the members of the A21978C group are therefore classified as cyclic depsipeptides.

While the clinical resistance to daptomycin is still very rare, sporadic case reports have still drawn a lot of attention, since daptomycin has become a drug of choice for many life-threatening infections. These observations have stimulated interest in developing novel daptomycin derivatives with improved activity and a broader action spectrum. Such development efforts would greatly benefit from an improved understanding of daptomycin's mode of action.

In the rest of this section, I will first give a brief review on how daptomycin was developed, and also on the previous progress in determining the action mode of daptomycin. At the end of this section, I will talk about the progress in daptomycin resistance research.

1.4.1 Preclinical development

The screening process is critical during drug development. It selects the candidates from a compound library for further evaluation. A large library can not only increase the chances of finding the candidates, but also provide a lot of information on possible further improvements. Here, I will focus on the major approaches that have been used for the construction of compound libraries for daptomycin analogues.

1.4.1.1 Semi-synthetic modification. It was observed early on that small changes to the acyl tail could give significantly different toxicity profiles within the A21978C group. Accordingly, screening a library of A21978C analogues having different lipid tails would be a logical approach to find new drugs.⁴⁸ However, purification of individual A21978C analogues from the fermentation mixture produced by *S. roseosporus* proved too laborious. Instead, a semi-synthetic method was developed to generate such a library.

The basic idea is to obtain the A21978C peptide core through deacylation of the whole naturally produced compound mixture. The peptide core can then be reacylated with different natural or synthetic acyl tails. The deacylation is catalyzed by a deacylase enzyme produced by *Actinoplanes utahensis* NRRL12052.²² However, if we go to the deacylation step directly, the A21978C core will have two free amino groups (Trp-1 and Orn-6) available for subsequent acylation. To circumvent this complication, the Orn group was protected by mono-*tert*-butyloxycarbonyl (*t*BOC) prior to deacylation. The monoacyl tails were reacted with the N-terminal of Trp-1 as activated fatty acyl esters. The *t*BOC group was then removed by trifluoroacetic acid (TFA). By screening the library generated by this method, the derivative with an *n*-decanoyl tail showed the best balance of antibacterial efficacy and low toxicity in animals, and it was chosen for further clinical development and became the drug known as daptomycin today.

While this semi-synthetic modification approach is good for making daptomycin analogues on an experimental scale, it is not ideal for producing the quantities required for clinical application. This difficulty was overcome through the addition of decanoic acid to the fermentation

broth. This yields daptomycin as the major product, which can then be obtained in homogeneous form through further purification.⁹⁰

In addition to the acyl tail modification, many other semi-synthetic modifications were also performed to expand the analogue library. These modifications include substitutions of the exocyclic amino acid residues¹³² and derivatizations of the Orn-6 side chain.⁸⁴

1.4.1.2 Combinatorial biosynthesis. The analogues produced by semi-synthesis can only represent limited structural diversity due to the lack of changes in the cyclic amino acid core. To overcome this limitation, an approach of combinatorial biosynthesis was used, which is based on the knowledge about the biosynthetic mechanism of A21978C (daptomycin), as well as of the related lipopeptide antibiotics A54145 and calcium-dependent antibiotic (CDA).

Daptomycin is synthesized by a non-ribosomal machinery within *S. roseosporus*, which relies on multiple enzymes at different stages (Figure 1.17).^{141,166} The assembly of the peptide core is carried out by three non-ribosomal peptide synthetases (NRPSs), DptA, DptBC, and DptD.^{13,14,132} Each of these synthetases comprises multiple modules (Figure 1.17C). All modules have a basic C-A-T domain structure, where domain C is for condensation, domain A is for activation (or adenylation), and domain T is for thiolation. The ATP-dependent activation occurs first. The activated L amino acid then forms a thioester with the T domain. The C domain finally reacts the aminoacyl residue with the C-terminus of the peptide located on the preceding T domain. In the process, the elongated peptide is transferred to the current T domain.

Three of the modules have an additional E domain, which is an epimerase that catalyzes the conversion of an L-amino acid to its corresponding D-isomer. Therefore, the amino acids are always acquired from solution as their L forms and are converted to the D forms after activation. This concerns residues D-Asn-2, D-Ala-8, and D-Ser-11. The synthesis of MeGlu-12 is assisted by DptI, an α -ketoglutarate methyltransferase.¹²⁰ The terminal module in DptD contains a thioesterase (Te) domain, which catalyzes the formation of an ester bond between Kyn-13 and Thr-4 to cyclize and release the completed lipopeptide.

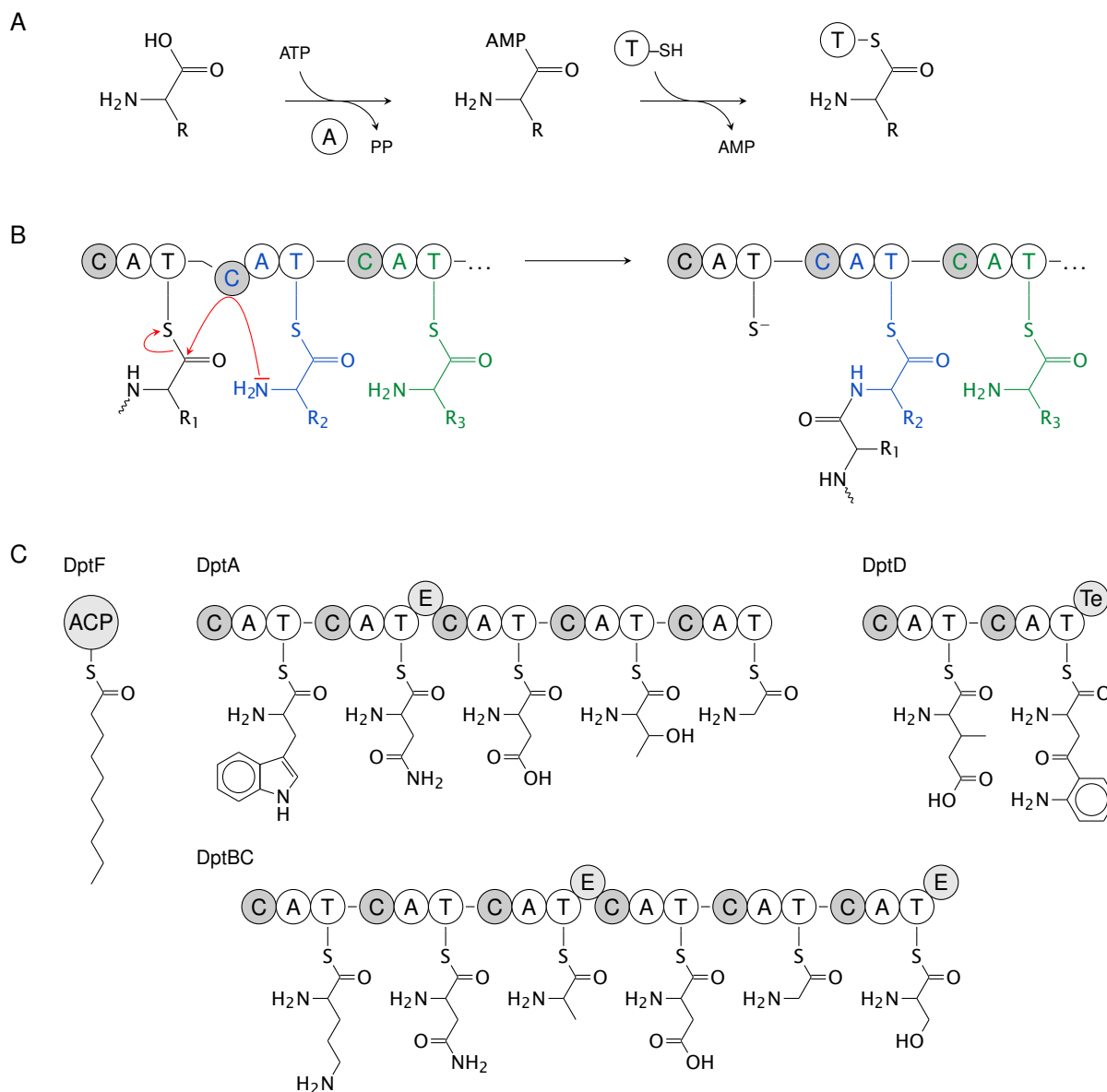


Figure 1.17 Biosynthesis of daptomycin by the Dpt non-ribosomal machinery. The incorporation of each amino acid is facilitated by a specific module that contains a C-A-T domain structure and an optional E domain, which mediate condensation, activation, thiolation, and epimerization, respectively. A: ATP-dependent activation and thiolation by the A and T domain of the cognate module. B: The C domain attaches its cognate amino acid to C-terminus of the peptide that is linked to preceding T domain. C: The synthesis of the peptide core is carried out in sequence by three large enzymes (DptA, DptBC, and DptD). Each of these enzymes contains multiple amino acid-conferring modules. The DptF module supplies activated acyl tails to DptA. The thioesterase domain (Te) at the end of DapD cyclizes and releases the lipopeptide. This figure is adopted from Dr. Muraih's thesis.¹⁴¹

DptE, an acyl-CoA ligase, and DptF, an acyl carrier, are required to initiate the condensation, respectively activating and delivering the fatty acid moiety (decanoic acid for daptomycin) to the N-terminus of Trp-1.²¹⁷ After the fatty acid has been attached, the condensation begins by release of Trp-1 and simultaneous elongation at its C-terminus with the following amino acid (Figure 1.17B). Then the peptide continues to grow in the same fashion. The overall condensation proceeds in the sequence of DptA, DptBC, and DptD.

Like A21978, both A54145 and calcium-dependent antibiotic (CDA) are lipodepsipeptides. A54145 is produced by *Streptomyces fradiae*²³ and CDA by *Streptomyces coelicolor* A(3)2.¹⁰⁶ They share many structural similarities with A21978C antibiotics: they all contain 10-membered cyclic peptides; the fatty acyl tails are attached to the N-terminal of their exocyclic residues (both of A21978C and A54145 have three exocyclic residues, while CDA has only one), and they all have a putative calcium-binding DXDG motif at the same position. They are also naturally produced by similar non-ribosomal systems as shown in Figure 1.18. The A54145 synthetase system comprises four NRPS subunits (LptA, LptB, LptC, and LptD), while CDA had three NRPS subunits (CdaPS1, CdaPS2, and CdaPS3). All of these NRPS subunits are constructed in the same module-domain architecture. Therefore, through the use of recombinant DNA techniques, novel synthetases can be assembled that combine different portions of the three natural systems. In the construction of such recombinant synthetases, three different approaches are plausible: (1) whole subunit substitution; (2) substitution of a module or domain within a specific subunit; and (3) disruption of genes involved in amino acid modification.

The NRPS subunits are encoded by overlapping genes in gene clusters, such as daptomycin's *dpt* gene cluster (Figure 1.18). It has been shown that sequential translation of these genes from one transcript is not essential for robust daptomycin production. When one or more of the *dptA*, *dptBC*, or *dptD* genes were deleted from the gene cluster, daptomycin production could be restored by introduction of the expression plasmids containing the missing genes. To facilitate genetic manipulation and combinatorial biosynthesis, three *dpt* genes were engineered

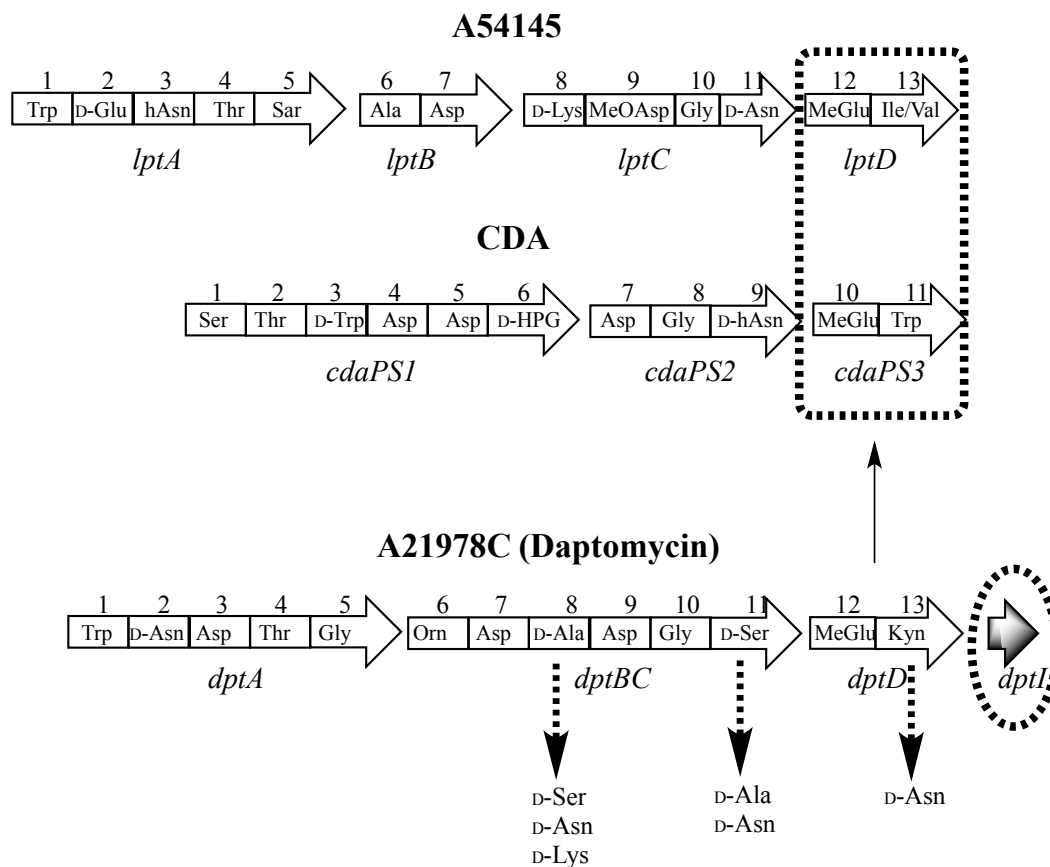


Figure 1.18 Combinatorial biosynthesis of daptomycin analogues. The four major combinatorial factors are: whole NRPS subunit substitutions (dashed box), modual or domain substitutions (dashed arrows), disruption of *dptI* gene (dashed oval), and lipid tail variations.

to express from different chromosomal loci under the control of separate promoters (*ermEp** promoters were used for *dptA* and *dptD* genes). Whole subunit exchange was achieved by deleting the *dptD* gene and replacing it with either the *cdaPS3* or the *lptD* genes from the CDA and A45145 synthesis pathways, respectively (dashed box in Figure 1.18). This yielded daptomycin analogues with Kyn-13 substituted by Trp-13 or with ILe/Val-13. The ambiguity in the latter case is due to the flexibility in substrate recognition for LptD.^{13,38,131}

With the help of module or domain substitutions, the amino acids incorporated by DapBC can be manipulated as well. The substituted module and domain sequences could be derived from either homologous or heterologous genes. During this process, the target sequence is

spliced out and the new sequence is introduced by fusing between the splicing sites. The homologous substitution was exemplified by the changes made on D-Ala-8 and D-Ser-11 within DapBC, which could be achieved by swapping the whole modules 8 and 11 or only their respective C-A-T domains. These exchanges produced variants with either or both of D-Ala-11 and D-Ser-8¹⁵³ (dashed line arrows in Figure 1.18). To replace D-Ala-8, D-Ser-11, and Kyn-13 with D-Asn, the sequence from homologous module-11 in A54145 *lptC* gene was introduced. Multiple modules can be exchanged concurrently as well. An analogue containing both D-Lys-8 and D-Asn-11 was produced when modules 8-11 from *dptBC* were replaced with modules 8-11 from *lptC*. In this analogue, the methoxylation on Asp-9 was found to be missing, which may have been caused by the lack of a tailoring enzyme gene.^{51,153}

The third variation is the deletion of the *dptI* gene, located downstream of the major NRPS genes, which leads to the production of analogues containing Glu-12 instead of MeGlu-12.¹⁵²

The number of peptide analogues obtained by recombinant techniques is then multiplied by the natural or precursed variations of lipid tails. In order to facilitate the final purification process, specific acyl tail precursors (such as *n*-decanoic acid for daptomycin) are fed to the fermentation process.

1.4.1.3 Chemoenzymatic synthesis. A major difficulty in the total synthesis of daptomycin is the formation of the ring-closing ester bond. One elegant strategy to overcome this obstacle consists in chemoenzymatic synthesis. This approach starts with solid-phase peptide synthesis, which replaces the natural peptide assembling by NRPSs. This yields a linear peptide, which is then cyclized using the natural thioesterase (Te domain). It has been shown that excised Te domains are capable of cyclizing a broad range of substrate peptides.¹⁰¹ During the process of synthesizing daptomycin analogues, the Te domain from CDA was used.⁷⁷ Daptomycin generated by this method has the same activity as the native compound.¹⁶⁶ Although chemoenzymatic synthesis provides more options for substituting amino acids and provides sufficient material for experimental study, it does not scale to the amounts required for clinical use.

1.4.1.4 Total chemical synthesis. One may wonder why more use has not been made of total chemical synthesis, which should be able to provide even more analogues. This is because all reported attempts have found this to be very difficult. The formation of the crucial ester linkage in daptomycin is especially challenging. Lam and colleagues synthesized daptomycin by using a combination of solution- and solid-phase chemistry.¹⁰⁸ To solve the ester link challenge, they first synthesized a branched tetradepsipeptide (consisting of Asp, Thr, Kyn, and Gly) in solution via a 12-step synthesis. The depsipeptide was then bound to a solid support for extension, and the final step of cyclization was completed in solution-phase again. This combined-phase method requires multiple HPLC purifications, which makes it very labour-intensive.

Very recently, Lohani, Taylor, and colleagues at the University of Waterloo have successfully synthesized daptomycin and a few analogues by entirely using solid-phase synthesis, which uses a combination α -azido and Fmoc amino acids. This novel approach has already yielded several derivatives with interesting properties (submitted for publication).

1.4.2 Clinical trials and applications

The initial clinical trials on daptomycin did not go quite as well as the preclinical studies. A treatment regimen involving two daily doses resulted in unacceptable adverse effects in the phase 2 trial. This result led to the termination of the daptomycin project by Eli Lilly. Almost a decade later, Cubist acquired the rights to the drug from Eli Lilly and initiated another round of clinical trials. The amount of drug applied in these trials was the same as before, but it was applied in a single daily dose instead of two. This counter intuitive approach turned out to be successful in reducing adverse effects and was the key to future approval.⁵⁹

Before the clinical introduction of daptomycin a decade ago, the first choice drug used in treatment for known or suspected MRSA infections was vancomycin. Since then, daptomycin has been used with increasing frequency as a primary drug. Some recent studies have suggested that daptomycin might even be a better choice than vancomycin for treating MRSA

bloodstream infections. It was found to be associated with lower mortality rate and fewer cases of persistent infections.^{140, 147}

Daptomycin has also proven valuable for “salvage treatment” for vancomycin, meaning that it has been used successfully after initial treatment with vancomycin had failed. Other options for treatment of VRE infections include linezolid and quinupristin-dalfopristin.^{91, 117} Both linezolid and quinupristin-dalfopristin have severe side effects, which limits their utility in long-term treatment.¹⁷⁰ However, daptomycin also has a shortcoming of its own: it is not effective for treating pneumonia. This has been attributed to pulmonary surfactant, which is assumed to bind and sequester daptomycin.¹⁸³

1.4.3 Mode of action

Since the discovery of daptomycin, many studies have attempted to elucidate its mode of action, and several different mechanisms have been proposed. While all studies agree that the antibacterial activity of daptomycin is Ca^{++} -dependent, most other aspects are subject to ongoing debate. To make it easier to follow, the proposed action modes can be divided into two general categories, namely, disruption of the cell membrane vs. inhibited synthesis of cell wall macromolecules, specifically peptidoglycan and lipoteichoic acids.

Allen and colleagues first suggested that daptomycin exerts its bactericidal activity through inhibiting the biosynthesis of peptidoglycan, and more specifically the early cytoplasmic stages of precursor synthesis. In their initial report,⁶ they compared the cellular effects of daptomycin with those of other antibiotics known to inhibit peptidoglycan biosynthesis, namely, vancomycin, amphomycin, and fosfomycin (see Figure 1.2). Unlike vancomycin or amphomycin, daptomycin did not cause the accumulation of UDP-MurNAc-pentapeptide inside *S. aureus* cells. A later study confirmed this observation and also showed that daptomycin did not inhibit the synthesis of lipid I and II (Step 3 and 4 in Figure 1.2).¹⁷⁴ Collectively, these findings indicate that any interference of daptomycin with murein synthesis would have to take place at a very early stage. Indeed, Allen *et al.* showed that daptomycin inhibited the synthesis of

UDP-MurNAc, an effect that is also seen with fosfomycin. While Allen did not identify a specific molecular target, they proposed that daptomycin inhibits the formation of early precursor molecules for peptidoglycan biosynthesis.⁶

This initial hypothesis was challenged by Boaretti and colleagues, who claimed that daptomycin binds to bacterial cell membrane irreversibly, which would prevent it from reaching any of the cytoplasmic targets that are involved in the synthesis of peptidoglycan precursor molecules.³¹ Allen and colleagues later revised their initial suggestion. They found that daptomycin does not affect the activity of enzymes that are involved in the synthesis of peptidoglycan precursor molecules; instead, daptomycin stopped the uptake of amino acids.⁵ They also noticed that daptomycin causes the release of intracellular potassium⁶ and the dissipation of the membrane potential.³ Combining all these findings, they proposed that the target for daptomycin is the energized cell membrane, and the inhibition of cell wall synthesis results from the disruption of membrane potential and energy metabolism by daptomycin.

Boaretti and colleagues also provided evidence that daptomycin has a stronger inhibitory effect on the synthesis of lipoteichoic acid than on that of other macromolecules, such as DNA, RNA, proteins, and peptidoglycan, which led them to propose that lipoteichoic acid (LTA) is the primary target for daptomycin.³¹ More experiments were performed to support their claim, but the results were not convincing. They tested the activity of daptomycin on *Enterococcus faecium* protoplasts.²¹ Protoplasts are cells with their cell wall removed. If an antibiotic only finds its target in the cell wall, it should have little effect on them. Their result showed daptomycin at MIC killed 99% of the cells within 60 minutes, while killing by vancomycin in the same time period was negligible. The opposite effects indicate the target for daptomycin might not be found in the cell wall as for vancomycin, but this was not addressed by the authors. At the same time, they showed that daptomycin has the strongest inhibitory effect on the synthesis of LTA during protoplast cell regeneration. Later on, they tried to identify the specific enzyme targets in cell membrane. Daptomycin was shown to bind to five proteins,²⁰ but none of these has been identified or shown to be involved in the synthesis of LTA.

The hypothetical inhibition of LTA biosynthesis was addressed again by Laganas and colleagues.¹⁰⁵ In their kinetic study, daptomycin was able to inhibit the synthesis of various macromolecules including RNA, LTA, and lipids, but the inhibition showed no kinetic preference for LTA biosynthesis. In the control experiment, rifampicin, an inhibitor to RNA polymerase, demonstrated clear kinetic specificity for RNA biosynthesis. Hence, it was suggested LTA biosynthesis was not the primary target. Laganas *et al.* also examined the effect of daptomycin on cells arrested in growth, where all macromolecular biosynthesis pathways are stopped. If daptomycin's activity required ongoing synthesis of LTA or any other macromolecules, it should not have any effect on these growth-arrested cells. In contrast to this prediction, it was observed that daptomycin was still very effective in killing these cells. It was also shown that adding exogenous LTA in excess did not affect the activity of daptomycin, which suggested daptomycin does not bind to LTA.

Despite their different views, all authors agree that the cell membrane is involved in the action mode of daptomycin. Artificial membrane studies showed that daptomycin could bind and insert into membrane without protein components.¹⁰⁷ Silverman and colleagues demonstrated that daptomycin's rapid bactericidal activity is closely correlated with the dissipation of the cell membrane potential, and that daptomycin triggers the release of K^+ . Based on these findings, as well as on the similarity to other membrane-damaging molecules, a multi-step mechanism of action, with the cell membrane as the primary target, was proposed¹⁸⁴ (Figure 1.19). According to this mechanism, (1) monomeric daptomycin monomer binds to the membrane in the presence of Ca^{++} , (2) bound daptomycin monomers oligomerize, and (3) oligomers form discrete channels to release K^+ and cause cell death.

Several later findings strongly supported this model and provided more details. The content of lipid phosphatidylglycerol (PG) in the bacterial cell membrane is crucial for daptomycin's bactericidal activity, and a reduced abundance of PG can give rise to daptomycin resistance.^{72,78,79} Fluorescence studies done on liposome models and on bacterial membrane vesicles showed that daptomycin, at concentrations similar to those required for antibacterial

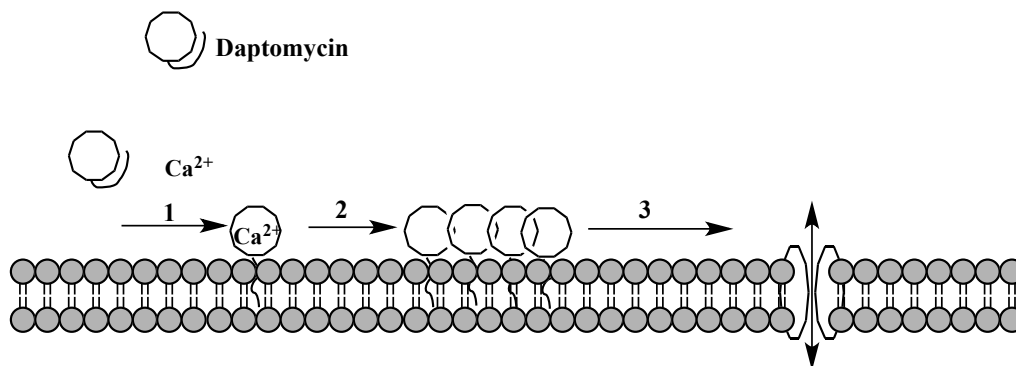


Figure 1.19 Proposed action mode of daptomycin. In the presence of Ca^{2+} , monomeric daptomycin binds to a susceptible membrane (1); the bound daptomycin monomers oligomerize (2); oligomers form discrete ion channels (3).¹⁸⁴

activity and with physiological levels of Ca^{2+} , can bind and form oligomers with 6–7 subunits on liposomes containing PG. Although daptomycin can bind to liposomes without PG (containing phosphatidylcholine only), this requires much higher than physiological concentrations of Ca^{2+} , and it does not result in oligomer formation.^{142–144}

A modified model, based mostly on NMR studies,^{85,95,194} suggested the calcium-dependent formation of micellar daptomycin oligomers with 14–16 subunits already in solution, before the interaction with membranes. These micelles are envisaged to approach the bacterial membrane and dissociate, where individual daptomycin molecules start to insert into the membrane. It should be noted that the concentration of daptomycin used in these NMR experiments (2mM) were much higher than the minimum inhibitory concentrationⁱ (MIC) ($\sim 0.5\mu\text{M}$). The above-mentioned fluorescence study¹⁴⁴ did not observe oligomerization in solution at concentrations close to MIC, which suggests that micelle formation occurs only at high concentration and is not relevant to the bactericidal mechanism.

While Muraih *et al.* showed the formation of oligomers on model membranes and bacterial cells, it should be noted that, up to this point, there was no direct evidence to show if these oligomers are involved in membrane permeabilization. Cotroneo and colleagues found that

ⁱMinimum inhibitory concentration: the lowest concentration of an antimicrobial that will inhibit the growth of a microorganism after overnight incubation.

daptomycin kills *S. aureus* cells without causing cell lysis or any membrane discontinuities visible by electron microscopy,⁴¹ which favors the formation of small and discrete pores. They also noticed daptomycin altered cell wall morphology with abnormal septation events.

Another group also characterized daptomycin-mediated alterations in cell morphology. Pogliano and colleagues showed that daptomycin induces curved membrane patches that attract the bacterial protein DivIVA.¹⁶⁴ DivIVA is involved in cell wall synthesis by recruiting other cell division enzymes. The correlation between daptomycin binding, localization of DivIVA, and altered cell morphology led them to propose a new twist on Silverman's model. When daptomycin is applied at a sub-lethal concentration, the daptomycin aggregates induce limited local alterations of cell morphology that become visible as cell bending and abnormal septations. When a lethal dose of daptomycin is given, multiple local alterations of the membrane are induced, which overwhelms the cells' ability to compensate. Certain small discontinuities on membrane might start to appear, which causes the leakage of ions and loss of membrane potential.

1.4.4 Resistance to daptomycin

As has been mentioned earlier, many variants of bacterial resistance have arisen through horizontal gene transfer. Although there is no such case reported regarding daptomycin, some of the potential sources of resistance genes have been investigated.

There is a gene, *dptP*, located very close to the synthetase gene cluster, which encodes a very basic protein (pI >11.5). It is assumed that this basic protein could directly neutralize the acidic daptomycin before transport.¹⁴

Among some of the daptomycin-resistant actinomycete isolates, daptomycin was found to be inactivated by hydrolysis of the ring-closing depsipeptide bond or by hydrolytic cleavage of the lipid tail. The inactivation of daptomycin by *Paenibacillus lautus* was found specifically caused by hydrolysis of the ring-closing ester bond.^{19,46} It is possible that the genes encoding these hydrolases could find their way to pathogenic bacteria.

In order to elucidate the resistance mechanisms in the clinical and laboratory-derived isolates, a number of hypotheses have since been proposed based on phenotypic observations and on DNA sequencing. All of them suggest that the bacteria gained their resistance through adaptation in cell wall homeostasis and membrane phospholipid metabolism.

One morphological characteristic observed in some daptomycin-resistant isolates is the thickening of cell walls.^{10,137,190} It has been suggested that such thickened walls act as reinforced physical barriers to impede access of daptomycin to its membrane targets. A number of genes in cell wall synthesis and metabolism were found to be upregulated following exposure to daptomycin.^{68,148} Many of these genes are regulated by an essential YycFG regulatory system.^{52,53} Mutations in YycFG have been identified in many daptomycin-resistant strains.^{72,89} It is possible that the thickened cell wall is the result of these mutations after a prolonged exposure to daptomycin.

Many of these genes are under the control of *vraSR* regulator, which is also upregulated. By inactivating *vraSR*, daptomycin-resistant *S. aureus* could be reverted back to a susceptible phenotype, which coincided with the restoration of a thinner cell wall.¹²⁹

The modification of the cell wall is not just limited to an increase in thickness. The overexpression of the *dlt* operon has been linked to daptomycin resistance. The *dlt* operon is responsible for the D-alanylation of wall teichoic acids, and its overexpression was shown to correlate with increased positive surface charge and reduced daptomycin binding to cells. Based on this observation, it was suggested that resistance might result from electrostatic repulsion between cell wall and daptomycin-Ca⁺⁺ complex.²²¹ However, it is noteworthy that daptomycin is negatively charged in solution, and that the cationic daptomycin-Ca⁺⁺ complex might not form until it is in very close proximity with the target membrane, at which point it would have already passed the cell wall. In a study on a resistant *S. aureus* strain with thickened cell walls, Bertsche and colleagues¹⁸ showed enhanced transcription of both the *tag* and *dlt* operons, which are responsible for the production of wall teichoic acid and for its D-alanylation, respectively. They suggested that resistance could be the result of multiple cell wall modifications. Hence, it

is possible that the resistance is due to the limited access to membrane conferred by a more densely packed cell wall.¹⁷¹

Changes in the fluidity of the cell membrane is also seen in some resistant *S. aureus* strains. The clinical resistant isolates tend to have more fluid membranes than their susceptible parental strains, whereas the ones selected by serial passaging in the laboratory tend to have more rigid membranes than their parental strains.^{91,93,137} The cell membrane fluidity is directly affected by the content of carotenoids. It has been shown that the increased production of carotenoid correlated with increased daptomycin MICs and enhanced membrane rigidity.¹³⁵ Nevertheless, strains that lack carotenoids have very fluid membranes and are also resistant to daptomycin.^{16,87} These contradicting observations were described as a “Goldilocks effect”, such that, for optimal activity for daptomycin, the membrane could be neither too fluid nor too rigid.^{16,91} However, how the membrane fluidity affects daptomycin activity at the molecular level is still unknown.

Mutations in the *mprF* gene are also found in many resistant *S. aureus* strains.⁷² This gene encodes a dual-functional membrane enzyme that catalyzes both the conversion of PG to lysyl-PG (Figure 1.20) in the inner leaflet of the membrane and the subsequent translocation to the outer leaflet.⁶⁴ The mutant enzymes found in resistant strains showed gains in function, which either increase the production of lysyl-PG or accelerate the flipping, which all result in an increase of lysyl-PG content in the outer membrane leaflet.^{93,163} Since lysyl-PG is positively charged, it has been suggested that the resistance could be the result of increased charge-charge repulsion to cationic daptomycin-Ca⁺⁺ complex, a similar mechanism as suggested for overexpression of *dlt* operon. It is also possible that the main effect of increased lysyl-PG synthesis is the concomitant reduction of PG in the membrane, which reduces the binding sites for daptomycin.⁷⁹

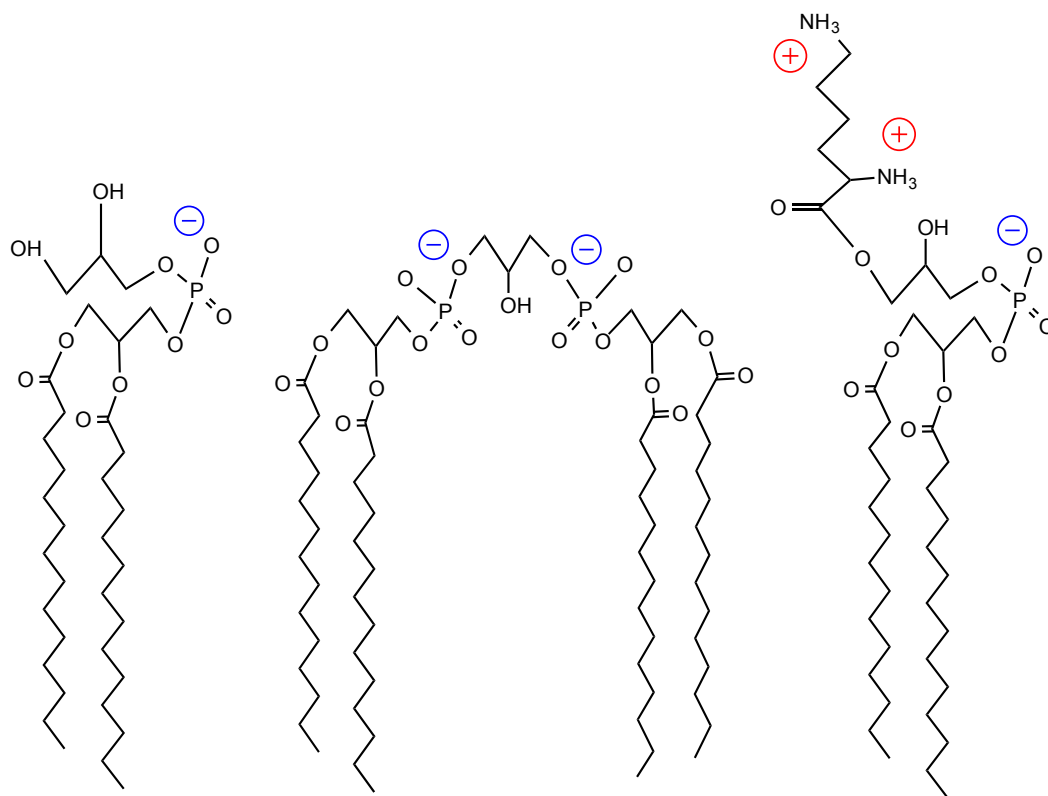


Figure 1.20 Chemical structures of lipid molecules: left, phosphatidylglycerol (PG), middle, cardiolipin (CL), and right, lysyl-phosphatidylglycerol (lysyl-PG). One CL molecule is synthesized by condensing two PG molecules. Lysyl-PG is produced by modifying the head group of PG. Daptomycin's activity depends on the membrane content of PG. The increased content of either CL or lysyl-PG (outer leaflet) has been suggested to cause resistance.

1.5 RESEARCH OBJECTIVES

Up to this point, ion channel formation is the best-defined and -supported model to explain daptomycin's mechanism of action. However, there are still many important questions that need to be answered by experiments. This thesis aimed to answer some of them.

1. Fluorescence studies have shown that daptomycin forms oligomers on liposome membranes and also on the cell membranes of susceptible bacteria. While oligomerization is thought to be required for bactericidal activity, this has not been experimentally demonstrated. This question is addressed in Chapter 2.

2. Daptomycin's rapid bactericidal activity correlates with membrane depolarization, which has been ascribed to permeabilization of the membrane toward K^+ .¹⁸⁴ However, the concentration of K^+ is higher inside the cell than outside, and a selective permeabilization for K^+ should cause hyperpolarization rather than depolarization. This suggests that the daptomycin permeabilizes the membrane toward ions other than K^+ also. Experiments that shed light on this question are presented in Chapter 3.
3. Apart from lysyl-PG, another lipid involved in resistance is cardiolipin (Figure 1.20), which is formed by condensing two PG molecules. Resistant *Enterococcus* strains were found to have mutations that enhance cardiolipin synthase activity.^{44,158} Does cardiolipin interact directly with daptomycin, and if so, how? This question is examined in Chapter 4.

Chapter 2

The role of oligomer formation in the antibacterial activity of daptomycin

2.1 INTRODUCTION

The lipopeptide antibiotic daptomycin is used clinically against infections by Gram-positive bacteria, including strains of staphylococci and enterococci that are resistant to other antibiotics.^{17,32,199} It binds to and causes depolarization of the bacterial cytoplasmic membrane, which is considered to be the mechanism of its rapid bactericidal action.^{3,184} Electron microscopy of daptomycin-exposed cells does not reveal any discontinuity of the lipid bilayer.⁴¹ Both this observation and the selective nature of the membrane permeability defect⁵ support the notion that daptomycin forms small, discrete membrane lesions. It was proposed earlier

The results presented in this chapter have been published in: “Mutual inhibition through hybrid oligomer formation of daptomycin and the semisynthetic lipopeptide antibiotic CB-182,462”, by Tianhua Zhang, Jawad K. Muraih, Evan Mintzer, Nasim Tishbi, Celine Desert, Jared Silverman, Scott Taylor, and Michael Palmer(2013), *Biochim. Biophys. Acta* 1828:302-8.

Authors’ contributions: The experiment depicted in Figure 2.4 was performed by E. Mintzer and N. Tishbi. The synthesis and purification of perylene-daptomycin were performed by S. Taylor. All other experiments were done by the thesis author. The experiments depicted in Figure 2.6 were replicated by J. Muraih.

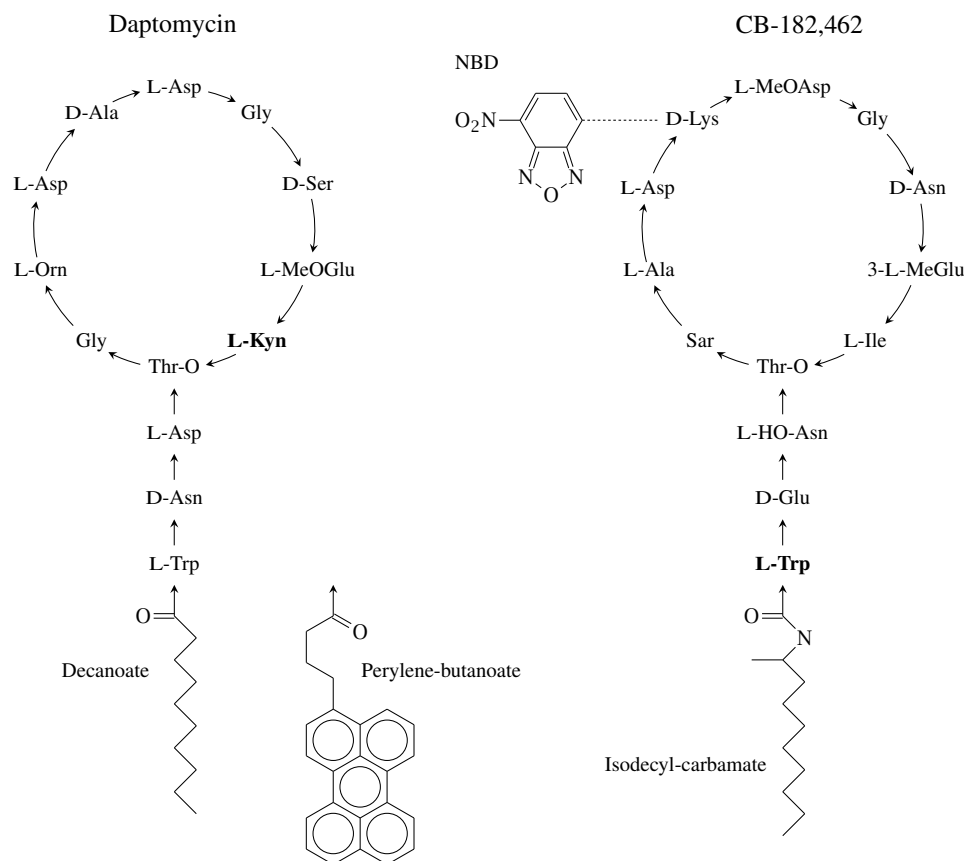


Figure 2.1 Structures of daptomycin and of CB-182,462 and of their labeled derivatives used in this study. Arrows indicate amide or ester bonds, in C to N or C to O direction. In perylene-daptomycin, a perylene-butanoyl residue replaces the N-terminally attached decanoyl residue found in daptomycin. CB-182,462 is a semisynthetic derivative of the natural compound A54145, in which the naturally occurring N-terminally linked fatty acyl residue is replaced by a substituted carbamyl residue. In NBD-CB-182,462, a nitrobenzoxadiazole (NBD) group is attached to the free amine in the side chain of D-lysine. Abbreviated names for non-standard amino acids: Orn, ornithine; MeOGlu, γ -methoxy-glutamate; kyn, kynurenine; HO-Asn, β -hydroxy-asparagine; MeOAsp, β -methoxy-aspartate. The two residues whose intrinsic fluorescence was used in some of the experiments, tryptophan in CB-182,462 and kynurenine in daptomycin, are set in boldface. Note that, in addition to the sequence similarity, the same positions are occupied by D- and L-amino acids in both molecules.

that these discrete lesions are formed by oligomeric assemblies of daptomycin molecules.¹⁸⁴ However, experimental evidence of oligomer formation has been obtained only recently,^{142,144} and direct proof of their involvement in membrane permeabilization is still lacking.

Daptomycin and antibiotic A54145 share the same architecture: both consist of 13 amino acids, including several non-standard ones (Figure 2.1).^{23,49} The ten C-terminal residues form a ring that is closed by an ester bond. The exocyclic N-terminal tryptophan carries a fatty acyl residue, which in the clinical drug preparation for daptomycin is decanoic acid, although the length of this acyl tail is subject to variation in the natural product. The two molecules also share significant sequence homology, with five identical residues and four more similar ones. We reasoned that testing the two molecules for their ability to form hybrid oligomers should provide information on the contributions of the conserved and the non-conserved residues, respectively, to the oligomerization process.

The experiments were performed with various fluorescent derivatives of daptomycin and of CB-182,462, a semisynthetic derivative of A54145.¹²⁴ Our results readily demonstrate the formation of such hybrid oligomers, both on model membranes and on bacterial cells; therefore, the amino acid residues conserved between daptomycin and CB-182,462 are sufficient for oligomerization. Remarkably, however, the hybrid oligomers exhibit reduced antibacterial activity. The observation of oligomers with impaired antibacterial activity shows, on the one hand, that the oligomer is indeed involved in the antibacterial effect. On the other hand, it indicates that oligomer formation as such is not sufficient for activity. Upon assembly, the oligomer must undergo some additional event, such as for example cooperative membrane insertion or the adoption of a very specific structure, in order to acquire bactericidal activity.

2.2 MATERIALS AND METHODS

2.2.1 Synthesis and purification of NBD-CB-182,462 and of perylene-daptomycin

Unlabeled CB-182,462 was provided by Cubist Pharmaceuticals Inc. (Lexington, MA, USA). Reaction of CB-182,462 with NBD-Cl (4-Chloro,7-nitro-2,1,3-benzoxadiazole; Fluka) and HPLC purification were performed as described before for NBD-daptomycin.¹⁴⁴ Molecular weight and homogeneity were confirmed by mass spectrometry on a Micromass Q-TOF UI-

tima GLOBAL mass spectrometer. The synthesis of perylene-daptomycin has been described as well.¹⁴²

2.2.2 Preparation of PC/PG large unilamellar vesicles (LUV)

The synthetic lipids 1,2-dimyristoyl-sn-glycero-3-phosphocholine (DMPC) and 1,2-dimyristoyl-sn-glycero-3-phospho-rac-(1'-glycerol) (DMPG; both from Avanti Polar Lipids, Alabaster, AL, USA) were used to prepare the vesicles. Equimolar amounts of DMPC and DMPG were weighed into a round-bottom flask and dissolved in chloroform/methanol (3:1). The solvent mixture was then evaporated with nitrogen to produce a lipid film, which was further dried under vacuum for 3 h and then dispersed in buffer. The resulting lipid suspension was extruded through a 100 nm polycarbonate filter 15 times, using a nitrogen-pressurized extruder to produce indicator-loaded large unilamellar liposomes^{126,144}

2.2.3 Isothermal titration calorimetry (ITC)

Binding of daptomycin, of CB-182,462, and of a 1/1 (mol) mixture of the two to lipid vesicles was measured calorimetrically at 25 °C using a VP-ITC from Microcal (GE Healthcare, Northampton, MA). LUV for this assay were prepared from equimolar dioleoyl-PG (DOPG) and dioleoyl-PC (DOPC) (5 mM total lipid) in buffer (10 mM HEPES, 100 mM sodium chloride, 1 mM CaCl₂ pH 7.4) by the freeze-thaw/extrusion method. Lipopeptides were dissolved in the same buffer. In a typical ITC experiment, the sample cell was filled with 23 μM lipopeptide solution and the reference cell with buffer. The 250 μL titration syringe was loaded with LUV suspension. Solutions and suspensions were degassed with stirring for 10 min prior to titrations. After system equilibration and a stable baseline was achieved, a 1 μL aliquot of LUV suspension was injected, the heat signal of which was excluded from data analysis according to the instrument's manufacturer's recommendation, followed by 2.5 μL injections at 6 min intervals until several successive injections generated low and constant heat signals. The cell contents were stirred by the injection syringe throughout the titration at a rate of 270 rpm.

Heat resulting from LUV dilution into buffer, which was small and constant (data not shown), was subtracted, and the baseline was adjusted manually to the average noise value prior to data analysis.⁸² Data were collected and analyzed using proprietary Origin software provided by Microcal. Thermodynamic parameters were derived from least squares analysis of the integrated heat signals using Origin's one-site model curve fitting routine. Experiments were performed at least in triplicate and derived parameters were reproducible within 15%.

2.2.4 Steady-state fluorescence measurements on PC/PG liposomes and on bacterial cells

Fluorescence emission spectra were acquired using a PTI QuantaMaster spectrofluorometer. Excitation wavelengths were 282 nm for tryptophan, 430 nm for perylene, and 465 nm for directly excited NBD fluorescence. Excitation and emission band passes were typically 2 nm but were occasionally adjusted in order to increase or reduce sensitivity. Unlabeled daptomycin and CB-182,462 or NBD-labeled CB-182,462 and perylene-labeled daptomycin were applied in the quantities indicated in the Results section (2.3) to the liposomes (200 or 250 μM total lipid) in HEPES/NaCl with calcium (5 mM). Samples were incubated for 5 or 10 min before acquisition of emission spectra, and in some instances measured repeatedly after longer time intervals as indicated.

For fluorescence measurements on bacteria, cells from a fresh overnight culture of *Bacillus subtilis* ATCC 1046 were harvested and repeatedly washed with HEPES/NaCl buffer by centrifugation in a table-top centrifuge. The pelleted cells were resuspended in approximately 20 volumes of buffer. Of the resulting cell suspension, 150 μL were incubated in the presence of CaCl_2 (5 mM) for 10 min with the amounts of labeled or unlabeled daptomycin and CB-182,462 stated in the Results section (2.3). The cells were again washed repeatedly by centrifugation with HEPES/NaCl/ CaCl_2 , resuspended in the same buffer and measured as described above for liposome samples.

2.2.5 Antibacterial activity of daptomycin and CB-182,462

Overnight cultures of *Bacillus subtilis* ATCC 1046 were grown at 37 °C in LB broth. Daptomycin and CB-182,462, alone or combined in various ratios, were serially diluted in LB broth supplemented with 5 mM CaCl₂ (the mixing ratios and dilutions are depicted in Figure 2.6 on page 65). Each serial dilution was inoculated with 1% by volume of the *Bacillus subtilis* overnight culture, and the culture tubes were incubated with shaking at 37 °C overnight. Growth was evaluated visually by turbidity. The transition from translucency (that is, inhibition) to high turbidity (growth) usually occurred abruptly. When intermediate turbidity was observed, which occurred at the most once in any given dilution series, the concentration in question was considered not inhibitory; that is, the minimum inhibitory concentration (MIC) was taken to be the lowest concentration without any visible turbidity. Growth and sterility controls were included in each experiment.

2.3 RESULTS

2.3.1 Oligomerization of CB-182,462 on liposome membranes

We have previously shown that daptomycin forms oligomers on model membranes and bacterial cells.^{142–144} While the similarity between the two compounds suggests that CB-182,462 should do the same, this has not been directly demonstrated. Therefore, a fluorescently labeled derivative was prepared with nitrobenzoxadiazole (NBD) attached to its unique free amino group (Figure 2.1). While the absorption of NBD is highest around 470 nm, there is a smaller absorption peak around 340 nm¹¹⁰ that overlaps the fluorescence emission spectrum of tryptophan. This allows the detection of FRET between the tryptophan of unlabeled CB-182,462 and the NBD-labeled derivative. In the experiment shown in Figure 2.2A, the two species were mixed before application to PC/PG liposomes in the presence of calcium. The tryptophan fluorescence of the unlabeled molecules is very strongly reduced by FRET, which indicates a close association of the two species. FRET is still observed, but to a lesser extent, when the

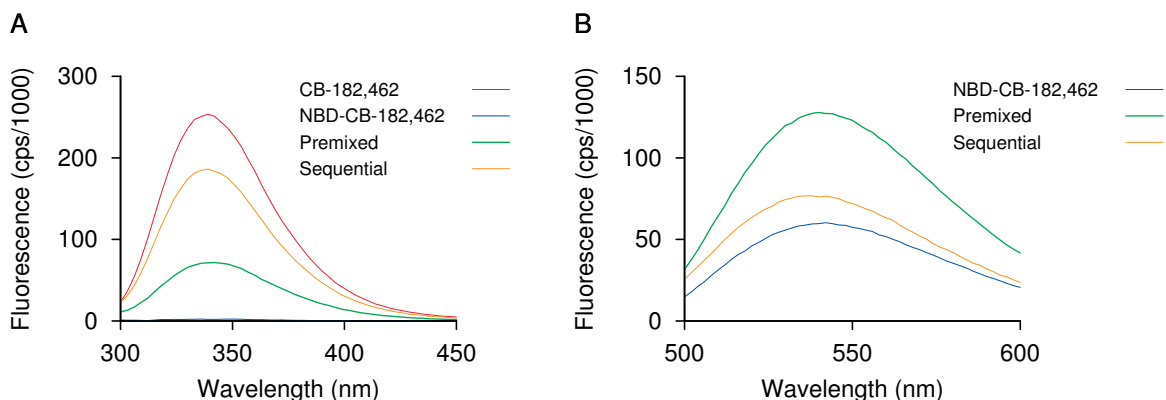


Figure 2.2 Formation of CB-182,462 oligomers on PC/PG liposomes. NBD-labeled CB-182,462 (0.96 μM) and unlabeled CB-182,462 (4.8 μM), alone or combination, were incubated with PC/PG (1:1, 200 μM total lipid) liposomes in the presence of calcium (5 mM). A: Tryptophan fluorescence upon excitation at 282 nm. NBD-CB-182,462 has virtually none, due to FRET from tryptophan to NBD. When the two compounds are mixed before application to liposomes, the tryptophan fluorescence is more strongly quenched than when they are applied separately with a time interval of 5 min between both applications. This is consistent with the formation of hybrid oligomers in the first case but mostly segregated oligomers in the second. The emission of NBD was not scanned in this experiment because it overlaps the secondary maximum of the excitation wavelength. B: Self-quenching of NBD-CB-182,462. Addition of unlabeled CB-182,462 before application to the PC/PG liposomes increases the fluorescence intensity of NBD-CB-182,462 upon direct excitation of NBD at 465 nm, indicating that the latter is subject to self-quenching in homogeneous oligomers. If the unlabeled CB-182,462 is added 5 min after the NBD-labeled sample, it has little effect on the extent of quenching.

two species are applied sequentially. Under these conditions, the labeled molecules and the unlabeled ones should undergo oligomerization separately, and therefore FRET will only occur between, but not within oligomers, which accounts for the reduced overall extent of FRET.

NBD exhibits concentration-dependent self-quenching.²⁷ The local concentration of NBD is higher, and therefore quenching is more pronounced, in pure NBD-CB-182,462 oligomers than in hybrid oligomers formed from a mixture of the NBD-labeled compound and an excess of the unlabeled one (Figure 2.2B). The results from both FRET and self-quenching experiments are completely analogous to our previous observations with daptomycin.¹⁴⁴

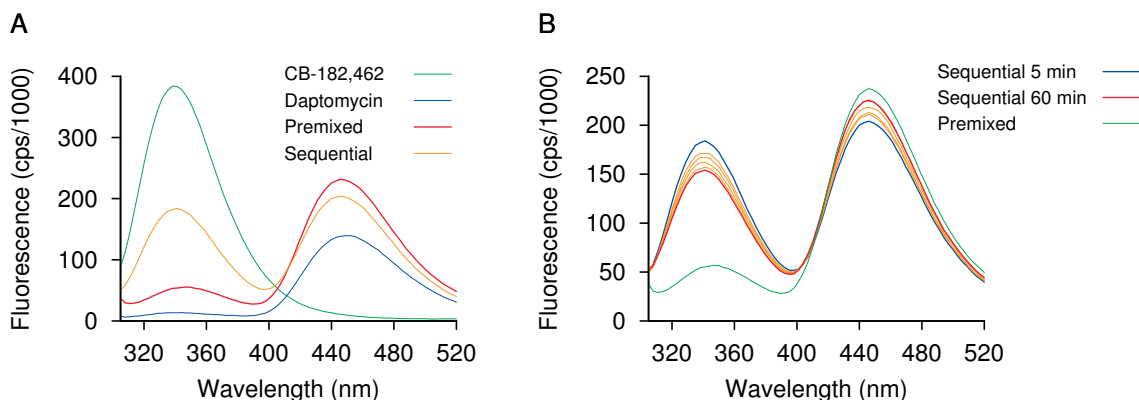


Figure 2.3 Formation of hybrid oligomers of native CB-182,462 and daptomycin on liposomes. A: When both compounds ($2 \mu\text{M}$ each) are mixed before addition to PC/PG liposomes ($250 \mu\text{M}$ total lipid) and calcium (5 mM), the tryptophan fluorescence of CB-182,462 is strongly reduced by FRET, and the kynurenine emission of daptomycin (around 445 nm) is increased. The extent of FRET is smaller when one compound is applied to the liposomes 5 min after the first one. B: Extended incubation of a sequentially prepared sample. The extent of FRET increases slightly with time, but after 60 min still does not approach that of a premixed sample, indicating that daptomycin and CB-182,462 mostly do not reassemble into hybrid oligomers within this time period. Thin yellow lines represent several time points between 5 and 60 min .

2.3.2 Formation of daptomycin/CB-182,462 hybrid oligomers on liposomes

The intrinsic fluorescence of tryptophan also overlaps the absorption spectrum of kynurenine, which in daptomycin causes virtually complete FRET from tryptophan to kynurenine.¹⁰⁷ FRET between tryptophan and kynurenine can also be used to detect formation of hybrid CB-182,462/daptomycin oligomers. When a premixed sample of the two is applied to PC/PG liposomes, the tryptophan fluorescence of CB-182,462 is largely suppressed by FRET (Figure 2.3A). Again, sequential application reduces FRET, which is consistent with formation of separate oligomers.

While daptomycin oligomers are largely stable on a time scale of one or a few hours,¹⁴⁴ it seems possible that hybrid oligomers of CB-182,462 might be less stable. In the experiment shown in Figure 2.3B, a sample prepared by sequential application of the two antibiotics was incubated, and the fluorescence emission measured repeatedly after various time intervals.

While the extent of FRET increases slightly with time, it remains much lower than that observed with a premixed sample after 60 min. This suggests that the rate of subunit exchange between oligomers is low, and oligomers are largely stable on the time scale of the experiment.

The stability of the hybrid oligomers was also examined by ITC. Figure 2.4 shows the ITC traces of daptomycin alone (A), CB-182,462 alone (C) and of an equimolar mixture (B) titrated with liposomes, which were prepared from an equimolar mixture of DOPC and DOPG. In all cases, early injections result in exothermic heat signals, which gradually decrease to very low spikes that represent heat of LUV dilution. Integration of the heat signals from these experiments produce the sigmoid curves typical for ITC experiments in which binding between membrane and drugs is specific and saturable. The titration profiles and the calculated energy terms for ΔH , $T\Delta S$ and ΔG (Figure 2.4D) are quite similar between the pure daptomycin and CB-182,462 samples on the one hand, and the equimolar mixture on the other, which supports the notion that the hybrid oligomers resemble the pure ones with respect to thermodynamic stability.

Another interesting aspect of the ITC results is the observed stoichiometry of the lipopeptides and phosphatidylglycerol, which is very close to 2 molecules of PG for each molecule of antibiotic. In a previous study using perylene excimer fluorescence and lipid bicelles, a stoichiometry of 1 was observed.¹⁴² One possible explanation for the discrepancy is that, in the liposome system, the lipopeptides interact only with the outer monolayer. Alternatively, it is possible that excimer fluorescence and thermal changes report on different stages of the membrane interaction that require only one and two molecules of PG, respectively. This question requires further study.

2.3.3 Formation of hybrid oligomers on bacterial cells

While PC/PG membranes are a useful model to observe the activity of daptomycin and CB-182,462, the lipid composition of bacterial membranes is different, and it is therefore pertinent to examine the formation of hybrid oligomers on bacterial cells as well. Due to the abundance

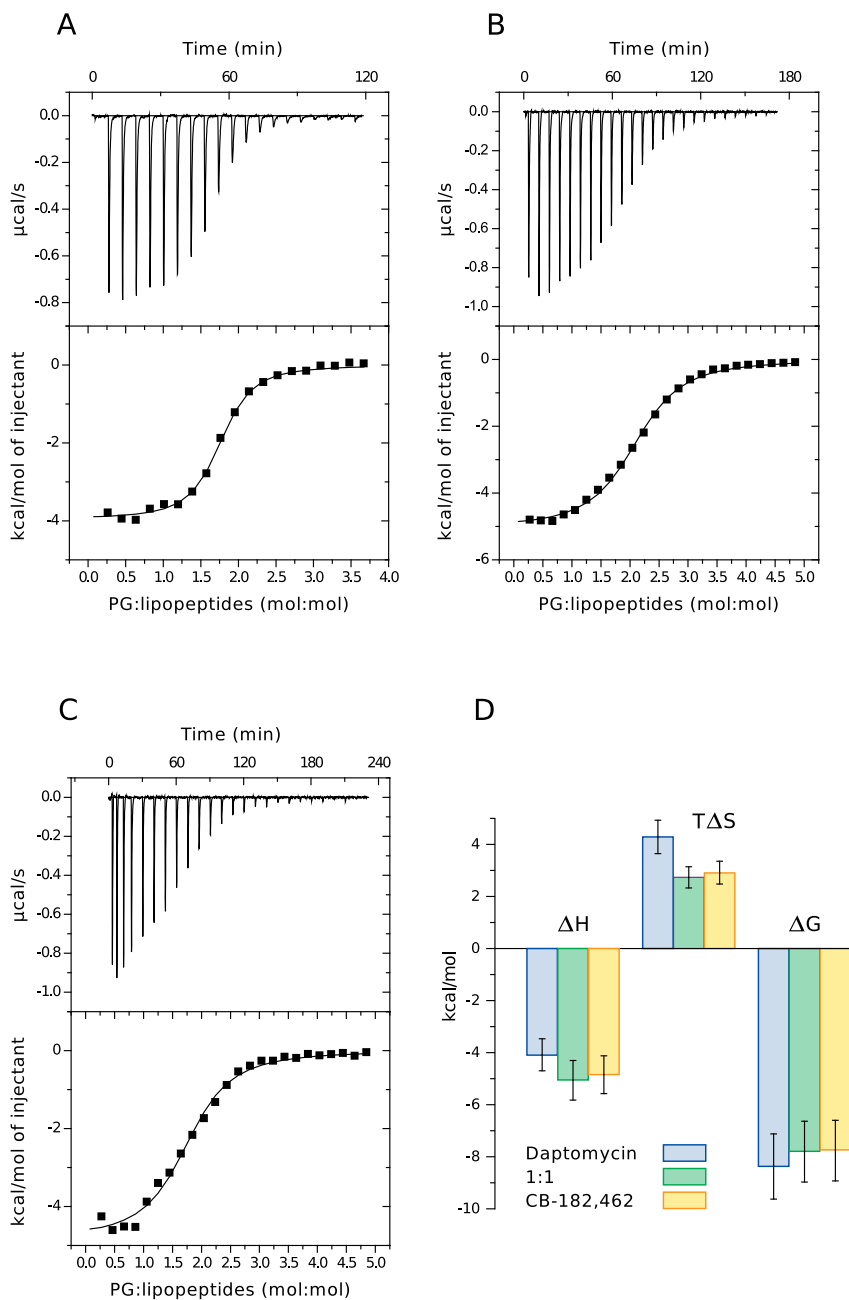


Figure 2.4 Interaction of homogeneous and hybrid oligomers with DOPC/DOPG membranes, studied with isothermal calorimetry (ITC). A–C: Raw ITC heat signals (top panels) and corresponding integrated isotherms (bottom panels) for titrations of pure daptomycin (A), equimolar daptomycin/CB-182,462 hybrids (B), and pure CB-182,462 (C) with 1/1 (mol/mol) PG/PC liposomes at 25 °C. Solid lines are best-fit curves obtained with Microcal’s Origin single binding site model. D: Summary of thermodynamic binding parameters. All experiments were performed at least in triplicate and results were reproducible within 15%. Representative isotherms are shown.

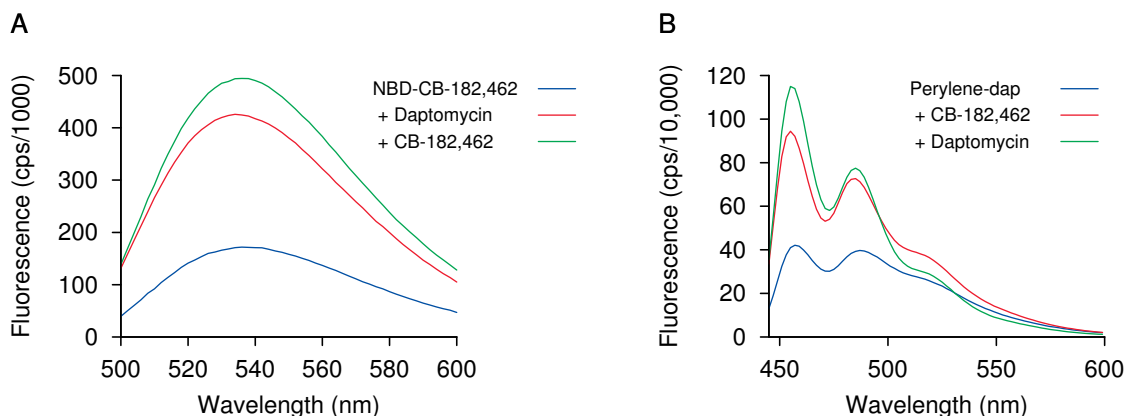


Figure 2.5 Formation of hybrid CB-182,462 oligomers on *Bacillus subtilis* cell membranes. A: Alleviation of NBD-CB-182,462 self-quenching by unlabeled CB-182,462 or daptomycin. NBD-CB-182,462 (4 μM), alone or premixed with unlabeled CB-182,462 or daptomycin (20 μM), was incubated with *Bacillus subtilis* ATCC 1046 cells in the presence of calcium (5 mM). After incubation for 10 min, the cells were washed repeatedly by centrifugation, resuspended in buffer, and the NBD fluorescence measured upon excitation at 465 nm. B: Inhibition of excimer formation by perylene-daptomycin by unlabeled daptomycin or CB-182,462. Perylene-daptomycin monomers emit maximally at 455 nm, whereas the excimers emit maximally at about 525 nm.¹⁴² Concentrations of labeled and unlabeled compounds, and other conditions were the same as in A.

of tryptophan in bacterial proteins, the intrinsic tryptophan fluorescence of CB-182,462 could not be used in these experiments. However, however, two alternative approaches allowed for the detection of hybrid oligomers on *Bacillus subtilis* cells.

In the first experiment (Figure 2.5A), the concentration-dependent self-quenching of NBD in NBD-labeled CB-182,462 was inhibited not only by unlabeled CB-182,462 but also using unlabeled daptomycin, which means daptomycin subunits intercalate between and separate the labeled molecules. In the second experiment (Figure 2.5B), the formation of perylene excimers in oligomers of perylene-labeled daptomycin¹⁴² is suppressed by both unlabeled daptomycin and unlabeled CB-182,462.

Between the two experiments, it is evident that both the labeled and the unlabeled forms of daptomycin and CB-182,462 are capable of hybrid oligomer formation on bacterial cell membranes.

2.3.4 Antibacterial activity of daptomycin/CB-182,462 mixtures

If two different drugs act independently but share the same target and mode of action, their mixtures will display additive effectiveness. This can be detected by isobolographic analysis.⁷³ In such an experiment, the concentrations of the two drugs in question are varied independently, and lines are drawn to connect equieffective dosages of various combinations. If the two drugs indeed behave additively, the equieffective dosages of all mixtures will fall on a straight line that also includes the equieffective dosages of the two pure drugs.

Figure 2.6A shows an isobologram for the minimum inhibitory concentrations (MICs) of daptomycin and CB-182,462. It is clear that the observed MICs deviate from such an ideal straight line. With the mixtures, greater than additive dosages are required to reach the MIC, indicating that the two drugs inhibit one another. The discrepancy is greatest with the equimolar mixture of the two antibiotics, indicating that mutual inhibition is most pronounced at this ratio (Figure 2.6B). While any binary mixture should produce a distribution of oligomers that vary with respect to both the fractions of the two antibiotics incorporated and the positions within the oligomer occupied by each, an equimolar ratio should maximize the extent of scrambling and minimize the residual fractions of homogeneous oligomers. The observation that mutual inhibition is strongest at this ratio therefore supports the notion that hybrid oligomers have impaired antibacterial activity.

2.4 DISCUSSION

In previous studies, it was shown that daptomycin forms oligomers on PG-containing membranes,^{142,144} and that the oligomers have a stoichiometry of approximately 6–7 subunits, or possibly twice that number.¹⁴³ A role of membrane-associated oligomers in the antibacterial activity of daptomycin has widely been assumed and accepted as plausible;¹⁸⁴ however, direct experimental evidence has been lacking. The mutual inhibition between daptomycin and the semisynthetic homologous lipopeptide CB-182,462 reported in this study constitutes the first

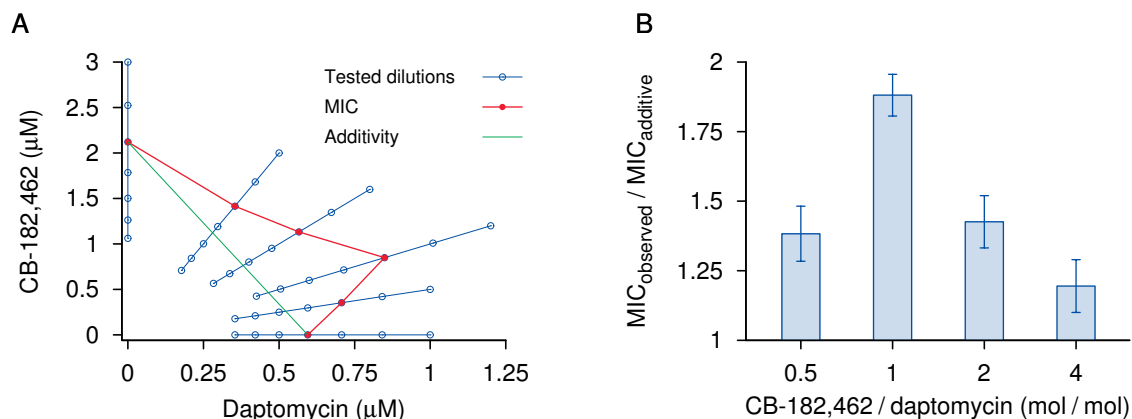


Figure 2.6 Mutual inhibition of bactericidal action between daptomycin and CB-182,462. A: Isobologram of MICs observed in an individual experiment. Daptomycin and CB-182,462 were admixed in LB medium and serially diluted at the ratios indicated; thin blue lines connect serial dilutions of the same starting mixture. *Bacillus subtilis* ATCC 1046 was pre-grown in LB broth and inoculated 1:100 into each serial dilution. In case of independent and additive action, all MICs should fall on a straight line connecting those of the pure antibiotics. The observed MICs of the mixtures deviate toward higher concentrations, indicating mutual inhibition. B: The ratio of the observed MIC to the hypothetical MIC expected from the linear additivity relation was calculated for each of the indicated mixing ratios. Data represent averages and standard deviations from six independent experiments. Higher ratios indicate greater mutual inhibition.

such evidence; for if each individual monomer contributed independently and proportionally to the antibacterial action, combinations of the two antibiotics should display strictly additive activity.

Considering the number of subunits (at least 6) and the efficiency of FRET between the two antibiotics (Figure 2.2A), it is likely that the oligomers produced by equimolar mixtures are indeed mostly hybrids, albeit with varying subunit stoichiometry. According to ITC, these oligomers have virtually the same stability as the homogeneous ones, which suggests that hybrid and homogeneous oligomers are also structurally similar. This is supported by the observation that equimolar mixtures exhibit only moderately reduced antibacterial activity, which means that some of the hybrids formed by this mixture are functionally active. Conceivably, the ones that are not active resemble a “pre-pore” stage that may also transiently exist with

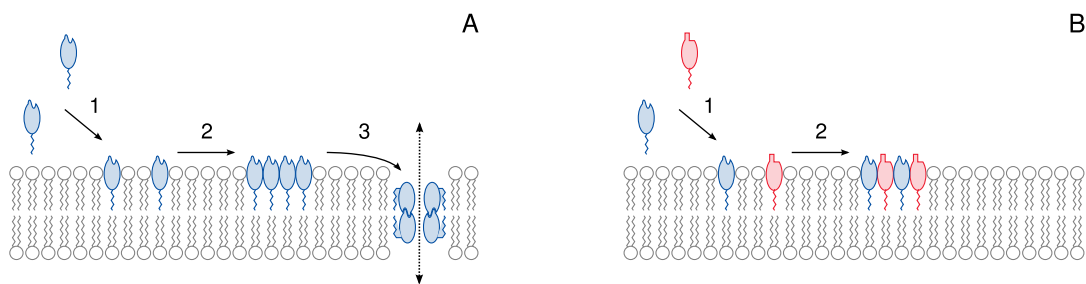


Figure 2.7 Hypothetical model for daptomycin action. A: Membrane binding (1) precedes oligomerization (2), which in turn must be followed by membrane insertion (3) in order to produce functional membrane lesions. B: In mixtures of CB-182,462 and daptomycin, oligomerization is preserved, but membrane insertion and permeabilization may be disrupted.

homogeneous oligomers, and which has to undergo an additional step to acquire bactericidal activity. A similar functional sequence exists with many pore-forming protein toxins, such as for example *Staphylococcus aureus* α -toxin,^{96,211} anthrax toxin protective antigen,¹³³ and the cholesterol-dependent cytolysins of Gram-positive bacteria,⁸⁸ all of which first assemble into oligomers atop the target membrane before cooperatively inserting into and then permeabilizing it. However, this hypothetical scenario, which is depicted in Figure 2.7, clearly needs to be addressed by further experimental study; it is not known at this time whether or not the inactive hybrid oligomers resemble a kinetic intermediate of the normal, active membrane lesion. The need for further experiments also pertains to the functional roles of individual amino acid residues in the daptomycin molecule. While our study makes an initial distinction between two functional groups of residues—namely, the ones shared between daptomycin and CB-182,462, which suffice for oligomerization, and those not shared between the two molecules, which make at least some contribution to oligomer activation—this level of resolution is clearly inadequate for construction of a detailed structural and functional model of the formation and activation of the oligomer. Studies with additional synthetic or genetically engineered^{151,195} molecular variants of daptomycin may help to address this question.

The high degree of specificity in the mutual interaction of the subunits within the daptomycin and CB-182,462 oligomers agrees with the considerable stability of the oligomers; even

the hybrids, which one might expect to be less stable than the homogeneous oligomers, appear mostly stable on a time scale longer than required for exercising the antibacterial effect.

Daptomycin has been likened to the large and structurally diverse functional family of antibacterial peptides.^{136,194} However, with most antibacterial peptides, oligomer formation seems to be rather fleeting and transient, or at least more readily reversible^{25,29,176,177} than with daptomycin and CB-182,462. It appears possible, therefore, that pore-forming protein toxins provide a more useful and valid paradigm than typical antimicrobial peptides to understand daptomycin's mode of action.

Chapter 3

Daptomycin forms cation- and size-selective pores in model membranes

3.1 INTRODUCTION

Daptomycin acts at the bacterial membrane. Various molecular targets and action modes have been proposed, including the inhibition of peptidoglycan¹³⁰ or lipoteichoic acid synthesis.³¹ However, the only effect consistently reported in studies from different laboratories consists in the depolarization of the bacterial cell membrane.^{3,5,169,184} Concomitantly with membrane depolarization, bacterial cells lose the ability to accumulate amino acid substrates, while leaving glucose uptake intact, indicating a selective nature of the membrane permeability defect.⁵ No membrane discontinuities have been observed by electron microscopy,⁴¹ also supporting the notion that the functional membrane lesion is discrete and small.

The results presented in this chapter have been published in: “Daptomycin forms cation- and size-selective pores in model membranes”, by TianHua Zhang, Jawad K. Muraih, Ben MacCormick, Jared Silverman, and Michael Palmer(2014), *Biochim. Biophys. Acta* 1838:2425-30.

Authors’ contributions: The calculation and fitting depicted in Figure 3.7 was performed by M. Palmer. All other experiments were done by the thesis author. Some experiments were replicated by B. MacCormick and J. Muraih.

Based on precedent from other membrane-damaging peptides and proteins, it was proposed early on that daptomycin acts through the formation of oligomeric transmembrane pores;¹⁸⁴ however, experimental evidence was only obtained more recently. Using various fluorescently labeled, functionally active daptomycin derivatives, oligomerization was observed both on model liposomes and on bacterial membranes,^{142–144} and it was subsequently shown that oligomerization is required for antibacterial action (see Chapter 2). The model liposomes used in those studies contained only phosphatidylcholine (PC), which is largely inert to daptomycin,¹⁴⁴ and phosphatidylglycerol (PG), which was required to induce binding at physiologically relevant calcium concentration, as well as to trigger oligomer formation.

It is noteworthy that the abundance of phosphatidylglycerol in bacterial cell membranes is also a major determinant in the susceptibility of bacteria to daptomycin.^{12,72,79} It was therefore of interest to determine whether the PC/PG liposome model also suffices to support the formation of the functional daptomycin pore, and if so, to characterize the pore's permeability properties. This study reports the corresponding experiments. The results show that daptomycin forms discrete pores on liposome membranes that are selective for cations of limited size.

3.2 MATERIALS AND METHODS

3.2.1 Preparation of indicator-loaded large unilamellar vesicles

The procedures for preparing the large unilamellar vesicles have been described in the preceding chapter (Section 2.2.2). The buffers used for dispersing the lipid film contained either pyranine or 5,5'-dithiobis-(2-nitrobenzoic acid) (DTNB) as an indicator for the permeabilization assays, and they varied in pH and salt composition as detailed in Table 1. Following polycarbonate membrane extrusion, the liposomes were subjected to gel filtration on a BioGel P-6DG column (Bio-Rad, Richmond, CA, USA) in order to remove untrapped indicator.

Table 3.1 Buffers and indicators used to detect membrane permeabilization toward different solutes. The indicators were dissolved in the corresponding hydration buffer, and the solution was then used to rehydrate PC/PG lipid films. After extrusion of the lipid dispersion through polycarbonate membranes, untrapped indicator was removed by gel filtration using the corresponding hydration buffer. In experiments with anionic or cationic test solute, pH gradients were established by diluting the liposome samples into reaction buffers with different pH levels. Pyranine (8-hydroxypyrene-1,3,6-trisulfonic acid) and DTNB (5,5'-dithiobis-(2-nitrobenzoic acid)) were obtained from Sigma.

Test solutes	Hydration buffer	Entrapped indicator	pH value
Cations	5 mM MES, 5mM Tricine, 5 mM NaCl, 5mM KCl, 250 mM Sucrose	5 mM pyranine	6.00
Anions	5 mM MES, 5mM Tricine, 5 mM NaCl, 5mM KCl, 250 mM Sucrose	5 mM pyranine	8.00
Neutral solutes	20 mM HEPES, 150 mM NaCl, 250 mM Sucrose	5 mM pyranine	7.00

The column buffers used in the gel filtration step matched those used for lipid film rehydration, except for the absence of pyranine or DTNB.

As indicated in Table 3.1, all loading buffers also contained 250 mM sucrose. This experimental detail was adopted from a previous study³⁷ and was found to improve the stability of the indicator-loaded liposomes.

3.2.2 Fluorescence measurements

With pyranine-loaded liposomes, time-based emission scans were acquired on a PTI QuantaMaster 4 system, the sample holder of which was thermostatted at 30 °C. Liposome suspensions were diluted to a final concentration of 250 μ M of total lipids into reaction buffer with 5 mM CaCl₂. Daptomycin (Cubist), carbonyl cyanide m-chlorophenyl hydrazine (CCCP, Sigma), and valinomycin or gramicidin (Sigma) were added as indicated to final concentrations of 1 μ M, 5 nM, 0.5 μ M, and 10 nM, respectively, in order to initiate the reaction. The fluo-

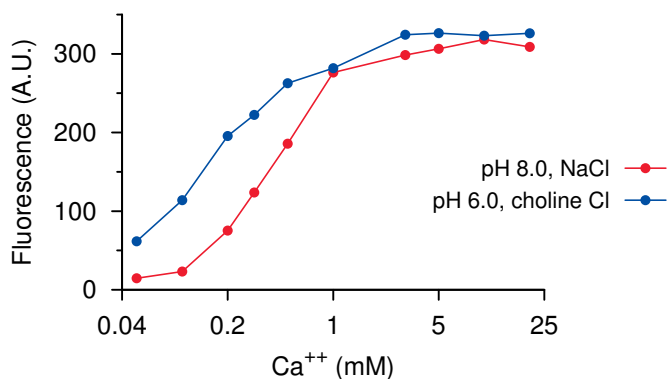


Figure 3.1 Binding of daptomycin to PC/PG membranes under conditions used in permeabilization assays. The binding of daptomycin to membranes can be monitored using its intrinsic kynurenine fluorescence as described.^{107,144} At both pH 6 and pH 8, binding of 1 μ M daptomycin reaches saturation at calcium concentrations lower than 5 mM.

rescence emission at 510 nm was recorded for 5 min, with excitation at 460 nm. Triton X-100 was then added to a final concentration of 0.1%, followed by one more minute of recording; this was done in order to disrupt the liposomes and so to establish the fluorescence intensity equivalent to 100% test solute permeation.

With cationic test solutes, the reaction buffer was similar to the corresponding liposome hydration buffer (see Table 3.1), but the concentration of the test solute was increased to 100 mM, and the pH value from 6.00 to 8.00. With the anionic test solute (Cl^-), the reaction buffer was similar to its hydration buffer, but choline chloride was added to 100 mM, and the pH value was lowered from 8.00 to 6.00. Using the intrinsic fluorescence of the kynurenine residue, we confirmed that daptomycin binds quantitatively to the model membranes under these experimental conditions (see Figure 3.1).

3.2.3 Spectrophotometric measurements

The permeation of thios into the liposomes was measured through reduction of entrapped DTNB, which was measured by its absorption at 412 nm ($\epsilon = 13,400 \text{ M}^{-1}\text{cm}^{-1}$). DTNB-loaded liposomes were diluted to a final concentration of 250 μ M total lipids into the corre-

sponding hydration buffer (Table 3.1) supplemented with 100 mM cysteine and 5 mM Ca^{++} . 1 μM daptomycin was added to initiate the reaction.

3.2.4 Assessment of flow rate of different cations through daptomycin pores

To convert observed changes of pyranine fluorescence to permeation rates of cations, a calibration curve for pyranine fluorescence as a function of pH was recorded. 200 mL of buffer (5 mM MES, 5 mM tricine, 5 mM NaCl, 5 mM KCl, 250 mM sucrose, pH 6.00; the same as used for the liposome interior when testing cation permeation) containing 2 μM pyranine was titrated with 1 M NaOH, while measuring both the pyranine fluorescence intensity at 510 nm and the pH value after each successive addition. The measured curve was fitted with the empirical polynomial function:

$$y = ax + bx^{1/2} + cx^{1/3} + dx^{1/4}$$

The fitted function was then used as a calibration curve to convert the measured time-based fluorescence traces to changes in the intra-liposomal proton concentration.

3.3 RESULTS

3.3.1 Effect of daptomycin on cation permeability

The permeability of liposomes for cations was measured using a coupled fluorescence assay that is based on the pH-sensitive indicator pyranine, whose fluorescence increases with the pH as its phenolic OH group dissociates between pH 6 and 8.5.³⁷ The experimental rationale, with potassium as an example, is illustrated in Figure 3.2. Dilution of the pyranine-loaded liposomes into the final reaction buffer containing 100 mM KCl at pH 8 creates two opposite ion concentration gradients across the liposome membrane: the K^+ concentration is higher outside, whereas the H^+ concentration is higher inside (Figure 3.2A). Addition of the proton

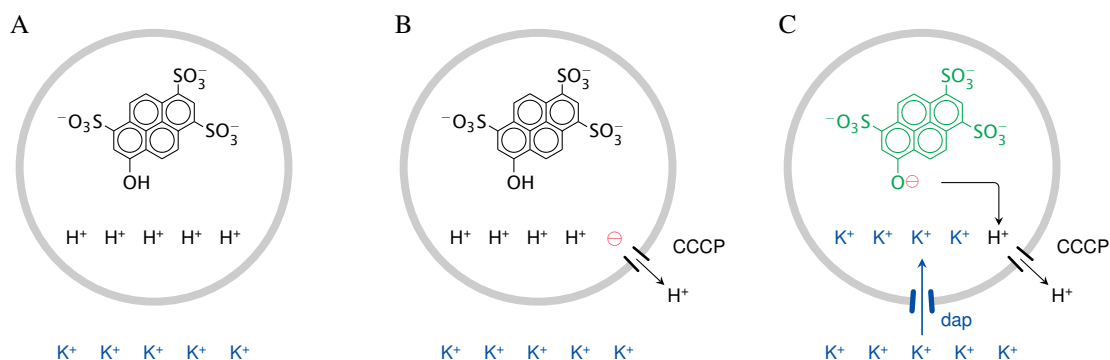


Figure 3.2 Schematic representation of the pyranine-based liposome permeabilization assay, using K^+ ions as an example. Liposomes loaded with pyranine were diluted into the final reaction buffer to create two opposite ion concentration gradients across the membrane (A). Application of the protonophore CCCP alone will create a diffusion potential, which will prevent a major efflux of protons (B). If daptomycin is added also and allows K^+ ions to enter, both ion gradients can dissipate, the pH in the liposome will rise, and pyranine fluorescence will increase (C).

ionophore CCCP alone to this system will cause little change to the pH within the liposomes, since the efflux of protons will very soon be restricted by the ensuing diffusion potential (Figure 3.2B). The internal pH will change significantly only after addition of daptomycin, if, and only if, daptomycin allows the influx of potassium ions. Both ion gradients will then dissipate, the interior pH will rise, and pyranine will dissociate and fluoresce (Figure 3.2C).

The findings obtained using this assay with different cations are illustrated in Figure 3.3. Panel A shows that the experiment works as expected with valinomycin, a potassium-specific ionophore. With potassium, but not with sodium, the combination of valinomycin and CCCP induces a rapid change that indicates swift dissipation of the proton gradient, facilitated by exchange of protons and potassium ions across the membrane. CCCP alone does not induce an appreciable change in fluorescence, while valinomycin alone shows a minor one; it may be that valinomycin has a limited ability to translocate protons bound to it, as has been suggested earlier.¹⁰³

Figure 3.3B shows the same experiment with daptomycin instead of valinomycin. Again, only the combination of daptomycin and CCCP induces a major change of fluorescence, while either agent alone induces negligible changes in fluorescence. This indicates that daptomycin

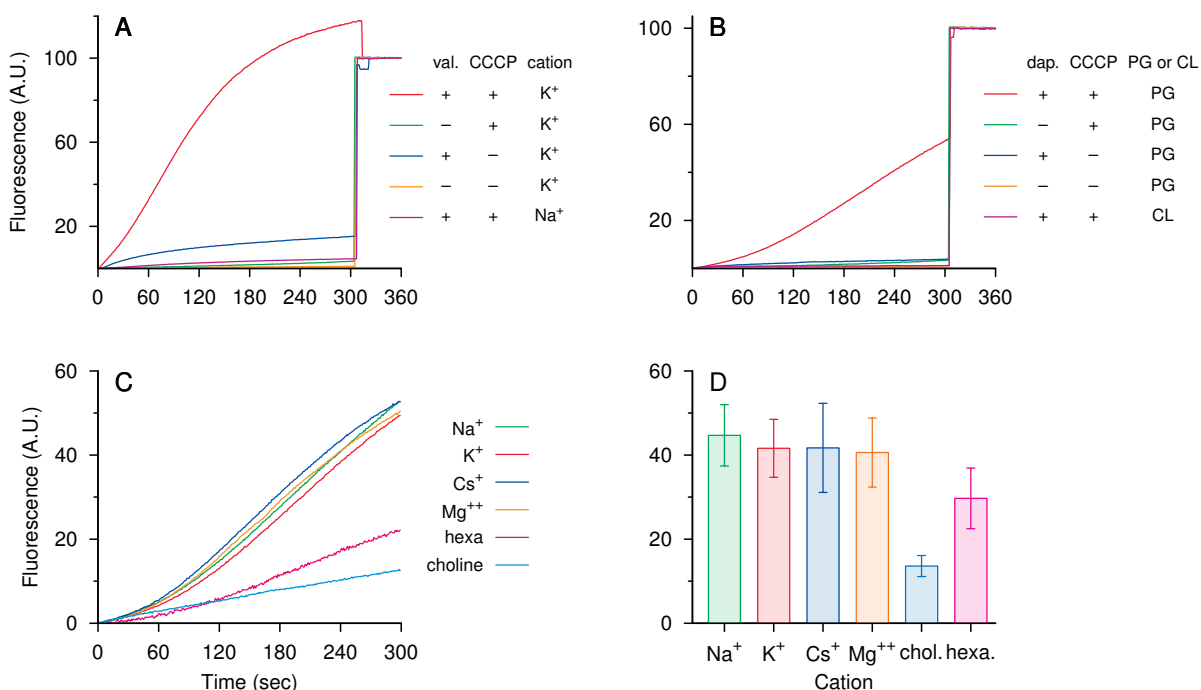


Figure 3.3 Time-based fluorescence traces of pyranine-loaded liposomes after exposure to different test solutes and permeabilizing agents, which were added at $t=0$. The interior pH was 6 and the exterior pH was 8. Test solutes added to the exterior buffer at 100 mM were KCl in B, and otherwise as indicated; “hexa” in C and D is hexamethonium. After 300 seconds, the samples were solubilized with Triton-X100, and the fluorescence monitored for another minute. The fluorescence intensity observed after Triton solubilization was used to normalize each fluorescence trace. A: Valinomycin (val., 0.5 μM) with CCCP (5 nM) permeabilizes liposomes for potassium, but not sodium. B: Daptomycin (1 μM) plus CCCP (5 nM) also causes permeabilization for potassium of membranes containing PG, but not cardiolipin. C: Permeabilization traces obtained with both daptomycin and CCCP present, after subtraction of the traces obtained with CCCP only. D: Averages and standard deviations of fluorescence intensities after 300 seconds of incubation, for 3 or 4 independent experiments performed as in C (“chol.” is choline).

allows the influx of potassium ions. Also note that the rate of fluorescence change induced with daptomycin/CCCP was significantly smaller than with valinomycin/CCCP, which indicates that under the given experimental conditions the rate of fluorescence change was constrained by daptomycin and not by CCCP. This latter conclusion is further supported by the experiments shown in Figure 3.4 and 3.5.

Furthermore, when CCCP was added several minutes after daptomycin in order to allow

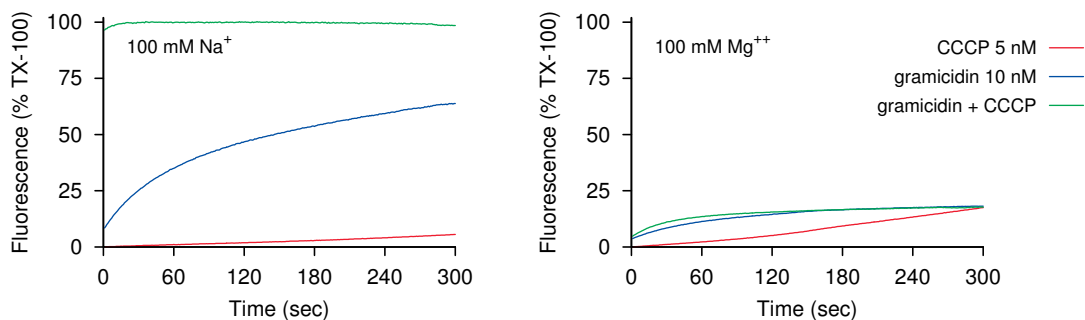


Figure 3.4 Permeabilization of pyranine-loaded liposomes by gramicidin for sodium and magnesium, respectively. Gramicidin forms channels in membranes that are selective for monovalent cations, including protons.⁶⁷ In the presence of sodium (left panel), gramicidin alone suffices to exchange sodium and protons across the liposome membrane. When carbonyl cyanide *m*-chlorophenyl hydrazone (CCCP) is added, complete permeabilization is virtually instantaneous. This indicates that, without CCCP, the rate of exchange was limited by proton transport, in keeping with the low free proton concentration ($1 \mu\text{M}$ inside the liposomes). The extent of permeabilization is minor when sodium is replaced with magnesium.

lead time for daptomycin pore assembly before triggering ion gradient dissipation, the ensuing fluorescence traces were very similar to those obtained with simultaneous application (data not shown). This indicates that the rate of ion flux was not limited by the process of pore assembly, but rather by the permeability of the already assembled pores.

When significantly higher concentrations of daptomycin were employed in combination with CCCP, the rate of permeabilization increased, but there was also a notable increase in the rate of fluorescence change in the absence of CCCP (data not shown). This agrees with a previous study showing that, at higher concentrations, daptomycin destabilizes and induces fusion of lipid bilayers.⁹⁴ We therefore used a concentration of $1 \mu\text{M}$ throughout; this value is similar to minimal inhibitory concentrations in susceptible bacteria.¹⁰⁵

To further investigate the ion selectivity and functional size of the pores formed by daptomycin, the same experimental conditions were used on a series of cations (Figure 3.3C). The various metal ions, choline, and hexamethonium (N,N,N,N',N',N'-hexamethylhexane-1,6-diaminium) were all used as their respective chloride salts and at the same molar concentrations. All metal ions produced a similar rate of fluorescence increase. Similar rates of

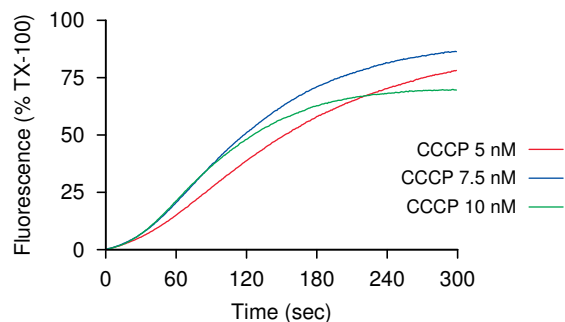


Figure 3.5 Permeabilization for sodium ions with 2 μM daptomycin and 5, 7.5 or 10 nM CCCP (traces with same amounts of CCCP only subtracted). The variation between curves is similar to that also observed between repetitions that use the same amounts of CCCP (compare Figure 3.3D). Overall ion gradient dissipation is clearly limited by daptomycin, not CCCP.

permeabilization were also observed with lithium, rubidium, barium, and calcium (data not shown); however, calcium is also a cofactor of daptomycin activity, which might conceivably skew this measurement. Compared to the metal cations, choline and hexamethonium produced significantly lower increases in fluorescence intensity (Figure 3.3C). Both are organic cations and, in unhydrated form, are larger than the metal ions.

3.3.2 Effect of daptomycin on the permeability for anions

To determine whether daptomycin pores also allow the permeation of anions, the assay format was varied slightly. Pyranine-loaded liposomes with high internal pH (8.00) were diluted into a reaction buffer containing 100 mM choline chloride at low pH (6.00), creating H^+ and Cl^- gradients that point the same way. Choline has been shown above to be only slowly transported by daptomycin, whereas proton transport by CCCP is fast (compare Figure 3.3A); therefore, an influx of chloride should mostly be compensated by a simultaneous influx of protons, lowering the interior pH and causing the fluorescence to drop. This, however, was not observed; the fluorescence intensity was not significantly affected by the presence of daptomycin, with or without CCCP (Figure 3.6A). We conclude that daptomycin pores have no or low permeability for chloride ions.

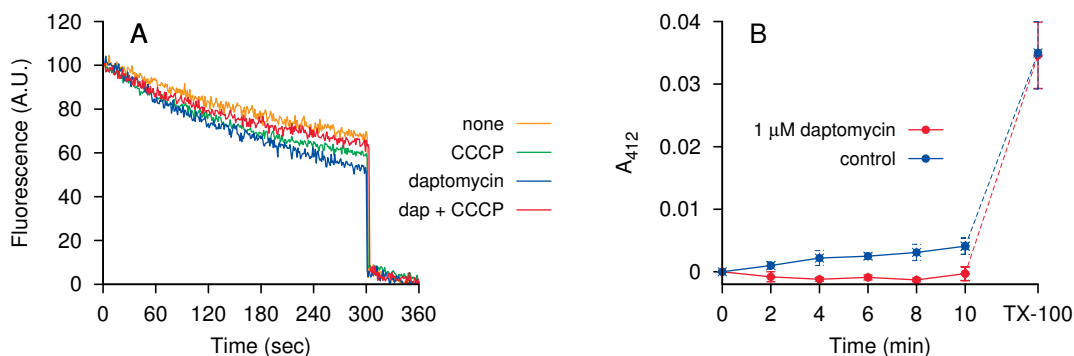


Figure 3.6 Absence of liposome permeabilization toward chloride (A) and cysteine (B). A: Pyranine-loaded liposomes with an interior pH of 6 were diluted 100 mM choline chloride, pH 8, and CCCP (5 nM) and daptomycin (1 μ M) were added at $t=0$. Permeabilization for chloride should have resulted in an accelerated dissipation of the pH gradient and concomitant drop in pyranine fluorescence. The experiment shown is one of 4 independent ones and is representative. B: Time course of reduction of DTNB entrapped in liposomes by 100 mM cysteine added to the outside, in the absence and presence of daptomycin (1 μ M). Reduction of DTNB results in an increase of the absorption at 412 nm. After the last reading at 10 minutes, samples were solubilized with Triton-X100, resulting in immediate complete DTNB reduction. Error bars are standard deviations from three independent experiments. Daptomycin does not increase in the permeation of cysteine into the liposomes.

3.3.3 Effect of daptomycin on the permeability for neutral solutes

DTNB (Ellman's reagent) is useful for the detection of thiol groups in compounds such as cysteine. Its disulfide bond is readily cleaved by thiols to produce 2-nitro-5-thiobenzoate, which absorbs at 412 nm.⁶³ We used it here to test the permeation of thiols across daptomycin pores. In this experiment, DTNB-loaded liposomes were added to a solution containing 100 mM of thiol.

The experiment shown in Figure 3.6B depicts the findings obtained with cysteine. Absorption was measured every 2 min over a period of 10 min, which showed no significant change until 0.1% Triton X-100 was added. Addition of 1 μ M daptomycin did not accelerate the reduction of DTNB (indeed it seemed to slightly delay it), indicating that the daptomycin pore allows no or only slow passage of cysteine across the membrane.

Cysteine has a neutral net charge, but it is not uncharged. Two uncharged thiols, dithiothreitol (DTT) and 2-mercaptoethanol, were also tested. These molecules, however, were found to swiftly enter the liposomes and reduce DTNB even at lower concentrations and in the absence of daptomycin, so that no conclusion could be reached as to their ability to be transported by daptomycin pores.

These findings do not allow us to clearly assess the ability of daptomycin to transport neutral solutes; cysteine transport may be limited either by lack of a positive charge or by its molecular size.

3.3.4 Estimation of the rate of ion flow across daptomycin pores

As illustrated in Figure 3.2, each proton that is to leave the liposome needs to be replaced by one (alkali metals and choline) or one half (magnesium and hexamethonium) cation that enters through a daptomycin pore. Therefore, a given decrease in the total (buffered and unbuffered) proton concentration corresponds to a proportional increase in the concentration of the test cation, and it is thus possible to estimate the rate of permeation through daptomycin pores from the rate of fluorescence change.

The relationship between pyranine fluorescence intensity and total proton concentration was determined empirically using NaOH to titrate pyranine-containing cation hydration buffer. The titration curve was mathematically fitted with an empirical polynomial function (Figure 3.7A), which was then used to convert the previously acquired fluorescence traces to changes of intravesicular cation concentrations (Figure 3.7B). The rates of change are highest for the alkali metal ions and lowest for magnesium and hexamethonium.

In Figure 3.7C, the rate of sodium transport during the first minute was approximated using a single-exponential fit. The parameters of this fit indicate an initial transport rate of 22 μM per second. To estimate the number of ions actually transported, we need to consider that the experiment observes the change in ion concentration only within the intraliposomal volume. Liposomes with 100 nm diameter and at a total lipid concentration of 250 μM should enclose

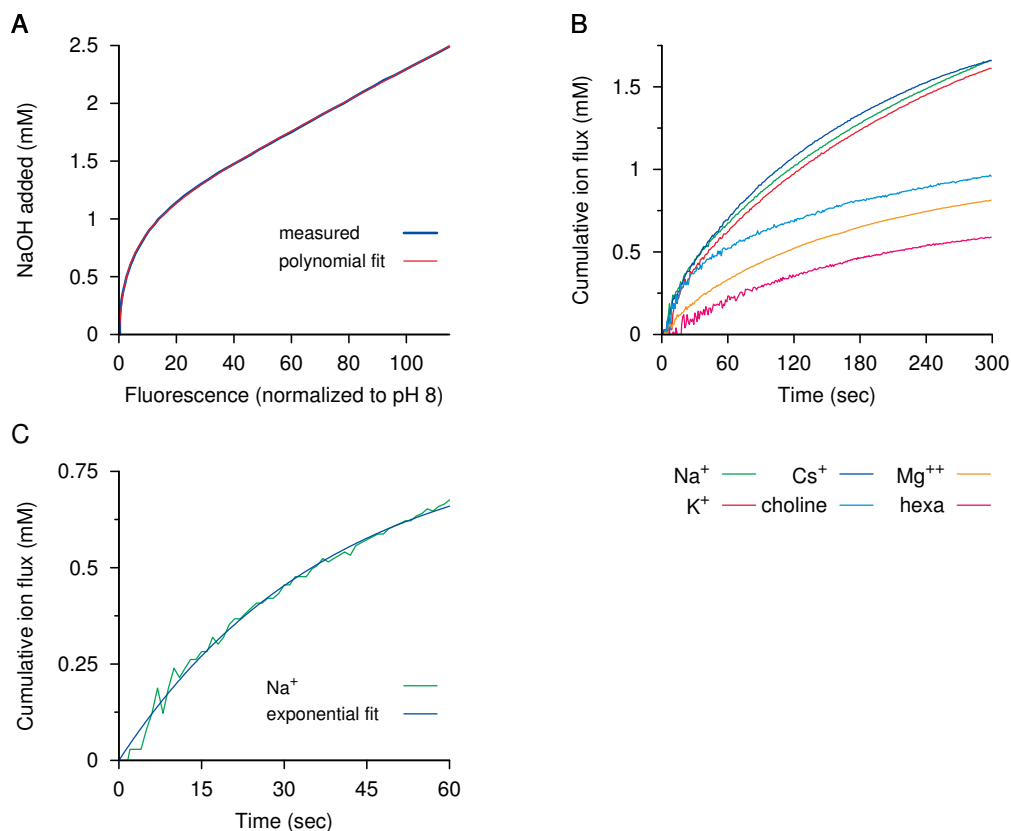


Figure 3.7 Conversion of observed pyranine fluorescence changes to cation flow rates. A calibration curve relating total (buffered and unbuffered) proton concentration to pyranine fluorescence intensity was obtained by titrating a solution matching the liposome interior with NaOH (A). A polynomial function was fitted to the measured values. In panel B, the polynomial function obtained in A was applied to the raw fluorescence traces shown in Figure 3C in order to transform them to ion fluxes. The flow rates for hexamethonium and Mg⁺⁺ were then divided by 2, as each of these cations is exchanged for 2 protons. In C, an exponential function was fitted to the transport curve for sodium in order to estimate the initial transport rate (see text for further details).

approximately 0.08% of the total volume. Therefore, an apparent ion transport rate of 22 $\mu\text{M/s}$ converts to a liposomal entry of only 18 nM/s from the bulk volume. The daptomycin concentration is 1 μM ; if all daptomycin molecules are indeed incorporated into functional pores, and each pore is an oligomer that consists of 7 or 8 subunits,¹⁴³ the average transport rate of each pore is approximately 0.12 sodium ions per second. While this is only a rough estimate, it is clear that ion transport by daptomycin is many orders of magnitude slower than

those of typical cellular ion channels or of gramicidin, which transports upward of 10^6 ions per second under similar conditions⁶⁷ (compare also Figure 3.4).

3.4 DISCUSSION

In previous experiments, it was shown that daptomycin forms oligomers on the membranes of liposomes consisting of PC and PG, as well as on bacterial cells.^{142,144} These oligomers were subsequently shown to contain approximately 7 subunits each¹⁴³ and to be involved in the bactericidal action of daptomycin. We recently proposed a revised and more detailed model, in which the oligomer comprises eight subunits, with four each in the inner and the outer membrane leaflet (see Chapter 4). Earlier studies had established that daptomycin depolarizes the cell membranes of susceptible bacteria.^{3,5,184} From the closely parallel observations obtained with the liposome model and with bacterial cells regarding oligomer formation, the question arose whether the functional daptomycin lesion could also be observed and characterized in the liposome model.

The findings reported here show that this is indeed the case. Daptomycin was found to permeabilize the liposome membranes in a cation-selective fashion. The rate of permeation was virtually the same for all alkali metal ions. It was approximately twice lower for magnesium, and lower again for the organic cations choline and hexamethonium, indicating that the pore also discriminates between different cations, most likely according to size.

When comparing the bare ions, without hydration shells, the two organic cations are much larger than all of the metal ions; both choline and hexamethonium contain tetramethylammonium as a moiety, which has an unhydrated diameter of 5.7 Å. In contrast, when we take the hydration shells into account, magnesium at 8.6 Å exceeds the alkali metals and the organic ions, which are all close to 7 Å (all ionic diameters according to²¹⁰). In membrane nanofiltration experiments,²⁰¹ sodium and potassium have been found to be more permeant than magnesium and calcium, and it was proposed that nanopore permeation involved the partial shedding of hydration shells. Partial dehydration may also be involved in ion permeation across the dapto-

mycin pore. The organic cations bind their hydration shells most weakly;⁸ nevertheless, they are less readily transported than the alkali metal ions, which suggests that daptomycin prefers ions with an effective radius below that of unhydrated choline or hexamethonium. Chloride, in both hydrated and unhydrated forms, is very similar in diameter to potassium; therefore, its exclusion is apparently not caused by size but may be due to electrostatic repulsion between it and one of the several acidic residues on the daptomycin molecule. It seems likely that the pore is also permeable for protons; however, due to the very low free (as opposed to buffered) proton concentration at near neutral pH, this would not result in a rapid dissipation of transmembrane proton gradients and therefore would not be detected in our assay.

The observations reported here agree rather well with previous reports on the permeabilization of bacterial cells. Daptomycin depolarizes *Bacillus* cells and disrupts their uptake of amino acids, which is mostly driven by cation cotransport, but does not induce leakage of already accumulated amino acids.⁵ The major cations that control the membrane potential are potassium and sodium. In an intact cell, the permeability is higher for potassium than for sodium, which creates a negative-inside membrane potential. Changing the permeability balance in favor of sodium will depolarize the membrane. This would occur with either sodium-selective channels or with non-selective pores such as those formed by daptomycin, which indeed reproducibly induces depolarization. Interestingly, one experimental study reported a short-lived yet distinct transient hyperpolarization, followed by depolarization.¹²⁴ The extracellular medium used in that study was low in sodium; in this situation, permeabilization for both sodium and potassium might produce a transient dominance of the strongly negative potassium equilibrium potential, which would then collapse as the cytosol becomes depleted of potassium through continued leakage.

A quantitative estimation of the rate of ion transport for a single daptomycin pore indicated that this rate is several orders of magnitude lower than that of gramicidin, another peptide antibiotic that permeabilizes membranes for cations. It must be noted that the transport rate obtained here for daptomycin is an average value; while it might indeed apply to each of the

functional pores in the ensemble, it is also possible that only a small fraction of all daptomycin oligomers form functional pores, with correspondingly greater permeability, or that the pores alternate between closed and open states, with the latter only prevailing during a small fraction of the time. While the conductivity properties of the individual daptomycin pore must be determined in future experiments, the low average conductivity, compared with a dedicated channel former such as gramicidin, might suggest that pore-formation may be only one of several aspects of daptomycin's bactericidal action. It should, however, be noted that no additional action mode has been biochemically substantiated.¹⁶⁹ Moreover, liposome permeabilization is readily observed with daptomycin concentrations equivalent to typical MIC values,¹⁸⁴ even though the ratio of daptomycin molecules to membrane lipids is lower in a liposome experiment than in a bacterial culture freshly inoculated for MIC measurement; this supports the notion that membrane permeabilization is relevant to antibacterial activity.

In sum, our study shows that a very simple artificial membrane model suffices to elicit and characterize the pore-forming activity of daptomycin. The only lipid specifically required for pore formation in our model is PG. A key role for PG *in vivo* is consistent with several studies on the causation of bacterial resistance to daptomycin.^{12,72,79} The availability of a simple yet sufficient liposome model for daptomycin pore formation should be useful in further characterizing the structure and action mode of daptomycin, as well as the molecular basis of bacterial resistance.

Chapter 4

Cardiolipin Prevents Membrane Translocation and Permeabilization by Daptomycin

4.1 INTRODUCTION

The antibacterial action mode of daptomycin (Figure 4.1) is not yet fully understood and may be multifaceted. Membrane permeabilization and interference with cell division have been demonstrated, whereas inhibition of cell wall synthesis remains somewhat contentious.¹⁰⁵ Membrane permeabilization can be observed in model liposomes and involves the formation of an oligomeric and cation- and size-selective pore, as detailed in the preceding chapter. Oligomerization and pore formation require phosphatidylglycerol (PG),¹² which is abundant in bacterial cell membranes but not in mammalian ones; this presumably contributes to the selectivity of the drug for bacteria.^{12, 78, 79, 137}

The results presented in this chapter have been published in: “Cardiolipin Prevents Membrane Translocation and Permeabilization by Daptomycin”, by TianHua Zhang, Jawad K. TianHua Zhang, Nasim Tishbi, Jennifer Herskowitz, Rachel L. Victor, Jared Silverman, Stephanie Uwumarenogie, Scott D. Taylor, Michael Palmer, and Evan Mintzer (2014), *J. Biol. Chem.* 289: 11584-91

Authors’ contributions: The experiments depicted in Figure 4.5 and 4.6 were performed by N. Tishbi, J. Herskowitz, R.L. Victor, and E. Mintzer. The synthesis and purification of perylene-daptomycin was performed by S. Taylor. All other experiments were done by the thesis author.

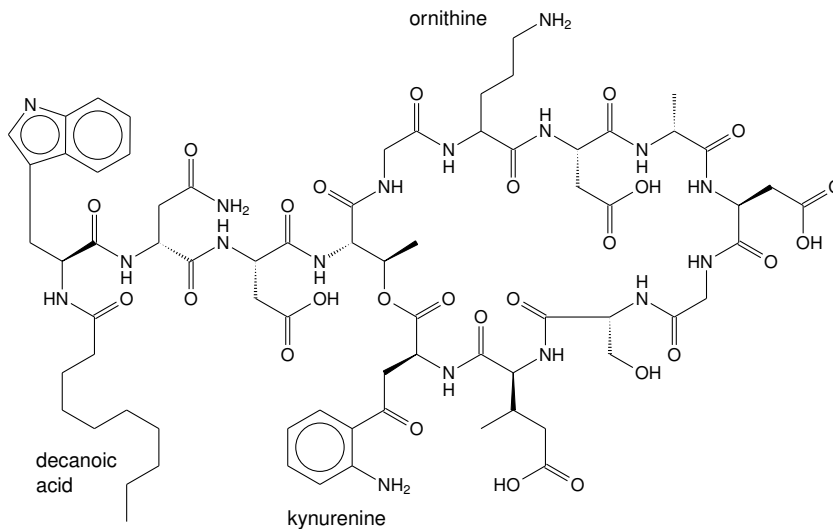


Figure 4.1 Structure of daptomycin. In NBD-daptomycin, the free amino group of ornithine is modified with NBD. In perylene-daptomycin, the N-terminally attached decanoyl residue is replaced by perylene-butanoic acid.¹⁴² Kynurenine has intrinsic fluorescence that can be used for FRET experiments in conjunction with NBD.¹⁴⁴

Since its approval for clinical use in 2003, daptomycin has assumed a major role in the treatment of infections with Gram-positive pathogens. Although the overall resistance situation is currently still favorable, resistant strains of *Staphylococcus aureus* and *Enterococcus* species occur. Genomic analysis of resistant strains indicate that resistance may involve changes in the lipid composition of the bacterial cell membrane. Such changes include the reduced synthesis of PG⁷⁹ and the increased conversion of PG to lysyl-phosphatidylglycerol (lysyl-PG).⁷² Because lysyl-PG is positively charged, it likely detracts from the calcium-mediated membrane binding of daptomycin, which would resemble its known inhibitory effect on cationic antimicrobial peptides.

Another set of mutations implicates cardiolipin. Mutations that enhance cardiolipin synthase activity⁴⁴ were found in resistant *Enterococcus* strains,¹⁵⁸ although replacement of the wild-type synthase with a mutant gene into a wild-type *Enterococcus faecalis* strain did not detectably change the susceptibility to daptomycin.²⁰⁷ Quantitative data on cardiolipin membrane levels in daptomycin-resistant *Enterococcus* strains are not available; therefore, whether

or not changes in cardiolipin content can increase the daptomycin resistance in vivo remains to be elucidated. Here, we examined the question whether or not cardiolipin can in principle affect the susceptibility of membranes to daptomycin. We found that cardiolipin may indeed protect lipid membranes from permeabilization. The inhibitory mechanism of cardiolipin is novel and surprising, and it provides further insight into the mechanism of daptomycin pore formation.

4.2 MATERIALS AND METHODS

4.2.1 Preparation of liposomes (LUV) for fluorescence experiments

The procedures for preparing the large unilamellar vesicles have been described in a preceding chapter (see Section 2.2.2). Lipid tetraoleyl-cardiolipin (TOCL) was also obtained from Avanti Polar Lipids (Alabaster, AL) and used as received. All lipids were mixed at the molar ratios indicated under “Results” (Section 4.3). All experiments involving these liposomes were carried out at 30 °C.

4.2.2 Preparation of liposomes (LUV) for ITC experiments

LUV were prepared using the freeze-thaw and extrusion method as described in Chapter 2. Lipid films were prepared by mixing appropriate volumes of pure DOPC, DOPG, and TOCL (Avanti) from stock solutions in chloroform and evaporating the solvent under a stream of nitrogen. The resulting films were hydrated in HBS (10 mM HEPES, 100 mM NaCl, 1 mM CaCl₂, pH 7.4) to a final total lipid concentration of 5 mM.

4.2.3 Measurement of membrane permeabilization with pyranine-loaded liposomes

This procedure was carried out exactly as described in the preceding chapter (Section 3.2.2).

4.2.4 Measurements of perylene excimer fluorescence

Perylene-daptomycin was prepared as described before.¹⁴² The compound was added to LUV at 2 μ M. Calcium was added to 5 mM, the samples were incubated for 5 min, and the fluorescence emission was recorded with excitation at 430 nm.

4.2.5 Isothermal calorimetry

Energetics of daptomycin binding to model membranes was investigated by high sensitivity isothermal titration calorimetry using a MicroCal VP-ITC instrument (GE Healthcare) as described in Section 2.2.3. Briefly, the sample cell (\sim 1.4 mL) was filled with 23 μ M daptomycin prepared in HBS containing 1 mM calcium, and the reference cell was filled with identical buffer. The 250- μ L syringe was loaded with 5 mM total lipid LUV suspension. Daptomycin solutions and lipid suspensions were degassed with stirring under vacuum for 20 min prior to each titration. After system equilibration and a preliminary 1 μ L injection that was omitted from data analysis, 2.5 μ L aliquots were injected into the sample cell at 6 min intervals. Data were collected by the MicroCal-customized Origin software. Baselines were normalized using the software Nitpic,⁹⁹ and the results were analyzed with the Origin “one binding site” model.

4.2.6 Langmuir monolayers

The ability of daptomycin to penetrate lipid monolayers was examined using a Langmuir surface balance and custom-built mini-trough from KSV-Nima (Biolin Scientific, Espoo, Finland). The aqueous subphase was HBS with 1 mM calcium, prepared with water purified through a Milli-Q system (Millipore, Molsheim, France). Lipid solutions were prepared by dissolving DOPC, DOPG, and TOCL in spectroscopy-grade chloroform to concentrations of \sim 1 mg/mL. The trough was filled with buffer, and the surface was cleaned by aspirating. Small aliquots of lipid solution were applied to the surface using a Hamilton digital syringe (Reno, NV) until an initial surface pressure of 20 mN/m was obtained. After allowing 10 min for solvent evaporation and monolayer equilibration, 50 μ L of 1 mM daptomycin, prepared in identical buffer,

were injected into the stirred subphase through a side port to avoid puncturing the monolayer. Daptomycin insertion into the lipid monolayer was monitored over time and detected by surface pressure increase at constant area. Each experiment was performed at least in triplicate.

4.2.7 Determination of daptomycin oligomer subunit stoichiometry by FRET

Nitrobenzoxadiazole-daptomycin (NBD-daptomycin) was prepared as described previously.¹⁴⁴ Fluorescence experiments and data analysis, too, were performed exactly as described before,¹⁴³ except that the lipid composition of the liposomes was varied as indicated in Section 4.3. Briefly, the stoichiometry is inferred from the extent of FRET between native daptomycin and NBD-daptomycin within hybrid oligomers, using the assumption of random co-assembly and experimental correction for FRET between neighbouring oligomers.

4.2.8 Dithionite quenching of NBD fluorescence

For the experiment shown in Figure 4.8A, NBD-phosphatidylethanolamine (NBD-PE) was obtained from Avanti and incorporated at 0.5% mol/mol into LUV that otherwise consisted of equal fractions of PC and PG. The liposomes were diluted into HBS supplemented with 25 mM calcium. We found it necessary to raise the concentration this high from the usual value of 5 mM to induce reaction between dithionite and liposomes containing PG; we assume that calcium alleviates the electrostatic repulsion between PG and dithionite. Daptomycin was added to 1 μ M where indicated, and the samples were incubated for 5 min before starting the fluorescence measurement (excitation wavelength, 465 nm; emission wavelength, 530 nm). After 1 min, dithionite was added (final concentration 10 mM), and the measurement was continued for another 5 min before the addition of Triton X-100 to solubilize the liposomes.

The experiments illustrated in Figure 4.8B were performed analogously, except that NBD-PE was omitted from the liposomes, and daptomycin was replaced with a mixture of NBD-daptomycin and native daptomycin (molar ratio 1:2; total final concentration 1 μ M). The inclusion of native daptomycin served to reduce NBD self-quenching.

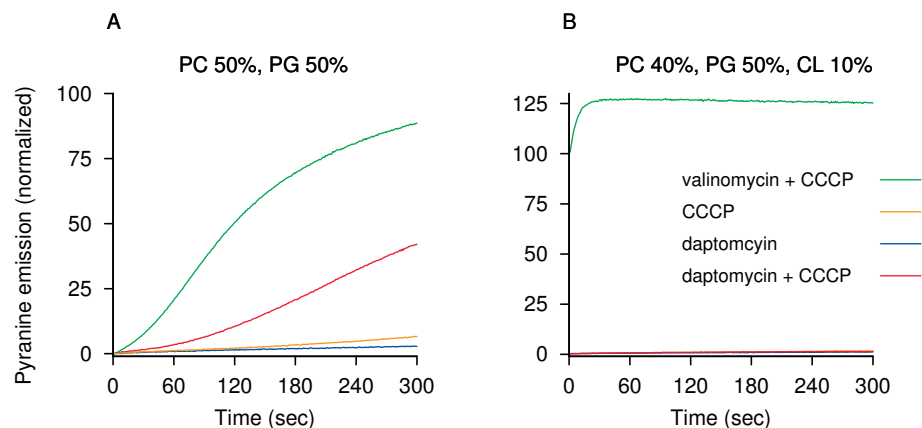


Figure 4.2 Permeabilization by daptomycin of liposomes composed of PC and PG (A) and PC, PG, and CL (B). The pH-sensitive fluorophore pyranine was entrapped in liposomes. The increase in its fluorescence by the efflux of protons was mediated by carbonyl cyanide *m*-chlorophenylhydrazone (CCCP), in exchange for potassium influx mediated by valinomycin (green) or daptomycin (red). Valinomycin is active on both membranes (but acts faster on the ones containing CL), whereas daptomycin permeabilizes only the membranes devoid of CL. The fluorescence intensity is scaled to that observed after solubilization with Triton X-100, which equals 100 units.

4.3 RESULTS

4.3.1 Cardiolipin Inhibits Membrane Permeabilization by Daptomycin

In the preceding chapter, we showed that daptomycin forms cation-selective pores of discrete size in liposomes composed of PC and PG. As shown in Figure 4.2, the addition of as little as 10% cardiolipin completely inhibits this pore formation.

In previous studies, we have shown that membrane permeabilization by daptomycin occurs in several successive stages, namely, monomer binding, oligomerization, and conversion of the oligomer to a functional pore.^{142–144} The following experiments were carried out to determine which of these stages is subject to inhibition by cardiolipin.

4.3.2 Binding and oligomerization of daptomycin on membranes containing cardiolipin

The binding of daptomycin to lipid membranes correlates with a strong increase in the intrinsic fluorescence of its kynurenine residue.¹⁰⁷ Binding also requires calcium, and the calcium con-

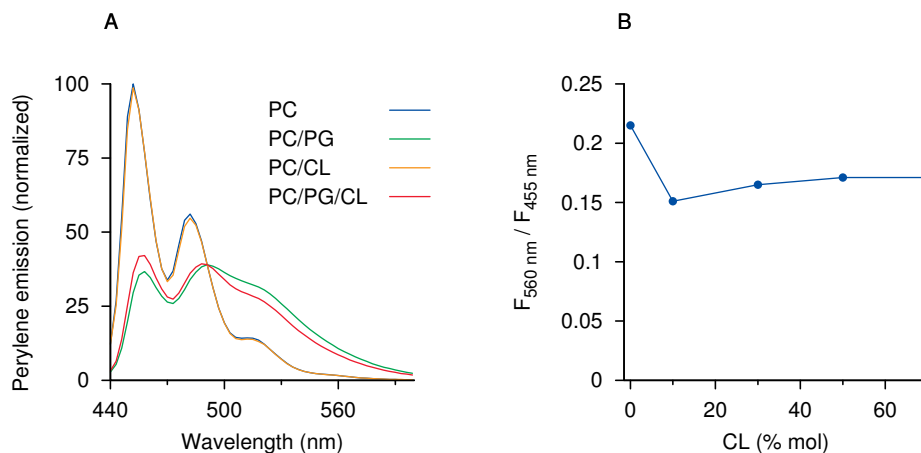


Figure 4.3 Fluorescence of perylene-daptomycin on liposomes containing PC alone or in various combinations with PG (mole fraction 30%) and CL (mole fraction 10%). A, on PC membranes as well as on PC/CL membranes, the spectrum is characteristic of the perylene monomer, indicating that oligomer formation does not occur. PC/PG membranes with or without 10% CL show a diminished monomer peak and a broad, overlapping excimer peak indicative of oligomer formation.¹⁴² The extent of excimer formation is slightly lower in the sample with CL. B, the ratio of emissions at 560 and 445 nm can be used to compare the extent of excimer formation. This ratio is shown here as a function of the CL mole fraction (0–70%). PG was constant at 30%, and the balance was made up by PC.

centration required to induce the half-maximal extent of this fluorescence increase ($[Ca]_{50}$) can be used to compare the affinity of daptomycin for membranes differing in lipid composition. The $[Ca]_{50}$ is ~ 12 mM calcium with pure DMPC membranes, 0.2 mM with DMPC/DMPG membranes (1:1), and 2 mM with DMPC/TOCL membranes. Thus, CL binds daptomycin more avidly than PC but less avidly than PG. When CL is added to PC and PG, the $[Ca]_{50}$ remains close to 0.2 mM, which suggests that on such membranes, daptomycin interacts with PG rather than CL (data not shown).

Oligomerization of membrane-bound daptomycin can be observed through excimer formation of a perylene-labeled daptomycin derivative.¹⁴² Figure 4.3A shows the fluorescence of perylene-daptomycin on membranes containing PC, PG, and CL in various combinations. As reported before,¹⁴² the emission spectrum observed on PC membranes is typical of perylene monomers, indicating the absence of daptomycin oligomer formation. On membranes con-

sisting of PC and PG, monomer intensity is reduced, and an overlapping, broad-based peak excimer peak centered around 520 nm appears, indicating daptomycin oligomer formation on these membranes.

The spectrum obtained with membranes containing PC and CL, but no PG, closely resembles the one from pure PC liposomes. Therefore, unlike PG, cardiolipin does not induce oligomerization of daptomycin. In contrast, membranes that contain both PG and CL do induce formation of excimers, and hence of daptomycin oligomers.

The extent of excimer formation can be compared using the ratio of the emission at 560 nm, where monomer fluorescence is negligible, with that at 455 nm, where monomer fluorescence is dominant. In Figure 4.3B, this ratio is shown as a function of CL molar fraction in the membrane. The extent of excimer formation drops noticeably from 0 to 10% CL and then increases slightly again as more CL is added. The potential significance of this finding is discussed below.

Another method for observing daptomycin oligomerization is the use of FRET between the kynurenine residue of the unlabeled molecule and the fluorescent label NBD attached to the ornithine side chain of a second daptomycin molecule; the NBD derivative retains full antibiotic activity.¹⁴⁴ This method has also been used to estimate the number of subunits in a single daptomycin oligomer to 6–7.¹⁴³ In those previous experiments, PC/PG membranes were used, which allow the formation of functional pores (Figure 4.2A). Because the addition of CL prevents pore formation, we considered that the oligomers that form in the presence of CL might be structurally different and contain a different number of subunits.

The experimental approach used in this experiment is fully explained in a previous study.¹⁴³ Briefly, native daptomycin and NBD-daptomycin are mixed in various proportions and then applied to liposome membranes. Interpretation is based on the assumptions of 1) oligomer stability on the time scale of the experiment, 2) random co-oligomerization, and 3) maximally effective FRET between the subunits of the same oligomer. Then, using experimental corrections for FRET between molecules that are part of separate oligomers, the number of subunits

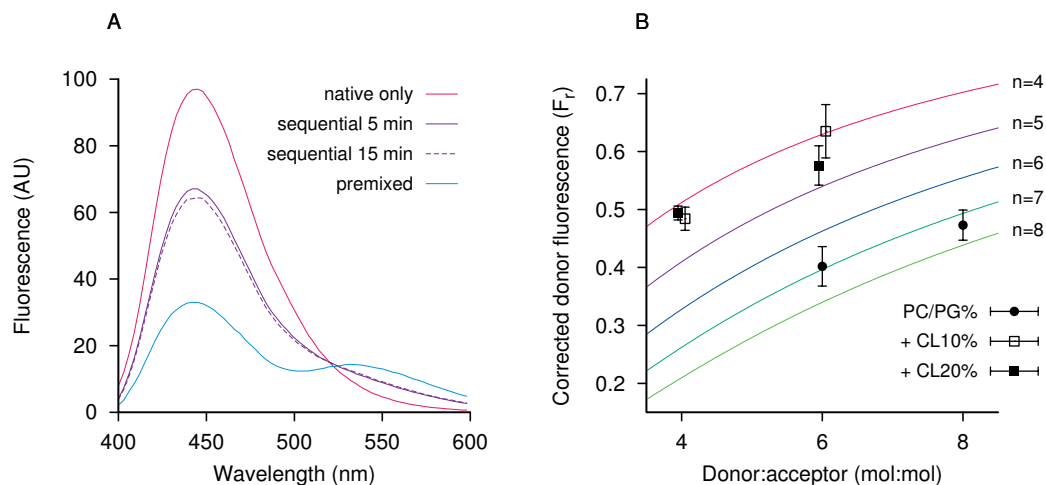


Figure 4.4 Estimation of subunit stoichiometry of the daptomycin oligomer by FRET between native daptomycin (donor) and NBD-daptomycin (acceptor). A, native daptomycin (3 μM final) and NBD-daptomycin (0.5 μM final) were added to liposomes containing PC (40%), PG(50%), and CL (10%), either sequentially, with incubation for 5 min between additions, or premixed. Emission spectra were acquired 5 and 15 min after the final addition. The peak at 450 nm represents the kynurenine emission of native daptomycin, whereas the peak at 540 nm is due to NBD. The donor emission of the sequential sample is higher than that of the premixed sample, which is due to the formation of segregated, stable oligomers. It is lower than that of donor alone, which is due to FRET between those segregated oligomers. The emission of the sequential sample remains almost the same after 15 min, which shows that the oligomers are stable on the time scale of the experiment. AU, arbitrary units. B, the two species were mixed before application to liposomes containing PG (50%), CL (0–20%, as indicated), and PC (balance to 100%) to induce the formation of hybrid oligomers. The corrected relative donor fluorescence (F_r) was obtained as described in reference.¹⁴³ The colored lines represent theoretical F_r functions for the indicated numbers of subunits; each data point represents the means \pm SD of 3 or 4 repeated experiments.

can be calculated from the reduction of donor fluorescence intensity that is observed in the presence of a given amount of acceptor.

Figure 4.4 shows that, indeed, the presence of cardiolipin changes the subunit stoichiometry. With cardiolipin, there were close to four subunits, whereas without CL, the number was close to seven, which is similar to the previously reported value.¹⁴³ These observations will be further discussed below.

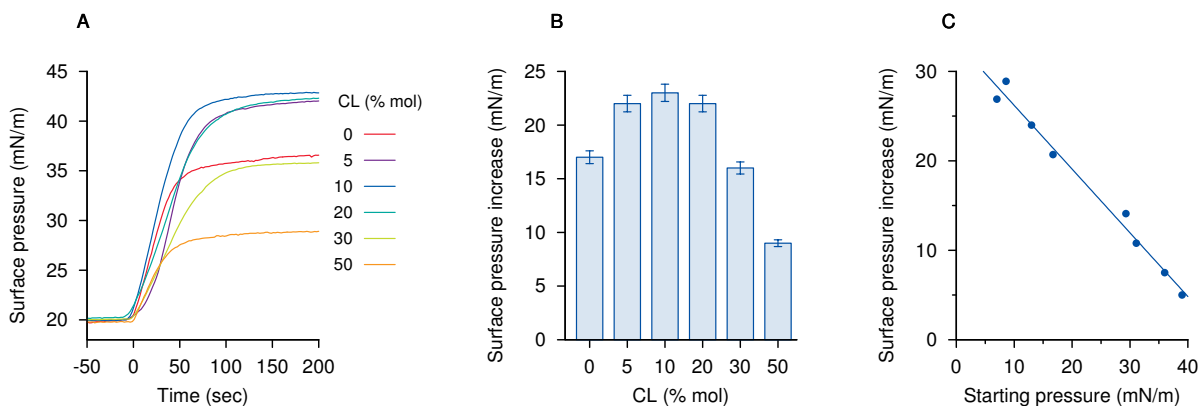


Figure 4.5 Surface pressure change of lipid monolayers consisting of CL (% mol/mol as indicated) and equal fractions of PC and PG, in response to injection of daptomycin into the subphase. A, time profiles; daptomycin was injected at $t = 0$ and at an initial surface pressure of 20 mN/m. B, changes in surface pressure derived from the data in panel A. Results were reproducible to within 5% ($n=3-5$). Each data point represents the means \pm SD of 3–5 repeated experiments. C, surface pressure change as a function of initial pressure on PC/PG membranes without CL. The surface pressure increment drops linearly with the starting pressure. The slope of the regression line is -0.885 ; at a slope of -1 , the final surface pressure would be entirely independent of the starting pressure.

4.3.3 Interaction of daptomycin with membranes containing CL by surface pressure and isothermal calorimetry (ITC)

To better understand the effect of CL on the membrane interaction of daptomycin, we studied a similar model system with Langmuir monolayers and with ITC. The insertion of daptomycin into PC/PG lipid monolayers can be observed as an increase in surface pressure. The addition of CL to this lipid mixture up to a molar fraction of 10% substantially enhances this response (Figure 4.5, A and B). This increase in the surface pressure differential indicates a deeper and/or more stable insertion of daptomycin molecules into monolayers containing CL. The surface pressure differential decreases again when CL is added to molar fractions of 20% or greater.

ITC was performed with LUV, which were added to a solution of daptomycin and calcium. Figure 4.6 shows that, relative to liposomes containing PC and PG only, the addition of CL up

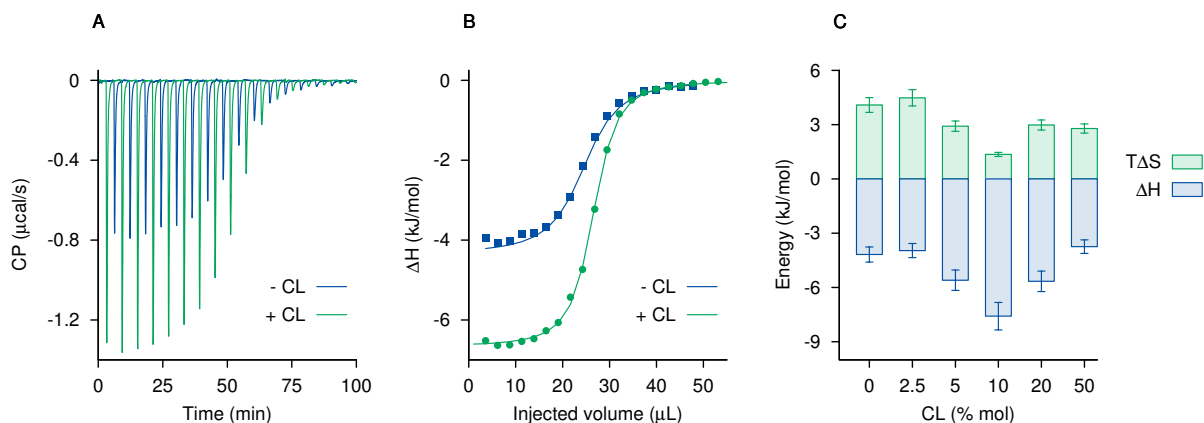


Figure 4.6 ITC experiments on daptomycin binding to PC/PG membranes with or without CL. A, representative raw traces. Each peak is caused by the injection of $2.5 \mu\text{l}$ of liposome suspension (see Section 4.2.5 for experimental details). B, integrals (data points) and single-site model fit curves for the traces shown in A. C, energies of interaction between daptomycin and liposome membranes (mole fraction of CL as indicated, balance of equal parts of PC and PG) obtained from a series of isothermal titrations ($n=2$ or 3 at each lipid composition). Each data point represents the means \pm SD of 3 or 4 repeated experiments.

to a molar fraction of 10% raised the enthalpy released by daptomycin binding significantly. This increase in negative enthalpy indicates a greater number of favorable molecular interactions between daptomycin and the lipid molecules of the membrane, which is consistent with the deeper membrane insertion of daptomycin molecules inferred from the surface pressure experiments.

The increase in negative enthalpy was accompanied by a decrease in entropy, as obtained by fitting a single-site binding model to the raw data. At a molar fraction of 20% or more CL, the changes to both the enthalpy and the entropy were partially reversible.

It may be noted that the response to changes in CL molar fraction was similar in three different assays, namely surface pressure, ITC, and perylene excimer fluorescence, which suggests that these assays reflect the same underlying effect of CL on the membrane interaction of daptomycin. In all three assays, the maximum signal was observed at a CL mole fraction of 10%, whereas higher mole fractions caused a partial reversal. We currently have no experimental basis on which to propose an explanation for this reversal. It may be noted that

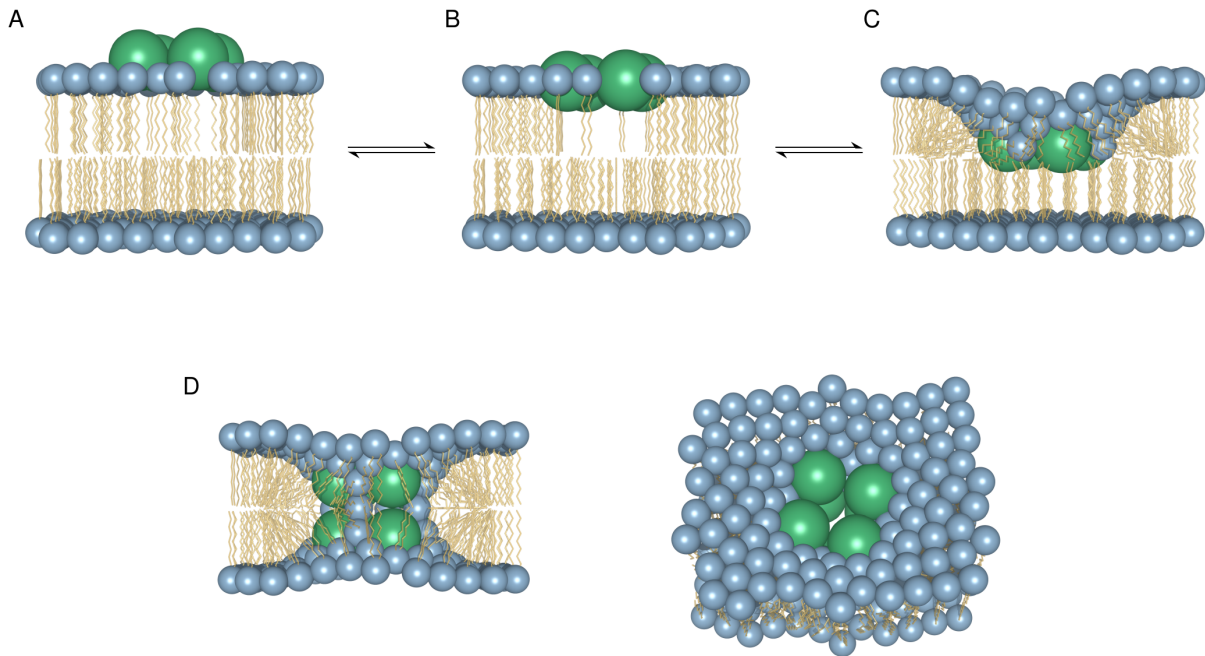


Figure 4.7 Hypothetical model of daptomycin membrane insertion, pore formation, and pore structure. A daptomycin tetramer forms in the outer membrane leaflet (A). Its insertion into the head group layer is limited by the distension and creation of voids in the acyl chain layer (B); this is unfavorable in terms of enthalpy and increases disorder (entropy). If CL is present, it provides extra bulk in the acyl chain layer, which stabilizes this situation and thus allows for deeper penetration of daptomycin. If CL is not present (C), head group distension and voids in the acyl layer may alternatively cause the outer leaflet to cave in, forming a half-toroidal structure. A tetramer as shown in C may flip to the other leaflet and then combine with a second tetramer in the outer leaflet, which gives an octameric pore (D).

molar fractions of CL higher than 10% are not common in bacterial membranes, so that this observation may not be relevant to the interaction of CL and daptomycin *in vivo*.

4.3.4 Cardiolipin inhibits membrane translocation of daptomycin

One question that had not been addressed in our previous studies is how daptomycin distributes between the two leaflets of the target membrane. The observation that cardiolipin both prevented pore formation and reduced the number of oligomer subunits by approximately half suggested the possibility that a functional pore might comprise subunits in both leaflets,

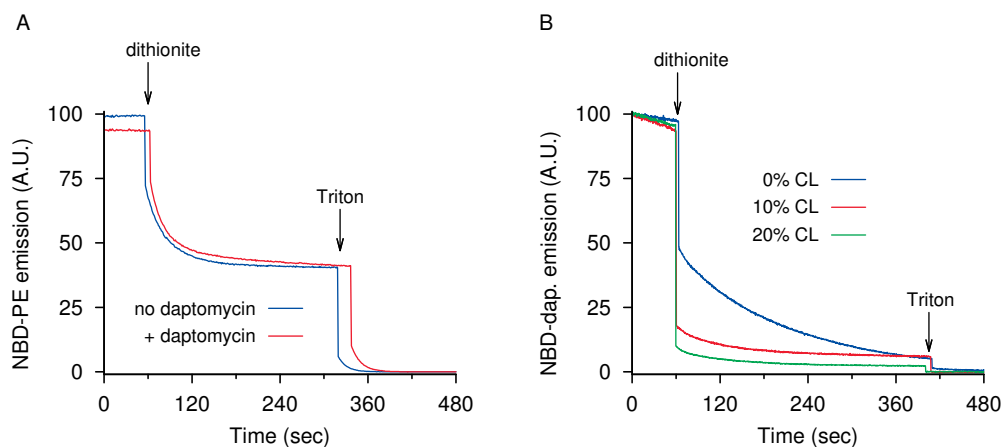


Figure 4.8 Distribution of daptomycin across inner and outer leaflets, examined with NBD fluorescence quenching using dithionite. **A:** Control. Dithionite (10mM) reduces only 50% of NBD-PE (0.5% in PC/PG membranes), both in the absence and in the presence of daptomycin. Therefore, dithionite continues to be excluded from membranes in the presence of daptomycin pores. A. U., arbitrary units. **B:** In PC/PG membranes containing 10 or 20 % CL, most of the NBD-daptomycin (NBD-dap) is reduced by dithionite instantly, indicating that it is confined to the outer leaflet. In contrast, in PC/PG membranes containing no CL, immediate reduction affects only 50% of NBD-daptomycin, whereas the remainder is reduced at a slower pace, presumably rate-limited by redistribution from the inner to the outer leaflet.

whereas the nonfunctional oligomers that form in the presence of cardiolipin might be confined to the outer membrane leaflet only (Figure 4.7). This hypothesis was tested using the fluorescence of NBD-daptomycin and its sensitivity to quenching with dithionite.

NBD is instantly reduced, and its fluorescence is abolished, by dithionite. Because dithionite is membrane-impermeant, this reaction can be used in liposome models to detect the accessibility of membrane-associated molecules from the outside.¹²⁸ A potential complication that arises here, however, is that daptomycin pores might allow dithionite to reach the liposome interior and reduce NBD-daptomycin also bound to the inner leaflet. Therefore, in a control experiment, a small amount of NBD-PE was incorporated into PC/PG liposomes, and its reduction by dithionite was monitored both with and without daptomycin. In both cases, the extent of reduction is close to 50%, which is consistent with a reduction of NBD-PE in the outer leaflet only (Figure 4.8A). Thus, in keeping with the observed cation selectivity of the dapto-

mycin pore that was discussed in the preceding chapter, dithionite does not appreciably enter the liposomes on the time scale of the experiment. Dithionite was also excluded by liposomes containing CL in addition to PC and PG, with or without daptomycin (data not shown).

Figure 4.8B depicts the results obtained with NBD-daptomycin; no NBD-PE was present in these experiments. When NBD-daptomycin was bound to membranes containing PC, PG, and either 10% or 20% CL, almost all NBD fluorescence was immediately quenched. In contrast, the extent of immediate quenching was only about 50% in membranes that contained PC and PG but no CL. The remainder of the fluorescence decayed more slowly with a half-life of ~60–90 s, which is presumably due to the redistribution of daptomycin from the inner to the outer leaflet. These findings support the notion that daptomycin is able to distribute symmetrically and reversibly between both membrane leaflets in PC/PG membranes, but unable to translocate across membranes containing 10 or 20% CL.

4.4 DISCUSSION

In this study, we have shown that cardiolipin inhibits the pore-forming activity of daptomycin in a liposome model. This study was prompted by genetic studies on daptomycin resistance, which suggest that bacteria may become more resistant to daptomycin by increasing the content of cardiolipin in their cell membranes. We found that inclusion of 10% CL in model membranes was sufficient to effectively suppress membrane translocation and pore formation in liposomes. This fractional amount of CL is at the upper end of the range reported for bacterial cell membranes,^{36,50,134} which suggests that this mechanism may be relevant for bacterial resistance to daptomycin. Formation of daptomycin pores in bacterial cell membranes, as detected by membrane depolarization, is well documented.^{3,124,184} It seems possible that an increased cardiolipin content would inhibit pore formation *in vivo*; however, this has yet to be experimentally examined. Daptomycin may also damage bacteria by more than one mechanism. If so, inhibition of pore formation may not suffice to prevent bactericidal action, and

additional resistance mechanisms would then be required to counter the other antibacterial action modes of the drug.

Whether or not the effect of CL observed *in vitro* has a role in bacterial resistance, the findings of our study do provide significant new insight into the mechanism of daptomycin action. Firstly, they show that oligomers can form in the outer leaflet alone. However, these oligomers do not form functional pores, and they do not reach the full number of subunits; instead, they contain only four subunits. Pore formation correlates with daptomycin reaching the inner membrane leaflet, and with an increase in the apparent subunit stoichiometry to 6–7.

To account for the collective findings, we propose a working model of pore formation that comprises the following steps (Figure 4.7): 1) calcium-mediated binding of monomeric daptomycin to PG in the outer leaflet of the target membrane; 2) formation of a tetramer from four bound monomers (this step occurs in the outer leaflet and is preserved in membranes that contain cardiolipin); 3) translocation of tetramers from the outer leaflet to the inner leaflet (this step is disrupted on membranes containing CL); and 4) alignment of two tetramers in the opposite leaflets to form an octameric functional pore.

In such an octamer, half of the subunits are located in the outer leaflet and hence subject to reduction by dithionite right away. The observation that the remainder of the NBD fluorescence is subject to protracted but ultimately complete reduction indicates that the translocation from the outer to the inner leaflet is reversible. The reverse translocation might conceivably involve the dissociation of octamers into tetramers. However, we could find no evidence of such a dissociation in preliminary experiments, and we therefore favor the view that translocation comes about through the trading of places between individual subunits within an intact octamer.

Although this model accounts for most of the available evidence without contortions, the postulated octamer obviously is at odds with the subunit stoichiometry (n) of 6–7 that was experimentally obtained with PC/PG membranes here and earlier.¹⁴³ Two effects might account for this discrepancy. Firstly, it is possible that not all tetramers assemble into octamers. In that case, the experimentally determined number would reflect an average of tetramers and

octamers, weighted for abundance. However, because we could not detect dissociation of octamers into tetramers, it seems likely that the number of free tetramers is low at equilibrium.

Secondly, as was pointed out in our previous study,¹⁴³ the stoichiometry obtained from FRET experiments may underestimate the true value. The efficiency of FRET is limited by the Förster distance, which was estimated to 2.7 nm for the couple of donor and acceptor labels used here (kynurenine in unlabeled daptomycin and NBD-daptomycin, respectively). The distance between subunits that belong to the same oligomer, yet reside in opposite membrane leaflets, might approach or even exceed this value, which would significantly diminish FRET. Because our analysis assumes FRET to be maximally effective between any two positions within the same oligomer,¹⁴³ a less than maximal FRET efficiency will cause the calculated number of subunits to underestimate the true value. Based on the currently available evidence, we consider this the most likely explanation.

If we assume the above model to be correct, the question arises exactly how cardiolipin may inhibit membrane translocation of daptomycin tetramers. This inhibitory effect was accompanied by several other changes. The slight drop of perylene excimer fluorescence (Figure 4.2B) may correspond to the fraction of excimers that form between perylene-daptomycin molecules in two opposite tetramers that are part of the same octamer, whereas the remaining excimer fluorescence arises from proximity within single tetramers. In liposomes, CL effected a notable increase in daptomycin binding enthalpy, which suggests an increase in the number of favorable molecular contacts.¹ In lipid monolayers, CL caused a greater increase in surface pressure in response to a given quantity of daptomycin. This suggests a deeper insertion of daptomycin into membranes containing moderate amounts of CL, which should increase the number of molecular contacts between daptomycin and the surrounding lipids, and therefore agrees with the findings from the ITC experiments.

A similar inhibitory effect of CL on membrane pore formation has previously been observed with the antimicrobial peptide magainin, and together with related findings has been interpreted in terms of lipid curvature strain.¹²⁵ According to this explanation, the peptide

claims space in the head group layer of the membrane. CL and other “cone-shaped” lipid species that provide more bulk in the hydrophobic acyl chain layer than in the head group layer accommodate the peptide, whereas lipids with larger head groups compete with it for space, promoting distension and bending of the head group layer, which leads to the formation of a toroidal pore.

The mechanism proposed for magainin may also underlie the effect of CL on daptomycin (Figure 4.7). Such a model might lead one to expect that, because of the greater competition for space in the head group layer of monolayers without CL, daptomycin insertion into such monolayers should raise the surface pressure to a greater extent than without CL, which is the opposite of what we observed (Figure 4.5). Possibly, the unstable situation illustrated in Figure 4.7B may relax by transitioning either toward the toroidal defect (Figure 4.7, C and D) or toward a less deeply inserted configuration, in which the bulk of the peptide remains outside of the lipid membrane and does not add lateral pressure to it (Figure 4.7A). In any event, an improved accommodation of daptomycin within CL-containing membranes would agree with the increase in negative enthalpy reported here. In this context, it is worth noting that CL is believed to be enriched in localized domains in bacterial cell membranes.⁹⁸ This might account for the inhomogeneous distribution of daptomycin on cell surfaces;¹⁶⁴ the correlation has, however, not been established.

A tighter interaction between daptomycin and membrane lipids might also account for the decrease in entropy that was observed concomitantly with increases in negative enthalpy. However, one should keep in mind that the entropy values were obtained through the use of a single-site binding model, and although this model is able to numerically fit the ITC titration curves rather well, we must not forget that daptomycin not only binds as a monomer but subsequently also forms oligomers, so that any model that assumes a one-step interaction can only be considered an approximation. Caution is therefore required with respect to interpreting the calculated entropy.

In sum, we have obtained evidence that supports a novel structural model of the daptomycin pore and suggests a possible mechanism of bacterial resistance to daptomycin. We presently have no way to further corroborate this hypothetical model. Nevertheless, it is interesting to note that many cation channels and pores have tetradic symmetry. Intriguingly, with the *Pseudomonas* lipopeptide tolaasin I, whose structure is not closely related to daptomycin, the very same kind of octameric symmetry spanning both leaflets has been obtained from *in silico* studies.⁹² We therefore feel that this structural model deserves consideration in future studies.

Chapter 5

Summary and future work

5.1 SUMMARY

At the beginning of this thesis in Section 1.5, I posed several questions concerning the action mode of daptomycin and the molecular basis of resistance to it. To answer these questions, three projects were designed and carried out that were described in the preceding chapters. The findings from these projects will be summarized here.

Daptomycin's bactericidal effect has been proposed to involve three steps: membrane binding, oligomerization, and membrane depolarization. Previous studies had shown that in the presence of a physiological level of Ca^{++} , daptomycin will only bind to and oligomerize on membranes containing PG.ⁱ Ca^{++} and PG are required both for oligomerization and for the bactericidal effect, which suggested that oligomerization is important for antibacterial activity.

In Chapter 2, we used the lipopeptide antibiotic CB-182,362, which is very similar to daptomycin in terms of structure and antibacterial activity. We showed that CB-182,362 can independently form oligomers on susceptible artificial and bacterial membranes, and moreover that

ⁱDaptomycin binds to membranes containing PC only or PC and CL, but only at non-physiologically high calcium concentrations; but there is no oligomer formation on these membranes.

it can also form stable hybrid oligomers when mixed with daptomycin. We then demonstrated that, within such hybrid oligomers, daptomycin and CB-182,362 exercise mutual inhibition. This finding indirectly shows that oligomerization is indeed an integral part of the bactericidal action mode. If it were not, that is, if each subunit of the oligomer exercised its antibacterial effect without requiring any cooperation from the neighbouring ones, the combination of daptomycin and CB-182,462 should act in a strictly additive fashion, and the reduced specific activity of hybrid oligomers relative to homogeneous ones could not be explained.

The mutual inhibition of the two compounds implies that at least some of the hybrid oligomers are inactive. The subunits of these inactive hybrids must be trapped within a non-functional structure. It seems possible that the inactive conformation resembles a transient stage in the formation of the regular, active oligomer; however, this cannot be proven with the available data.

In the current model of daptomycin action, the step following oligomerization is pore formation. Previous studies have shown daptomycin's activity is correlated with membrane depolarization, which has been hypothetically attributed to K^+ leakage. However, selective K^+ leakage should cause hyperpolarization rather than depolarization, since this ion is more concentrated inside the cell than outside. One would therefore expect that ions other than K^+ can also pass through the daptomycin pores. Before our work, the selectivity of the pore had not been systematically studied.

In Chapter 3, we showed that a liposome model can be used to detect and characterize the permeability properties of the daptomycin pores. We found that daptomycin indeed forms discrete pores on PG-containing liposomes. These pores have the highest permeabilities for Na^+ , K^+ , and other alkali metal ions. The rate of permeation is approximately twice lower for Mg^{++} , and yet lower again for the organic cations choline and hexamethonium. Anions like Cl^- and the zwitterion cysteine are excluded. These findings indicate the daptomycin pores are selective for cations, and the permeability for these cations is limited by their sizes.

These findings also complement previous *in vivo* observations and suggest that the observed

depolarization of bacterial cell membrane is mainly caused by the influx of Na^+ . The quantitative analysis showed the average conductivity of daptomycin pore is very low, several orders of magnitude lower than that of gramicidin. In comparison to daptomycin's rapid bactericidal activity, it is possible that only some of the oligomers function as active pores, suggesting the possibility that pore-formation is only one of the several contributing factors to daptomycin's antibacterial activities.

An increased activity of cardiolipin synthesis has been observed in resistant *Enterococcus* strains. The exact role of cardiolipin in the resistance mechanism is not yet understood. The findings from Chapters 2 and 3 have paved the way for us to test the effect of cardiolipin in each step of the proposed mechanism of action.

In Chapter 4, 10 or 20 molar % of CL was included in PG-containing model liposomes. Fluorescence studies showed that the binding and oligomerization of daptomycin on these membranes were not inhibited, but the membrane permeabilization for cations was completely abolished. This suggested that the oligomers formed on CL-containing membranes are not active.

The inactive and active oligomers were found different in both size and distribution across the membrane leaflets. A FRET-based technique was applied to estimate the subunit numbers. On the CL-containing liposomes, each oligomer comprises approximately four daptomycin molecules, whereas on the susceptible membranes, this number is nearly twice as high.

The membrane-impermeant fluorescence quencher dithionite was used to assess the distribution of membrane-bound NBD-daptomycin. On CL-containing liposomes, almost all of the fluorescence signal was quenched right away, indicating the oligomers were confined to the outer leaflet of the membrane. In contrast, on the susceptible liposomes, only about half of the NBD-daptomycin was subject to immediate quenching, indicating that membrane-bound daptomycin was evenly distributed on both inner and outer leaflets. These findings revealed that cardiolipin inhibited the membrane translocation of daptomycin.

To sum up all the findings, a refined model for the molecular action mode of daptomycin

was proposed. Monomeric daptomycin first binds to PG on the outer leaflet of membrane in the presence of Ca^{++} . Then, four bound monomers form a tetramer before being translocated across the membrane to the inner leaflet. Finally, two tetramers on the opposite leaflets line up to form an octameric ion pore. The presence of CL prevents the membrane translocation for tetramer and the ultimate pore formation.

5.2 FUTURE WORK

5.2.1 Solid-state NMR for daptomycin pore structure

As demonstrated by the fluorescence studies presented in chapters 2 and 4, the formation of oligomers with an accurate and intact structure is critical for daptomycin's bactericidal activity and ability to permeabilize the membrane. In order to better understand the mechanism of pore formation, high-resolution structures would be very helpful. Fluorescence studies alone cannot provide such high-resolution structures. NMR studies in solution have been attempted, but this approach could not provide data of sufficient quality, due to certain experimental limitations, such as sample aggregation. Preliminary results suggest that solid-state NMR may be an option to circumvent these limitations.

5.2.2 Mechanism of resistance caused by lysyl-PG

An increase of CL and lysyl-PG content in cell membrane has been linked to the daptomycin resistance by many studies. We have shown in Chapter 4 that CL has a very specific way to prevent membrane permeabilization. With lysyl-PG, this has not been studied; it remains to be seen whether or not resistance can be demonstrated in a liposome model, and if so, which step is inhibited. It is even possible that additional aspects of the action mode may be discovered, just as turned out to be the case with CL.

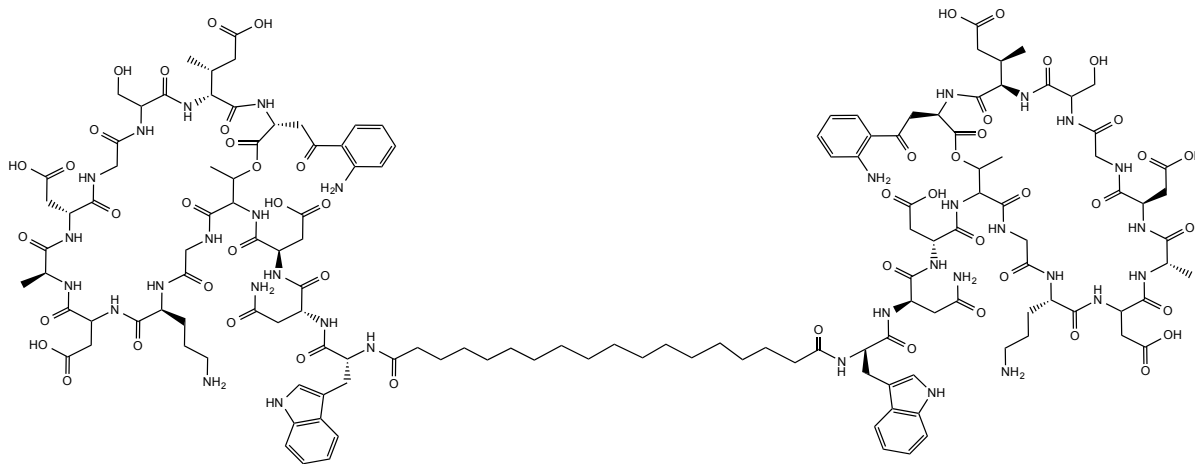


Figure 5.1 Structure of a synthetic daptomycin dimer. Two peptide head groups are linked by one long bivalent acyl tail.

5.2.3 Interaction between daptomycin and the bacterial cell wall

Since oligomer formation is important for daptomycin's activity, one might expect that tethering together daptomycin molecules to dimers or larger oligomers might increase its antibacterial activity. Recently, a daptomycin dimer (Figure 5.1) has been synthesized by Dr. Scott Taylor's group. The dimer comprises two daptomycin peptide groups that are linked by a long bivalent acyl tether. During initial tests, this compound showed no antibacterial activity. However, it showed very similar characteristics to native daptomycin in terms of ion permeability through liposomal membranes. These preliminary observations raise the question whether the dimer may be too big to traverse the cell wall, and so be unable to reach its intended target. Note that this relates to the previously discussed hypothesis that resistance may be caused by thickened cell wall (see Section 1.4.4). To verify this, an antibacterial activity test could be carried out on protoplast cells, which lack a cell wall.

5.2.4 Quantitative analysis of membrane binding and oligomerization

The binding and oligomerization of daptomycin have mostly been described at a qualitative level. The ability to quantitatively monitor these steps can offer a more in-depth understand-

ing of interaction daptomycin with lipids, and also between the subunits within the oligomer. Steady-state and time-resolved fluorescence analysis of pyrene excimer formation has been widely used to characterize non-covalent interactions within and between polymers.^{54,55} Due to the spectral overlap between the emission of pyrene and the absorbance of kynurenine, pyrene-labeled daptomycin is not suitable for such studies, since pyrene excitation is lost through intramolecular FRET. However, the daptomycin-related lipopeptide A54145 lacks a kynurenine residue and can therefore be used in pyrene-based fluorescence experiments. The excimer fluorescence of this compound can provide insight into daptomycin and other membrane bound peptide oligomers. Stopped-flow fluorescence experiments can also be used as a supplementary approach.

5.2.5 Potentials with synthetic daptomycin analogues

Recently, Lohani, Taylor, and colleagues have synthesized daptomycin and several analogues entirely using solid-phase based method (see Section 1.4.1.4), which has shown the potential to produce a large library of daptomycin analogues. In their studies, the activity of analogues that contain amino acid substitutions at position 12 and 13 (Figure 5.2) were assessed. The analogue containing Glu-12 instead of MeGlu-12 was found less (approximately 8-fold) active than daptomycin, which confirms the importance of methyl group for activity as had been shown by earlier studies.^{77,152,153} The analogue with changed stereochemistry at the methyl group (Dap-(2S,3S)-MeGlu-12) was found much less (approximately 40-fold) than the native daptomycin (Dap-(2S,3R)MeGlu-12), which shows the stereochemistry of methyl group also could significantly affect activity. Interestingly, the analogue containing double substitutions (Glu-12,Trp-13) has the similar activity level as daptomycin. Whereas another double substituted analogue (Glu-12,Tyr-13) is about 40-fold less active than daptomycin. Future studies on these analogues with membrane models could potentially reveal more details in daptomycin's structure-function relationships. The development of total synthesis can also facilitate

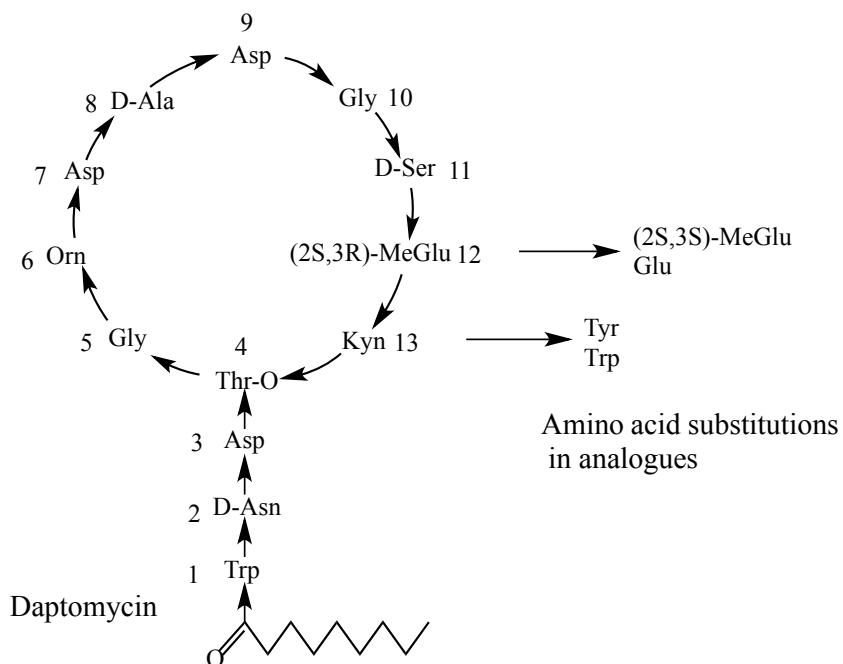


Figure 5.2 Structures of daptomycin and analogues. The analogues contain amino acid substitutions at position 12 and 13 as pointed by arrows.

the search for analogues with improved activity, possibly the ones that are unaffected by lung surfactant¹⁸³ and are still safe for clinical use.

Bibliography

- [1] T. Abraham, R. N. A. H. Lewis, R. S. Hodges, and R. N. McElhaney. Isothermal Titration Calorimetry Studies of the Binding of a Rationally Designed Analogue of the Antimicrobial Peptide Gramicidin S to Phospholipid Bilayer Membranes. *Biochemistry*, 44(6):2103–2112, Jan. 2005.
- [2] R. K. Agrawal, P. Penczek, R. A. Grassucci, and J. Frank. Visualization of elongation factor G on the Escherichia coli 70S ribosome: the mechanism of translocation. *Proceedings of the National Academy of Sciences*, 95(11):6134–8, May 1998.
- [3] W. E. Alborn, N. E. Allen, and D. A. Preston. Daptomycin disrupts membrane potential in growing *Staphylococcus aureus*. *Antimicrobial Agents and Chemotherapy*, 35(11):2282–2287, Nov. 1991.
- [4] B. B. Aldridge, M. Fernandez-Suarez, D. Heller, V. Ambravaneswaran, D. Irimia, M. Toner, and S. M. Fortune. Asymmetry and aging of mycobacterial cells lead to variable growth and antibiotic susceptibility. *Science*, 335(6064):100–104, 2012.
- [5] N. E. Allen, W. E. J. Alborn, and J. N. J. Hobbs. Inhibition of membrane potential-dependent amino acid transport by daptomycin. *Antimicrob Agents Chemother*, 35(12):2639–2642, 1991.
- [6] N. E. Allen, J. N. Hobbs, and W. E. Alborn. Inhibition of peptidoglycan biosynthesis in gram-positive bacteria by LY146032. *Antimicrobial agents and chemotherapy*, 31(7):1093–9, July 1987.
- [7] R. I. Aminov. A brief history of the antibiotic era: lessons learned and challenges for the future. *Frontiers in Microbiology*, 1(December):134, Jan. 2010.

- [8] E. V. Anslyn and D. A. Dougherty. *Modern Physical Organic Chemistry*. University Science, 2006.
- [9] R. D. Arbeit, D. Maki, F. P. Tally, E. Campanaro, B. I. Eisenstein, and Others. The safety and efficacy of daptomycin for the treatment of complicated skin and skin-structure infections. *Clinical Infectious Diseases*, 38(12):1673, 2004.
- [10] C. A. Arias, D. Panesso, D. M. McGrath, X. Qin, M. F. Mojica, C. Miller, L. Diaz, T. T. Tran, S. Rincon, E. M. Barbu, J. Reyes, J. H. Roh, E. Lobos, E. Sodergren, R. Pasqualini, W. Arap, J. P. Quinn, Y. Shamoo, B. E. Murray, and G. M. Weinstock. Genetic basis for in vivo daptomycin resistance in enterococci. *The New England Journal of Medicine*, 365(10):892–900, Sept. 2011.
- [11] M. E. Azzam and I. D. Algranati. Mechanism of puromycin action: fate of ribosomes after release of nascent protein chains from polysomes. *Proceedings of the National Academy of Sciences*, 70(12):3866–9, Dec. 1973.
- [12] R. H. Baltz. Daptomycin: mechanisms of action and resistance, and biosynthetic engineering. *Current opinion in chemical biology*, 13(2):144–51, Apr. 2009.
- [13] R. H. Baltz, P. Brian, V. Miao, and S. K. Wrigley. Combinatorial biosynthesis of lipopeptide antibiotics in streptomyces roseosporus. *Journal of Industrial Microbiology and Biotechnology*, 33(2):66–74, 2006.
- [14] R. H. Baltz, V. Miao, and S. K. Wrigley. Natural products to drugs: daptomycin and related lipopeptide antibiotics. *Natural Product Reports*, 22(6):717–741, 2005.
- [15] E. J. Bassett, M. S. Keith, G. J. Armelagos, D. L. Martin, and A. R. Villanueva. Tetracycline-labeled human bone from ancient Sudanese Nubia (A.D. 350). *Science*, 209(4464):1532–1534, Sept. 1980.

-
- [16] A. S. Bayer, T. Schneider, and H.-G. Sahl. Mechanisms of daptomycin resistance in *Staphylococcus aureus*: role of the cell membrane and cell wall. *Annals of the New York Academy of Sciences*, 1277:139–58, Jan. 2013.
- [17] J. M. Bell, J. D. Turnidge, H. S. Sader, and R. N. Jones. Antimicrobial activity and spectrum of daptomycin: results from the surveillance program in Australia and New Zealand (2008). *Pathology*, 42(5):470, 2010.
- [18] U. Bertsche, C. Weidenmaier, D. Kuehner, S.-J. Yang, S. Baur, S. Wanner, P. Francois, J. Schrenzel, M. R. Yeaman, and A. S. Bayer. Correlation of daptomycin resistance in a clinical *Staphylococcus aureus* strain with increased cell wall teichoic acid production and D-alanylation. *Antimicrobial Agents and Chemotherapy*, 55(8):3922–3928, 2011.
- [19] K. Bhullar, N. Waglechner, A. Pawlowski, K. Koteva, E. D. Banks, M. D. Johnston, H. A. Barton, and G. D. Wright. Antibiotic resistance is prevalent in an isolated cave microbiome. *PLoS One*, 7(4):e34953, 2012.
- [20] M. Boaretti and P. Canepari. Identification of daptomycin-binding proteins in the membrane of *Enterococcus hirae*. *Antimicrobial Agents and Chemotherapy*, 39(9):2068–2072, 1995.
- [21] M. Boaretti, P. Canepari, M. del Mar Lleò, and G. Satta. The activity of daptomycin on *Enterococcus faecium* protoplasts: indirect evidence supporting a novel mode of action on lipoteichoic acid synthesis. *Antimicrobial Agents and Chemotherapy*, 31(2):227–235, 1993.
- [22] L. D. Boeck, D. S. Fukuda, B. J. Abbott, and M. Debono. Deacylation of A21978C, an acidic lipopeptide antibiotic complex, by *Actinoplanes utahensis*. *Journal of Antibiotics*, 41(8):1085–1092, 1988.

- [23] L. D. Boeck, H. R. Papiska, R. W. Wetzel, J. S. Mynderse, D. S. Fukuda, F. P. Mertz, and D. M. Berry. A54145, a new lipopeptide antibiotic complex: discovery, taxonomy, fermentation and HPLC. *Journal of Antibiotics*, 43(6):587–593, 1990.
- [24] E. Bouza and P. Muñoz. Monotherapy versus combination therapy for bacterial infections. *Medical Clinics of North America*, 84(6):1357–1389, 2000.
- [25] K. A. Brogden. Antimicrobial peptides: pore formers or metabolic inhibitors in bacteria? *Nature Reviews. Microbiology*, 3(3):238–50, Mar. 2005.
- [26] E. D. Brown, E. I. Vivas, C. T. Walsh, and R. Kolter. MurA (MurZ), the enzyme that catalyzes the first committed step in peptidoglycan biosynthesis, is essential in *Escherichia coli*. *Journal of Bacteriology*, 177(14):4194–4197, 1995.
- [27] R. S. Brown, J. D. Brennan, and U. J. Krull. Self-quenching of nitrobenzoxadiazole labeled phospholipids in lipid membranes. *Journal of Chemical Physics*, 100(8):6019, 1994.
- [28] B. Cabrer, D. Vázquez, and J. Modolell. Inhibition by elongation factor EF G of aminoacyl-tRNA binding to ribosomes. *Proceedings of the National Academy of Sciences*, 69(3):733–6, Mar. 1972.
- [29] D. S. Cafiso. Alamethicin: A peptide model for voltage gating and protein-membrane interactions. In *Annual Review of Biophysics and Biomolecular Structure*, volume 23, pages 141–165. 1994.
- [30] C. Calvori, L. Frontali, L. Leoni, and G. Tecce. Effect of rifamycin on protein synthesis. *Nature*, 207:417–418, 1965.
- [31] P. Canepari, M. Boaretti, M. M. Lleó, G. Satta, and M. Del Mar Lleo. Lipoteichoic acid as a new target for activity of antibiotics: mode of action of daptomycin (LY146032). *Antimicrobial Agents and Chemotherapy*, 34(6):1220–6, June 1990.

- [32] R. Cantón, P. Ruiz-Garbajosa, R. L. Chaves, and A. P. Johnson. A potential role for daptomycin in enterococcal infections: what is the evidence? *Journal of Antimicrobial Chemotherapy*, 65(6):1126, 2010.
- [33] Centers for Disease Control and Prevention (CDC). Antibiotic resistance threats in the United States, 2013. 2013.
- [34] J. Chevalier, J.-M. Pagès, and M. Malléa. *In Vivo* Modification of Porin Activity Confering Antibiotic Resistance to *Enterobacter aerogenes*. *Biochemical and Biophysical Research Communications*, 266(1):248–251, 1999.
- [35] B. C. Chung, J. Zhao, R. A. Gillespie, D.-Y. Kwon, Z. Guan, J. Hong, P. Zhou, and S.-Y. Lee. Crystal structure of MraY, an essential membrane enzyme for bacterial cell wall synthesis. *Science (New York, N.Y.)*, 341(6149):1012–6, Aug. 2013.
- [36] S. Clejan, T. A. Krulwich, K. R. Mondrus, and D. Seto-Young. Membrane lipid composition of obligately and facultatively alkalophilic strains of *Bacillus* spp. *Journal of Bacteriology*, 168(1):334–340, Oct. 1986.
- [37] N. R. Clement and J. Michael Gould. Pyranine (8-hydroxy-1,3,6-pyrenetrisulfonate) as a probe of internal aqueous hydrogen ion concentration in phospholipid vesicles. *Biochemistry*, 20(6):1534–1538, 1981.
- [38] M.-F. Coëffet-Le Gal, L. Thurston, P. Rich, V. Miao, and R. H. Baltz. Complementation of daptomycin dpta and dptd deletion mutations in trans and production of hybrid lipopeptide antibiotics. *Microbiology*, 152(10):2993–3001, 2006.
- [39] M. Cook, E. Molto, and C. Anderson. Fluorochrome labelling in roman period skeletons from Dakhleh oasis, Egypt. *American Journal of Physical Anthropology*, 80(2):137–143, 1989.

- [40] B. D. Cookson. Review The emergence of mupirocin resistance: a challenge to infection control and antibiotic prescribing practice. *Journal of Antimicrobial Chemotherapy*, pages 11–18, 1998.
- [41] N. Cotroneo, R. Harris, N. Perlmutter, T. Beveridge, and J. A. Silverman. Daptomycin exerts bactericidal activity without lysis of *Staphylococcus aureus*. *Antimicrobial Agents and Chemotherapy*, 52(6):2223–5, June 2008.
- [42] N. R. Cozzarelli. DNA gyrase and the supercoiling of DNA. *Science*, 207(4434):953–960, 1980.
- [43] L. Cui and X.-Z. Su. Discovery, mechanisms of action and combination therapy of artemisinin. *Expert Review of Anti-infective Therapy*, 7(8):999–1013, 2009.
- [44] M. Davlieva, W. Zhang, C. A. Arias, and Y. Shamoo. Biochemical Characterization of Cardiolipin Synthase Mutations Associated with Daptomycin Resistance in Enterococci. *Antimicrobial Agents and Chemotherapy*, 57(1):289–296, Jan. 2013.
- [45] V. M. D’Costa, K. M. McGrann, D. W. Hughes, and G. D. Wright. Sampling the antibiotic resistome. *Science*, 311(5759):374–377, 2006.
- [46] V. M. D’Costa, T. A. Mukhtar, T. Patel, K. Koteva, N. Waglechner, D. W. Hughes, G. D. Wright, and G. De Pascale. Inactivation of the lipopeptide antibiotic daptomycin by hydrolytic mechanisms. *Antimicrobial Agents and Chemotherapy*, 56(2):757–64, Feb. 2012.
- [47] E. Dé, A. Baslé, M. Jaquinod, N. Saint, M. Malléa, and G. Molle. A new mechanism of antibiotic resistance in Enterobacteriaceae induced by a structural modification of the major porin. *Molecular Microbiology*, 41(1):189–198, 2001.
- [48] M. Debono, B. J. Abbott, R. M. Molloy, D. S. Fukuda, A. H. Hunt, V. M. Daupert, F. T. Counter, J. L. Ott, C. B. Carrell, L. C. Howard, and Others. Enzymatic and chem-

- ical modifications of lipopeptide antibiotic A21978C: the synthesis and evaluation of daptomycin (LY146032). *Journal of Antibiotics*, 41(8):1093, 1988.
- [49] M. Debono, M. Barnhart, C. B. Carrell, J. A. Hoffmann, J. L. Occolowitz, B. J. Abbott, D. S. Fukuda, R. L. Hamill, K. Biemann, and W. C. Herlihy. A21978C, a complex of new acidic peptide antibiotics: isolation, chemistry, and mass spectral structure elucidation. *Journal of Antibiotics*, 40(6):761–777, June 1987.
- [50] J. A. F. O. den Kamp, I. Redai, and L. L. M. van Deenen. Phospholipid Composition of *Bacillus subtilis*. *Journal of Bacteriology*, 99(1):298–303, July 1969.
- [51] S. Doekel, M.-F. Coëffet-Le Gal, J.-Q. Gu, M. Chu, R. H. Baltz, and P. Brian. Non-ribosomal peptide synthetase module fusions to produce derivatives of daptomycin in *streptomyces roseosporus*. *Microbiology*, 154(9):2872–2880, 2008.
- [52] S. Dubrac, P. Bisicchia, K. M. Devine, and T. Msadek. A matter of life and death: cell wall homeostasis and the walkr (yycgf) essential signal transduction pathway. *Molecular microbiology*, 70(6):1307–1322, 2008.
- [53] S. Dubrac, I. G. Boneca, O. Poupel, and T. Msadek. New insights into the walk/walr (yycg/yycf) essential signal transduction pathway reveal a major role in controlling cell wall metabolism and biofilm formation in *staphylococcus aureus*. *Journal of bacteriology*, 189(22):8257–8269, 2007.
- [54] J. Duhamel. New insights in the study of pyrene excimer fluorescence to characterize macromolecules and their supramolecular assemblies in solution. *Langmuir*, 28(16):6527–6538, 2012.
- [55] J. Duhamel. Global analysis of fluorescence decays to probe the internal dynamics of fluorescently labeled macromolecules. *Langmuir*, 30(9):2307–2324, 2013.

- [56] R. L. Dunne, L. A. Dunn, P. Upcroft, P. J. O'Donoghue, and J. a. Upcroft. Drug resistance in the sexually transmitted protozoan *Trichomonas vaginalis*. *Cell Research*, 13(4):239–49, Aug. 2003.
- [57] W. Y. Edward, G. McDermott, H. I. Zgurskaya, H. Nikaido, and D. E. Koshland. Structural basis of multiple drug-binding capacity of the acrb multidrug efflux pump. *Science*, 300(5621):976–980, 2003.
- [58] D. I. Edwards. Mechanisms of selective toxicity of metronidazole and other nitroimidazole drugs. *The British journal of venereal diseases*, 56(5):285–290, 1980.
- [59] B. I. Eisenstein, F. B. Oleson, and R. H. Baltz. Daptomycin: from the mountain to the clinic, with essential help from Francis Tally, MD. *Clinical Infectious Diseases*, 50(Suppl 1):S10–5, Jan. 2010.
- [60] G. M. Eliopoulos, C. Thauvin, B. Gerson, and R. C. Moellering. In Vitro Activity and Mechanism of Action of A21978C1 , a Novel Cyclic Lipopeptide Antibiotic L-Asp L-Orn D-Ser L-Kyn L L-Thr L-Asp. *Antimicrobial Agents and Chemotherapy*, 27(3):357–362, 1985.
- [61] G. M. Eliopoulos, S. Willey, E. Reiszner, P. G. Spitzer, G. Caputo, and R. C. Moellering. In vitro and in vivo activity of LY 146032, a new cyclic lipopeptide antibiotic. *Antimicrobial Agents and Chemotherapy*, 30(4):532–5, Oct. 1986.
- [62] C. A. Elkins and H. Nikaido. Substrate specificity of the rnd-type multidrug efflux pumps acrb and acrd of *Escherichia coli* is determined predominately by two large periplasmic loops. *Journal of bacteriology*, 184(23):6490–6498, 2002.
- [63] G. L. Ellman. Tissue sulfhydryl groups. *Archives of Biochemistry and Biophysics*, pages 70–77, 1959.

-
- [64] C. M. Ernst and A. Peschel. Broad spectrum antimicrobial peptide resistance by MprF mediated aminoacylation and flipping of phospholipids. *Molecular Microbiology*, 80(2):290–299, 2011.
- [65] M. E. Falagas, P. I. Rafailidis, and D. K. Matthaiou. Resistance to polymyxins: Mechanisms, frequency and treatment options. *Drug Resistance Updates*, 13(4-5):132–8, 2010.
- [66] Z. Feng and R. G. Barletta. Roles of Mycobacterium smegmatis Racemase in the Mechanisms of Action of and Resistance to the Peptidoglycan Roles of Mycobacterium smegmatis D -Alanine : D -Alanine Ligase and D -Alanine Racemase in the Mechanisms of Action of and Resistance to the Pepti. *Antimicrobial Agents and Chemotherapy*, 2003.
- [67] A. Finkelstein and O. S. Andersen. The gramicidin a channel: A review of its permeability characteristics with special reference to the single-file aspect of transport. *Journal of Membrane Biology*, 59(3):155–171, Oct. 1981.
- [68] A. Fischer, S.-J. Yang, A. S. Bayer, A. R. Vaezzadeh, S. Herzig, L. Stenz, M. Girard, G. Sakoulas, A. Scherl, and M. R. Yeaman. Daptomycin resistance mechanisms in clinically derived *Staphylococcus aureus* strains assessed by a combined transcriptomics and proteomics approach. *Journal of Antimicrobial Chemotherapy*, 66(8):1696–1711, 2011.
- [69] A. Fleming. On the antibacterial action of cultures of a penicillium, with special reference to their use in the isolation of B. influenzae. *British Journal of Experimental Pathology*, 10(31):226–236, 1929.
- [70] H. G. Floss and T.-W. Yu. Rifamycin mode of action, resistance, and biosynthesis. *Chemical reviews*, 105(2):621–632, 2005.

- [71] R. Following and H. Therapy. Tetracycline Antibiotics: Mode of Action, Applications, Molecular Biology, and Epidemiology of Bacterial Resistance. *Microbiology and Molecular Biology Reviews*, 65(2):232–260, 2001.
- [72] L. Friedman, J. D. Alder, and J. A. Silverman. Genetic changes that correlate with reduced susceptibility to daptomycin in *Staphylococcus aureus*. *Antimicrobial agents and chemotherapy*, 50(6):2137–45, June 2006.
- [73] P. K. Gessner. Isobolographic analysis of interactions: an update on applications and utility. *Toxicology*, 105(2-3):161–179, Dec. 1995.
- [74] S. H. Gillespie. Evolution of drug resistance in Mycobacterium tuberculosis: clinical and molecular perspective. *Antimicrobial Agents and Chemotherapy*, 46(2):267–274, 2002.
- [75] S. H. Gillespie. Evolution of drug resistance in mycobacterium tuberculosis: clinical and molecular perspective. *Antimicrobial agents and chemotherapy*, 46(2):267–274, 2002.
- [76] N. Grindley, M. Lauth, R. Wells, R. Wityk, J. Salvo, and R. Reed. Transposon-mediated site-specific recombination: Identification of three binding sites for resolvase at the *res* sites of $\gamma\delta$ and *tn 3*. *Cell*, 30(1):19–27, 1982.
- [77] J. Grünewald, S. A. Sieber, C. Mahlert, U. Linne, and M. A. Marahiel. Synthesis and derivatization of daptomycin: a chemoenzymatic route to acidic lipopeptide antibiotics. *Journal of the American Chemical Society*, 126(51):17025–17031, 2004.
- [78] A.-B. Hachmann, E. R. Angert, and J. D. Helmann. Genetic analysis of factors affecting susceptibility of *Bacillus subtilis* to daptomycin. *Antimicrobial agents and chemotherapy*, 53(4):1598–609, Apr. 2009.
- [79] A.-B. Hachmann, E. Sevim, A. Gaballa, D. L. Popham, H. Antelmann, and J. D. Helmann. Reduction in membrane phosphatidylglycerol content leads to daptomycin re-

- sistance in *Bacillus subtilis*. *Antimicrobial Agents and Chemotherapy*, 55(9):4326–37, Sept. 2011.
- [80] K. J. Harder, H. Nikaido, and M. Matsushashi. Mutants of *Escherichia coli* that are resistant to certain beta-lactam compounds lack the ompF porin. *Antimicrobial Agents and Chemotherapy*, 20(4):549–552, 1981.
- [81] G. Hartmann, W. Behr, K.-A. Beissner, K. Honikel, and A. Sippel. Antibiotics as inhibitors of nucleic acid and protein synthesis. *Angewandte Chemie International Edition in English*, 7(9):693–701, 1968.
- [82] H. Heerklotz, A. D. Tsamaloukas, and S. Keller. Monitoring detergent-mediated solubilization and reconstitution of lipid membranes by isothermal titration calorimetry. *Nature Protocols*, 4(5):686–697, Apr. 2009.
- [83] F. Heffron, B. J. McCarthy, H. Ohtsubo, and E. Ohtsubo. Dna sequence analysis of the transposon tn3: three genes and three sites involved in transposition of tn3. *Cell*, 18(4):1153–1163, 1979.
- [84] J. Hill, J. Siedlecki, I. Parr, M. Morytko, X. Yu, Y. Zhang, J. Silverman, N. Controneo, V. Laganas, T. Li, et al. Synthesis and biological activity of *n*-acylated ornithine analogues of daptomycin. *Bioorganic & medicinal chemistry letters*, 13(23):4187–4191, 2003.
- [85] S. W. Ho, D. Jung, J. R. Calhoun, J. D. Lear, M. Okon, W. R. Scott, R. E. Hancock, and S. K. Straus. Effect of divalent cations on the structure of the antibiotic daptomycin. *European biophysics journal*, 37(4):421–433, 2008.
- [86] J. E. Hodgson, S. P. Curnock, K. G. Dyke, R. Morris, D. R. Sylvester, and M. S. Gross. Molecular characterization of the gene encoding high-level mupirocin resistance in *Staphylococcus aureus* J2870. *Antimicrobial Agents and Chemotherapy*, 38(5):1205–8, May 1994.

- [87] D. C. Holt, M. T. Holden, S. Y. Tong, S. Castillo-Ramirez, L. Clarke, M. A. Quail, B. J. Currie, J. Parkhill, S. D. Bentley, E. J. Feil, et al. A very early-branching staphylococcus aureus lineage lacking the carotenoid pigment staphyloxanthin. *Genome biology and evolution*, 3:881–895, 2011.
- [88] E. M. Hotze, E. M. Wilson-Kubalek, J. Rossjohn, M. W. Parker, A. E. Johnson, and R. K. Tweten. Arresting pore formation of a cholesterol-dependent cytolysin by disulfide trapping synchronizes the insertion of the transmembrane beta-sheet from a prepore intermediate. *Journal of Biological Chemistry*, 276(11):8261–8, Mar. 2001.
- [89] B. P. Howden, C. R. McEvoy, D. L. Allen, K. Chua, W. Gao, P. F. Harrison, J. Bell, G. Coombs, V. Bennett-Wood, J. L. Porter, et al. Evolution of multidrug resistance during staphylococcus aureus infection involves mutation of the essential two component regulator walkr. *PLoS pathogens*, 7(11):e1002359, 2011.
- [90] F. M. Huber, R. L. Pieper, and A. J. Tietz. The formation of daptomycin by supplying decanoic acid to *Streptomyces roseosporus* cultures producing the antibiotic complex A21978C. *Journal of Biotechnology*, 7(4):283–292, Apr. 1988.
- [91] R. M. Humphries, S. Pollett, and G. Sakoulas. A current perspective on daptomycin for the clinical microbiologist. *Clinical microbiology reviews*, 26(4):759–80, Oct. 2013.
- [92] G. H. Jo, S. H. Lee, J. Y. Hyun, K. R. Kang, and Y. H. Lim. In silico study of the ion channel formed by tolaasin i produced by pseudomonas tolaasii. *Journal of microbiology and biotechnology*, 21(10):1097–1100, 2011.
- [93] T. Jones, M. R. Yeaman, G. Sakoulas, S.-J. Yang, R. A. Proctor, H.-G. Sahl, J. Schrenzel, Y. Q. Xiong, and A. S. Bayer. Failures in clinical treatment of *Staphylococcus aureus* infection with daptomycin are associated with alterations in surface charge, membrane phospholipid asymmetry, and drug binding. *Antimicrobial agents and chemotherapy*, 52(1):269–278, 2008.

- [94] D. Jung, J. P. Powers, S. K. Straus, and R. E. W. Hancock. Lipid-specific binding of the calcium-dependent antibiotic daptomycin leads to changes in lipid polymorphism of model membranes. *Chemistry and Physics of Lipids*, 154(2):120–8, Aug. 2008.
- [95] D. Jung, A. Rozek, M. Okon, and R. E. Hancock. Structural transitions as determinants of the action of the calcium-dependent antibiotic daptomycin. *Chemistry & biology*, 11(7):949–957, 2004.
- [96] R. Jursch, A. Hildebrand, G. Hobom, J. Tranum-Jensen, R. Ward, M. Kehoe, and S. Bhakdi. Histidine residues near the N terminus of staphylococcal alpha-toxin as reporters of regions that are critical for oligomerization and pore formation. *Infection and Immunity*, 62(6):2249–2256, 1994.
- [97] F. M. Kahan, J. S. Kahan, P. J. Cassidy, and H. Kropp. The Mechanism Of Action of Fosfomycin (Phosphonomycin). *Annals of the New York Academy of Sciences*, 235(1):364–386, 1974.
- [98] F. Kawai, M. Shoda, R. Harashima, Y. Sadaie, H. Hara, and K. Matsumoto. Cardiolipin Domains in *Bacillus subtilis* Marburg Membranes. *Journal of Bacteriology*, 186(5):1475–1483, Mar. 2004.
- [99] S. Keller, C. Vargas, H. Zhao, G. Piszczek, C. A. Brautigam, and P. Schuck. High-Precision Isothermal Titration Calorimetry with Automated Peak-Shape Analysis. *Analytical Chemistry*, 84(11):5066–5073, Apr. 2012.
- [100] A. M. King, S. A. Reid-Yu, W. Wang, D. T. King, G. De Pascale, N. C. Strynadka, T. R. Walsh, B. K. Coombes, and G. D. Wright. Aspergillomarasmine a overcomes metallo-[bgr]-lactamase antibiotic resistance. *Nature*, 510(7506):503–506, 2014.
- [101] R. M. Kohli, C. T. Walsh, and M. D. Burkart. Biomimetic synthesis and optimization of cyclic peptide antibiotics. *Nature*, 418(6898):658–661, 2002.

-
- [102] R. K. Koripella, Y. Chen, K. Peisker, C. S. Koh, M. Selmer, and S. Sanyal. Mechanism of elongation factor-G-mediated fusidic acid resistance and fitness compensation in *Staphylococcus aureus*. *Journal of Biological Chemistry*, 287(36):30257–67, Aug. 2012.
- [103] J. Kríz, J. Dybal, and E. Makrlík. Valinomycin-proton interaction in low-polarity media. *Biopolymers*, 82(5):536–48, Aug. 2006.
- [104] A. Kumar and H. P. Schweizer. Bacterial resistance to antibiotics: active efflux and reduced uptake. *Advanced Drug Delivery Reviews*, 57(10):1486–513, July 2005.
- [105] V. Laganas, J. Alder, and J. A. Silverman. In Vitro Bactericidal Activities of Daptomycin against *Staphylococcus aureus* and *Enterococcus faecalis* Are Not Mediated by Inhibition of Lipoteichoic Acid Biosynthesis. *Antimicrobial Agents and Chemotherapy*, 47(8):2682–2684, July 2003.
- [106] J. Lakey, E. Lea, B. Rudd, H. Wright, and D. Hopwood. A new channel-forming antibiotic from streptomyces coelicolor a3 (2) which requires calcium for its activity. *Journal of general microbiology*, 129(12):3565–3573, 1983.
- [107] J. H. Lakey and M. Ptak. Fluorescence indicates a calcium-dependent interaction between the lipopeptide antibiotic LY 146032 and phospholipid membranes. *Biochemistry*, 27(13):4639–4645, June 1988.
- [108] H. Y. Lam, Y. Zhang, H. Liu, J. Xu, C. T. Wong, C. Xu, and X. Li. Total synthesis of daptomycin by cyclization via a chemoselective serine ligation. *Journal of the American Chemical Society*, 135(16):6272–6279, 2013.
- [109] P. Lambert. Bacterial resistance to antibiotics: modified target sites. *Advanced Drug Delivery Reviews*, 57(10):1471–85, July 2005.

-
- [110] D. Lancet and I. Pecht. Spectroscopic and immunochemical studies with nitrobenzoxadiazolealanine, a fluorescent dinitrophenyl analog. *Biochemistry*, 16(23):5150–5157, 1977.
- [111] M. Landy, N. W. Larkum, E. J. Oswald, and F. Streightoff. Increased synthesis of p-aminobenzoic acid associated with the development of sulfonamide resistance in staphylococcus aureus. *Science*, 97(2516):265–267, 1943.
- [112] R. Leclercq and P. Courvalin. Bacterial resistance to macrolide, lincosamide, and streptogramin antibiotics by target modification. *Antimicrobial agents and chemotherapy*, 35(7):1267, 1991.
- [113] A. Lee, W. Mao, M. S. Warren, A. Mistry, K. Hoshino, R. Okumura, H. Ishida, and O. Lomovskaya. Interplay between efflux pumps may provide either additive or multiplicative effects on drug resistance. *Journal of bacteriology*, 182(11):3142–3150, 2000.
- [114] B. A. Legaree, C. B. Adams, and A. J. Clarke. Overproduction of penicillin-binding protein 2 and its inactive variants causes morphological changes and lysis in escherichia coli. *Journal of bacteriology*, 189(14):4975–4983, 2007.
- [115] A. H. Lin, R. W. Murray, T. J. Vidmar, and K. R. Marotti. The oxazolidinone eperzolid binds to the 50S ribosomal subunit and competes with binding of chloramphenicol and lincomycin. *Antimicrobial agents and chemotherapy*, 41(10):2127–31, Oct. 1997.
- [116] D. G. Lindmark and M. Müller. Antitrichomonad action, mutagenicity, and reduction of metronidazole and other nitroimidazoles. *Antimicrobial Agents and Chemotherapy*, 10(3):476–482, 1976.
- [117] C. Liu, A. Bayer, S. E. Cosgrove, R. S. Daum, S. K. Fridkin, R. J. Gorwitz, S. L. Kaplan, A. W. Karchmer, D. P. Levine, and B. E. Murray. Clinical practice guidelines by the Infectious Diseases Society of America for the treatment of methicillin-resistant

- Staphylococcus aureus* infections in adults and children. *Clinical Infectious Diseases*, pages e18–e55, 2011.
- [118] O. Lomovskaya, H. I. Zgurskaya, and H. Nikaido. It takes three to tango. *Nature biotechnology*, 20(12):1210–1212, 2002.
- [119] S. Magnet and J. S. Blanchard. Molecular insights into aminoglycoside action and resistance. *Chemical Reviews*, 105(2):477–98, Feb. 2005.
- [120] C. Mahlert, F. Kopp, J. Thirlway, J. Micklefield, and M. A. Marahiel. Stereospecific enzymatic transformation of α -ketoglutarate to (2 s, 3 r)-3-methyl glutamate during acidic lipopeptide biosynthesis. *Journal of the American Chemical Society*, 129(39):12011–12018, 2007.
- [121] A. S. Mankin. Macrolide myths. *Current Opinion in Microbiology*, 11(5):414–21, Oct. 2008.
- [122] W. Mao, M. S. Warren, D. S. Black, T. Satou, T. Murata, T. Nishino, N. Gotoh, and O. Lomovskaya. On the mechanism of substrate specificity by resistance nodulation division (rnd)-type multidrug resistance pumps: the large periplasmic loops of mexd from *Pseudomonas aeruginosa* are involved in substrate recognition. *Molecular microbiology*, 46(3):889–901, 2002.
- [123] D. H. Mariam, Y. Mengistu, S. E. Hoffner, and D. I. Andersson. Effect of rpoB mutations conferring rifampin resistance on fitness of *Mycobacterium tuberculosis*. *Antimicrobial Agents and Chemotherapy*, 48(4):1289–1294, 2004.
- [124] C. Mascio, K. Townsend, N. Cotroneo, and J. Silverman. Microbiological characterization of a novel lipopeptide antibiotic with activity in pulmonary surfactant. In *49th Interscience Conference on Antimicrobial Agents and Chemotherapy*. San Francisco, CA, USA, pages 12–15, 2009.

-
- [125] K. Matsuzaki, K.-i. Sugishita, N. Ishibe, M. Ueha, S. Nakata, K. Miyajima, and R. M. Epanand. Relationship of Membrane Curvature to the Formation of Pores by Magainin 2. *Biochemistry*, 37(34):11856–11863, Aug. 1998.
- [126] L. D. Mayer, M. J. Hope, and P. R. Cullis. Vesicles of variable sizes produced by a rapid extrusion procedure. *Biochimica et Biophysica Acta*, 858(1):161–168, 1986.
- [127] D. Mazel. Integrons: agents of bacterial evolution. *Nature Reviews Microbiology*, 4(8):608–620, 2006.
- [128] J. C. McIntyre and R. G. Sleight. Fluorescence assay for phospholipid membrane asymmetry. *Biochemistry*, 30(51):11819–11827, Dec. 1991.
- [129] S. Mehta, A. X. Cuirolo, K. B. Plata, S. Riosa, J. A. Silverman, A. Rubio, R. R. Rosato, and A. E. Rosato. VraSR two-component regulatory system contributes to mprF-mediated decreased susceptibility to daptomycin in in vivo-selected clinical strains of methicillin-resistant *Staphylococcus aureus*. *Antimicrobial Agents and Chemotherapy*, 56(1):92–102, 2012.
- [130] D. Mengin-Lecreulx. Inhibition of peptidoglycan biosynthesis in *Bacillus megaterium* by daptomycin. *FEMS Microbiology Letters*, 69(3):245–248, June 1990.
- [131] V. Miao, M.-F. Coëffet-Le Gal, K. Nguyen, P. Brian, J. Penn, A. Whiting, J. Steele, D. Kau, S. Martin, R. Ford, et al. Genetic engineering in *Streptomyces roseosporus* to produce hybrid lipopeptide antibiotics. *Chemistry & biology*, 13(3):269–276, 2006.
- [132] V. Miao, M.-F. Coëffet-LeGal, P. Brian, R. Brost, J. Penn, A. Whiting, S. Martin, R. Ford, I. Parr, M. Bouchard, et al. Daptomycin biosynthesis in *Streptomyces roseosporus*: cloning and analysis of the gene cluster and revision of peptide stereochemistry. *Microbiology*, 151(5):1507–1523, 2005.

- [133] C. J. Miller, J. L. Elliott, and R. J. Collier. Anthrax Protective Antigen:Prepore-to-Pore Conversion. *Biochemistry*, 38(32):10432–10441, July 1999.
- [134] N. N. Mishra and A. S. Bayer. Correlation of Cell Membrane Lipid Profiles with Daptomycin Resistance in Methicillin-Resistant *Staphylococcus aureus*. *Antimicrobial Agents and Chemotherapy*, 57(2):1082–1085, Feb. 2013.
- [135] N. N. Mishra, G. Y. Liu, M. R. Yeaman, C. C. Nast, R. A. Proctor, J. McKinnell, and A. S. Bayer. Carotenoid-related alteration of cell membrane fluidity impacts staphylococcus aureus susceptibility to host defense peptides. *Antimicrobial agents and chemotherapy*, 55(2):526–531, 2011.
- [136] N. N. Mishra, J. McKinnell, M. R. Yeaman, A. Rubio, C. C. Nast, L. Chen, B. N. Kreiswirth, and A. S. Bayer. In vitro cross-resistance to daptomycin and host defense cationic antimicrobial peptides in clinical methicillin-resistant *Staphylococcus aureus* isolates. *Antimicrobial Agents and Chemotherapy*, 55(9):4012–8, Sept. 2011.
- [137] N. N. Mishra, S.-J. Yang, A. Sawa, A. Rubio, C. C. Nast, M. R. Yeaman, and A. S. Bayer. Analysis of Cell Membrane Characteristics of In Vitro-Selected Daptomycin-Resistant Strains of Methicillin-Resistant *Staphylococcus aureus* . *Antimicrobial Agents and Chemotherapy*, 53(6):2312–2318, June 2009.
- [138] D. Moazed and H. F. Noller. Chloramphenicol, erythromycin, carbomycin and vernamycin B protect overlapping sites in the peptidyl transferase region of 23S ribosomal RNA. *Biochimie*, 69(8):879–884, Aug. 1987.
- [139] T. Mohammadi, V. van Dam, R. Sijbrandi, T. Vernet, A. Zapun, A. Bouhss, M. Diepeveen-de Bruin, M. Nguyen-Disteche, B. de Kruijff, and E. Breukink. Identification of ftsw as a transporter of lipid-linked cell wall precursors across the membrane. *The EMBO Journal*, 30(8):1425–1432, 2011.

- [140] C. L. Moore, P. Osaki-Kiyan, N. Z. Haque, M. B. Perri, S. Donabedian, and M. J. Zervos. Daptomycin versus vancomycin for bloodstream infections due to methicillin-resistant staphylococcus aureus with a high vancomycin minimum inhibitory concentration: a case-control study. *Clinical infectious diseases*, page cir764, 2011.
- [141] J. K. Muraih. *Mode of Action of Daptomycin, a Lipopeptide Antibiotic*. PhD thesis, University of Waterloo, 2012.
- [142] J. K. Muraih, J. Harris, S. D. Taylor, and M. Palmer. Characterization of daptomycin oligomerization with perylene excimer fluorescence: stoichiometric binding of phosphatidylglycerol triggers oligomer formation. *Biochimica et Biophysica Acta*, 1818(3):673–8, Mar. 2012.
- [143] J. K. Muraih and M. Palmer. Estimation of the subunit stoichiometry of the membrane-associated daptomycin oligomer by FRET. *Biochimica et Biophysica Acta*, 1818(7):1642–1647, Feb. 2012.
- [144] J. K. Muraih, A. Pearson, J. Silverman, and M. Palmer. Oligomerization of daptomycin on membranes. *Biochimica et Biophysica Acta*, 1808(4):1154–60, Apr. 2011.
- [145] S. Murakami, R. Nakashima, E. Yamashita, T. Matsumoto, and A. Yamaguchi. Crystal structures of a multidrug transporter reveal a functionally rotating mechanism. *Nature*, 443(7108):173–179, 2006.
- [146] S. Murakami, R. Nakashima, E. Yamashita, and A. Yamaguchi. Crystal structure of bacterial multidrug efflux transporter acrb. *Nature*, 419(6907):587–593, 2002.
- [147] K. P. Murray, J. Zhao, S. L. Davis, R. Kullar, K. Kaye, P. Lephart, and M. J. Rybak. Early use of daptomycin versus vancomycin for methicillin-resistant staphylococcus aureus bacteremia with vancomycin mic > 1 mg/l: a matched cohort study. *Clinical infectious diseases*, page cit112, 2013.

-
- [148] A. Muthaiyan, J. A. Silverman, R. K. Jayaswal, and B. J. Wilkinson. Transcriptional profiling reveals that daptomycin induces the staphylococcus aureus cell wall stress stimulon and genes responsive to membrane depolarization. *Antimicrobial agents and chemotherapy*, 52(3):980–990, 2008.
- [149] D. Nathans. Puromycin inhibition of protein synthesis: incorporation of puromycin into peptide chains. *Proceedings of the National Academy of Sciences*, 51(4):585, 1964.
- [150] M. L. Nelson, A. Dinardo, J. Hochberg, and G. J. Armelagos. Brief communication: Mass spectroscopic characterization of tetracycline in the skeletal remains of an ancient population from Sudanese Nubia 350-550 CE. *American Journal of Physical Anthropology*, 143(1):151–4, Sept. 2010.
- [151] K. T. Nguyen, X. He, D. C. Alexander, C. Li, J.-Q. Gu, C. Mascio, A. Van Praagh, L. Mortin, M. Chu, J. A. Silverman, P. Brian, and R. H. Baltz. Genetically engineered lipopeptide antibiotics related to A54145 and daptomycin with improved properties. *Antimicrobial Agents and Chemotherapy*, 54(4):1404–13, Apr. 2010.
- [152] K. T. Nguyen, D. Kau, J.-Q. Gu, P. Brian, S. K. Wrigley, R. H. Baltz, and V. Miao. A glutamic acid 3-methyltransferase encoded by an accessory gene locus important for daptomycin biosynthesis in streptomyces roseosporus. *Molecular microbiology*, 61(5):1294–1307, 2006.
- [153] K. T. Nguyen, D. Ritz, J.-Q. Gu, D. Alexander, M. Chu, V. Miao, P. Brian, and R. H. Baltz. Combinatorial biosynthesis of novel antibiotics related to daptomycin. *Proceedings of the National Academy of Sciences*, 103(46):17462–17467, 2006.
- [154] M. Noda, Y. Kawahara, A. Ichikawa, Y. Matoba, H. Matsuo, D.-G. Lee, T. Kumagai, and M. Sugiyama. Self-protection mechanism in D-cycloserine-producing *Streptomyces lavendulae*. Gene cloning, characterization, and kinetics of its alanine racemase and D-

- alanyl-D-alanine ligase, which are target enzymes of D-cycloserine. *Journal of Biological Chemistry*, 279(44):46143–52, Oct. 2004.
- [155] H. Ochman, J. G. Lawrence, and E. A. Groisman. Lateral gene transfer and the nature of bacterial innovation. *Nature*, 405(6784):299–304, 2000.
- [156] B. Ostash and S. Walker. Moenomycin family antibiotics: chemical synthesis, biosynthesis, and biological activity. *Natural Product Reports*, 27(11):1594–1617, 2010.
- [157] A. C. Palmer and R. Kishony. Opposing effects of target overexpression reveal drug mechanisms. *Nature communications*, 5, 2014.
- [158] K. L. Palmer, A. Daniel, C. Hardy, J. Silverman, and M. S. Gilmore. Genetic basis for daptomycin resistance in enterococci. *Antimicrobial Agents and Chemotherapy*, 55(7):3345–3356, 2011.
- [159] M. Palmer. Efflux of cytoplasmically acting antibiotics from gram-negative bacteria: periplasmic substrate capture by multicomponent efflux pumps inferred from their cooperative action with single-component transporters. *Journal of bacteriology*, 185(17):5287–5289, 2003.
- [160] M. Palmer, A. Chan, T. Dieckmann, and J. Honek. *Biochemical Pharmacology*. Wiley & Sons, first edit edition, 2012.
- [161] S. M. Patel and L. D. Saravolatz. Monotherapy versus combination therapy. *Medical Clinics of North America*, 90(6):1183 – 1195, 2006. Antimicrobial Therapy.
- [162] U. Patel, Y. P. Yan, F. W. Hobbs, J. Kaczmarczyk, a. M. Slee, D. L. Pompliano, M. G. Kurilla, and E. V. Bobkova. Oxazolidinones mechanism of action: inhibition of the first peptide bond formation. *Journal of Biological Chemistry*, 276(40):37199–205, Oct. 2001.

- [163] A. Y. Peleg, S. Miyakis, D. V. Ward, A. M. Earl, A. Rubio, D. R. Cameron, S. Pillai, R. C. Moellering, and G. M. Eliopoulos. Whole genome characterization of the mechanisms of daptomycin resistance in clinical and laboratory derived isolates of *Staphylococcus aureus*. *PloS one*, 7(1):e28316, Jan. 2012.
- [164] J. Pogliano, N. Pogliano, and J. A. Silverman. Daptomycin-mediated reorganization of membrane architecture causes mislocalization of essential cell division proteins. *Journal of Bacteriology*, 194(17):4494–504, Sept. 2012.
- [165] C. R. H. Raetz and C. Whitfield. Lipopolysaccharide endotoxins. *Annual Review of Biochemistry*, 71:635, 2002.
- [166] L. Robbel and M. A. Marahiel. Daptomycin, a bacterial lipopeptide synthesized by a nonribosomal machinery. *Journal of Biological Chemistry*, 285(36):27501–27508, 2010.
- [167] M. C. Roberts, J. Sutcliffe, P. Courvalin, L. B. Jensen, J. Rood, and H. Seppala. Nomenclature for macrolide and macrolide-lincosamide-streptogramin b resistance determinants. *Antimicrobial Agents and Chemotherapy*, 43(12):2823–2830, 1999.
- [168] C. Rodriguez-Fonseca, R. Amils, and R. A. Garrett. Fine structure of the peptidyl transferase centre on 23 S-like rRNAs deduced from chemical probing of antibiotic-ribosome complexes. *Journal of Molecular Biology*, 247(2):224–35, Mar. 1995.
- [169] E. Rubinchik, T. Schneider, M. Elliott, W. R. P. Scott, J. Pan, C. Anklin, H. Yang, D. Dugourd, A. Müller, K. Gries, S. K. Straus, H. G. Sahl, and R. E. W. Hancock. Mechanism of action and limited cross-resistance of new lipopeptide MX-2401. *Antimicrobial Agents and Chemotherapy*, 55(6):2743–54, June 2011.
- [170] E. Rubinstein, R. Isturiz, H. C. Standiford, L. G. Smith, T. H. Oliphant, S. Cammarata, B. Hafkin, V. Le, and J. Remington. Worldwide assessment of linezolid’s clinical safety

- and tolerability: comparator-controlled phase III studies. *Antimicrobial Agents and Chemotherapy*, 47(6):1824–1831, 2003.
- [171] R. Saar-Dover, A. Bitler, R. Nezer, L. Shmuel-Galia, A. Firon, E. Shimoni, P. Trieu-Cuot, and Y. Shai. D-alanylation of lipoteichoic acids confers resistance to cationic peptides in group b streptococcus by increasing the cell wall density. *PLoS pathogens*, 8(9):e1002891, 2012.
- [172] M. Schindler and M. J. Osborn. Interaction of Divalent Cations and Polymyxin B with lipopolysaccharide. *Biochemistry*, 18(20):4425–4430, 1979.
- [173] F. Schlünzen, E. Pyetan, P. Fucini, A. Yonath, and J. M. Harms. Inhibition of peptide bond formation by pleuromutilins: the structure of the 50S ribosomal subunit from *Deinococcus radiodurans* in complex with tiamulin. *Molecular Microbiology*, 54(5):1287–94, Dec. 2004.
- [174] T. Schneider, K. Gries, M. Josten, I. Wiedemann, S. Pelzer, H. Labischinski, and H.-G. Sahl. The lipopeptide antibiotic friulimicin b inhibits cell wall biosynthesis through complex formation with bactoprenol phosphate. *Antimicrobial agents and chemotherapy*, 53(4):1610–1618, 2009.
- [175] M. A. Seeger, A. Schiefner, T. Eicher, F. Verrey, K. Diederichs, and K. M. Pos. Structural asymmetry of acrb trimer suggests a peristaltic pump mechanism. *Science*, 313(5791):1295–1298, 2006.
- [176] Y. Shai. Mechanism of the binding, insertion and destabilization of phospholipid bilayer membranes by α -helical antimicrobial and cell non-selective membrane-lytic peptides. *Biochimica et Biophysica Acta*, 1462(1-2):55–70, Dec. 1999.
- [177] Y. Shai. Mode of action of membrane active antimicrobial peptides. *Biopolymers*, 66(4):236–48, Jan. 2002.

-
- [178] L.-T. Sham, E. K. Butler, M. D. Lebar, D. Kahne, T. G. Bernhardt, and N. Ruiz. MurJ is the flippase of lipid-linked precursors for peptidoglycan biogenesis. *Science*, 345(6193):220–222, 2014.
- [179] J. A. Shapiro. Molecular model for the transposition and replication of bacteriophage μ and other transposable elements. *Proceedings of the National Academy of Sciences*, 76(4):1933–1937, 1979.
- [180] L. L. Shen and A. G. Pernet. Mechanism of inhibition of DNA gyrase by analogues of nalidixic acid: the target of the drugs is DNA. *Proceedings of the National Academy of Sciences*, 82(2):307–311, 1985.
- [181] D. L. Shinabarger, K. R. Marotti, R. W. Murray, a. H. Lin, E. P. Melchior, S. M. Swaney, D. S. Dunyak, W. F. Demyan, and J. M. Buysse. Mechanism of action of oxazolidinones: effects of linezolid and eperezolid on translation reactions. *Antimicrobial Agents and Chemotherapy*, 41(10):2132–6, Oct. 1997.
- [182] L. L. Silver. Challenges of antibacterial discovery. *Clinical Microbiology Reviews*, 24(1):71–109, Jan. 2011.
- [183] J. A. Silverman, L. I. Mortin, A. D. G. Vanpraagh, T. Li, and J. Alder. Inhibition of daptomycin by pulmonary surfactant: in vitro modeling and clinical impact. *Journal of Infectious Diseases*, 191(12):2149–52, June 2005.
- [184] J. A. Silverman, N. G. Perlmutter, and H. M. Shapiro. Correlation of Daptomycin Bactericidal Activity and Membrane Depolarization in *Staphylococcus aureus*. *Antimicrobial Agents and Chemotherapy*, 47(8):2538–2544, July 2003.
- [185] S. M. Simon and G. Blobel. A protein-conducting channel in the endoplasmic reticulum. *Cell*, 65(3):371–380, 1991.

-
- [186] S. M. Simon and G. Blobel. Signal peptides open protein-conducting channels in *e. coli*. *Cell*, 69(4):677–684, 1992.
- [187] A. E. Simor, T. L. Stuart, L. Louie, C. Watt, M. Ofner-Agostini, D. Gravel, M. Mulvey, M. Loeb, A. McGeer, E. Bryce, and A. Matlow. Mupirocin-resistant, methicillin-resistant *Staphylococcus aureus* strains in Canadian hospitals. *Antimicrobial Agents and Chemotherapy*, 51(11):3880–6, Nov. 2007.
- [188] A. Sippel and G. Hartmann. Mode of action of rifamycin on the rna polymerase reaction. *Biochimica et Biophysica Acta (BBA)-Nucleic Acids and Protein Synthesis*, 157(1):218–219, 1968.
- [189] O. Sköld. *Antibiotics and antibiotic resistance*. John Wiley & Sons, 2011.
- [190] M. E. Steed, C. Vidailiac, W. E. Rose, P. Winterfield, G. W. Kaatz, and M. J. Rybak. Characterizing vancomycin-resistant Enterococcus strains with various mechanisms of daptomycin resistance developed in an in vitro pharmacokinetic/pharmacodynamic model. *Antimicrobial Agents and Chemotherapy*, 55(10):4748–4754, 2011.
- [191] K. J. Stone and J. L. Strominger. Mechanism of Action of Bacitracin: Complexation with Metal Ion and C55-Isoprenyl Pyrophosphate. *Proceedings of the National Academy of Sciences*, 68(12):3223–3227, Dec. 1971.
- [192] K. J. Stone and J. L. Strominger. Inhibition of sterol biosynthesis by bacitracin. *Proceedings of the National Academy of Sciences*, 69(5):1287–9, May 1972.
- [193] D. R. Storm and J. L. Strominger. Complex Formation between Bacitracin Peptides and Isoprenyl Pyrophosphates: The Specificity of Lipid-Peptide Interactions . *Journal of Biological Chemistry*, 248(11):3940–3945, June 1973.

- [194] S. K. Straus and R. E. W. Hancock. Mode of action of the new antibiotic for Gram-positive pathogens daptomycin: comparison with cationic antimicrobial peptides and lipopeptides. *Biochimica et Biophysica Acta*, 1758(9):1215–23, Sept. 2006.
- [195] M. Strieker and M. A. Marahiel. The structural diversity of acidic lipopeptide antibiotics. *ChemBiochem : a European Journal of Chemical Biology*, 10(4):607–16, Mar. 2009.
- [196] A. Sugino, N. P. Higgins, P. O. Brown, C. L. Peebles, and N. R. Cozzarelli. Energy coupling in DNA gyrase and the mechanism of action of novobiocin. *Proceedings of the National Academy of Sciences*, 75(10):4838–4842, 1978.
- [197] A. Sugino, C. L. Peebles, K. N. Kreuzer, and N. R. Cozzarelli. Mechanism of action of nalidixic acid: purification of Escherichia coli nalA gene product and its relationship to DNA gyrase and a novel nicking-closing enzyme. *Proceedings of the National Academy of Sciences*, 74(11):4767–4771, 1977.
- [198] S. M. Swaney, H. Aoki, M. C. Ganoza, and D. L. Shinabarger. The oxazolidinone linezolid inhibits initiation of protein synthesis in bacteria. *Antimicrobial Agents and Chemotherapy*, 42(12):3251–3255, 1998.
- [199] F. P. Tally, M. Zeckel, M. M. Wasilewski, C. Carini, C. L. Berman, G. L. Drusano, and F. B. Oleson. Daptomycin: a novel agent for Gram-positive infections. *Expert Opinion in Investigational Drugs*, 8(8):1223–1238, 1999.
- [200] H. Tanaka, R. Oiwa, S. Matusukura, and S. Omura. Amphomycin inhibits phospho-N-acetylmuramyl-pentapeptide translocase in peptidoglycan synthesis of *Bacillus*. *Biochemical and Biophysical Research Communications*, 86(3):902–908, Feb. 1979.
- [201] B. Tansel, J. Sager, T. Rector, J. Garland, R. F. Strayer, L. Levine, M. Roberts, M. Hummerick, and J. Bauer. Significance of hydrated radius and hydration shells on ionic permeability during nanofiltration in dead end and cross flow modes. *Separation and Purification Technology*, 51(1):40–47, Aug. 2006.

- [202] T. Tenson, M. Lovmar, and M. Ehrenberg. The Mechanism of Action of Macrolides, Lincosamides and Streptogramin B Reveals the Nascent Peptide Exit Path in the Ribosome. *Journal of Molecular Biology*, 330(5):1005–1014, July 2003.
- [203] E. B. Tikhonova, Q. Wang, and H. I. Zgurskaya. Chimeric analysis of the multicomponent multidrug efflux transporters from gram-negative bacteria. *Journal of bacteriology*, 184(23):6499–6507, 2002.
- [204] G. S. Timmins and V. Deretic. Mechanisms of action of isoniazid. *Molecular Microbiology*, 62(5):1220–7, Dec. 2006.
- [205] A. Tomasz. The Mechanism of the Irreversible Antimicrobial Effects of Penicillins: How the Beta-Lactam Antibiotics Kill and Lyse Bacteria. *Annual Review of Microbiology*, 33(1):113–137, Oct. 1979.
- [206] C. S. Toro, S. R. Lobos, I. Calderón, M. Rodríguez, and G. C. Mora. Clinical isolate of a porinless *Salmonella typhi* resistant to high levels of chloramphenicol. *Antimicrobial Agents and Chemotherapy*, 34(9):1715–1719, 1990.
- [207] T. T. Tran, D. Panesso, H. Gao, J. H. Roh, J. M. Munita, J. Reyes, L. Diaz, E. A. Lobos, Y. Shamoo, N. N. Mishra, A. S. Bayer, B. E. Murray, G. M. Weinstock, and C. A. Arias. Whole-Genome Analysis of a Daptomycin-Susceptible *Enterococcus faecium* Strain and Its Daptomycin-Resistant Variant Arising during Therapy. *Antimicrobial Agents and Chemotherapy*, 57(1):261–268, Jan. 2013.
- [208] E. E. Udo, L. E. Jacob, and B. Mathew. Genetic analysis of methicillin-resistant *Staphylococcus aureus* expressing high- and low-level mupirocin resistance. *Journal of Medical Microbiology*, 50(10):909–15, Oct. 2001.
- [209] P. Upcroft and J. A. Upcroft. Drug Targets and Mechanisms of Resistance in the Anaerobic Protozoa Drug Targets and Mechanisms of Resistance in the Anaerobic Protozoa. *Clinical Microbiology Reviews*, 14(1), 2001.

-
- [210] A. Volkov, S. Paula, and D. Deamer. Two mechanisms of permeation of small neutral molecules and hydrated ions across phospholipid bilayers. *Bioelectrochemistry and Bioenergetics*, 42(2):153–160, May 1997.
- [211] B. Walker, O. Braha, S. Cheley, and H. Bayley. An intermediate in the assembly of a pore-forming protein trapped with a genetically-engineered switch. *Chemistry & Biology*, 2(2):99–105, Feb. 1995.
- [212] R. J. Wargel, C. A. Hadur, and F. C. Neuhaus. Mechanism of D-cycloserine action: transport mutants for D-alanine, D-cycloserine, and glycine. *Journal of Bacteriology*, 105(3):1028–35, Mar. 1971.
- [213] D. J. Waxman and J. L. Strominger. Penicillin-binding proteins and the mechanism of action of beta-lactam antibiotics. *Annual Review of Biochemistry*, 52:825–69, Jan. 1983.
- [214] W. Wehrli. Rifampin: mechanisms of action and resistance. *Review of Infectious Diseases*, 5(Supplement 3):S407–S411, 1983.
- [215] B. Weisblum. Erythromycin Resistance by Ribosome Modification. *Antimicrobial Agents and Chemotherapy*, 39(3):577–585, 1995.
- [216] D. N. Wilson. Ribosome-targeting antibiotics and mechanisms of bacterial resistance. *Nature Reviews Microbiology*, 12(1):35–48, 2014.
- [217] M. Wittmann, U. Linne, V. Pohlmann, and M. A. Marahiel. Role of dpte and dptf in the lipidation reaction of daptomycin. *FEBS journal*, 275(21):5343–5354, 2008.
- [218] G. D. Wright. Bacterial resistance to antibiotics: enzymatic degradation and modification. *Advanced Drug Delivery Reviews*, 57(10):1451–70, July 2005.
- [219] L. Xiong, P. Kloss, S. Douthwaite, M. Andersen, S. Swaney, D. L. Shinabarger, A. S. Mankin, and N. M. Andersen. Oxazolidinone Resistance Mutations in 23S rRNA of *Escherichia coli* Reveal the Central Region of Domain V as the Primary Site of Drug

- Action Oxazolidinone Resistance Mutations in 23S rRNA of *Escherichia coli* Reveal the Central Region of Domain V as the Pri. *Journal of Bacteriology*, 2000.
- [220] T. Yanagisawas and T. Judy. Protein Structure of Isoleucyl-tRNA Synthetase with Pseudomonic Acid Resistance of. *Journal of Biological Chemistry*, 269(39):24304–24309, 1994.
- [221] S.-J. Yang, B. N. Kreiswirth, G. Sakoulas, M. R. Yeaman, Y. Q. Xiong, A. Sawa, and A. S. Bayer. Enhanced expression of *dltabcd* is associated with the development of daptomycin nonsusceptibility in a clinical endocarditis isolate of *Staphylococcus aureus*. *Journal of Infectious Diseases*, 200(12):1916–1920, 2009.
- [222] M. B. Yarmolinsky and L. Gabriel. Inhibition by puromycin of amino acid incorporation into protein. *Proceedings of the National Academy of Sciences*, 45(12):1721, 1959.
- [223] K. D. Young. A flipping cell wall ferry. *Science*, 345(6193):139–140, 2014.
- [224] Y. Yuan, S. Fuse, B. Ostash, P. Sliz, D. Kahne, and S. Walker. Structural Analysis of the Contacts Anchoring Moenomycin to Peptidoglycan Glycosyltransferases and Implications for Antibiotic Design. *ACS Chemical Biology*, 3(7):429–436, July 2008.
- [225] Y. Zhang, B. Heym, B. Allen, D. Young, and S. Cole. The catalase–peroxidase gene and isoniazid resistance of *Mycobacterium tuberculosis*. *Nature*, 358(6387):591–593, Aug. 1992.